

Electronic Thesis and Dissertation Repository

3-29-2016 12:00 AM

Photosynthetic acclimation to warming and elevated CO₂ in two Antarctic vascular plant species

Vi NT Bui
The University of Western Ontario

Supervisor
Danielle Way
The University of Western Ontario

Graduate Program in Biology

A thesis submitted in partial fulfillment of the requirements for the degree in Master of Science
© Vi NT Bui 2016

Follow this and additional works at: <https://ir.lib.uwo.ca/etd>



Part of the [Other Physiology Commons](#), [Other Plant Sciences Commons](#), and the [Plant Biology Commons](#)

Recommended Citation

Bui, Vi NT, "Photosynthetic acclimation to warming and elevated CO₂ in two Antarctic vascular plant species" (2016). *Electronic Thesis and Dissertation Repository*. 3654.
<https://ir.lib.uwo.ca/etd/3654>

This Dissertation/Thesis is brought to you for free and open access by Scholarship@Western. It has been accepted for inclusion in Electronic Thesis and Dissertation Repository by an authorized administrator of Scholarship@Western. For more information, please contact wlsadmin@uwo.ca.

Abstract

Climate change can affect the performance of the only two vascular plant species found in Antarctica, *Deschampsia antarctica* and *Colobanthus quitensis*. I investigated the response of these two species to warming and elevated CO₂ in terms of photosynthesis and leaf anatomy. While photosynthesis increased directly with rising temperature and CO₂, it showed no acclimation to changes in growth temperature, and a small degree of acclimation to growth under elevated CO₂. Likewise, leaf anatomy displayed little plasticity in response to changes in the growth environment, although *D. antarctica*'s stomatal groove structure was modified under warming, likely to reduce water loss. Biomass accumulation in both species increased at elevated growth CO₂; however, warming suppressed growth in the warmest treatments in *D. antarctica*, and under all warming treatments in *C. quitensis*. My results proposed mechanisms for past trends of expanding population in both species and predictions of their performance in future climates.

Keywords

Antarctica, biomass, *Colobanthus quitensis*, *Deschampsia antarctica*, elevated CO₂, leaf anatomy, photosynthesis, stomatal groove, thermal acclimation, warming.

Co-Authorship Statement

This work was conducted under the supervision of Dr. Danielle Way, in collaboration with Drs. León Bravo and Carolina Sanhueza. All the experimental design, data collection, and data analysis was done by myself in collaboration with Drs. Way, Bravo, and Sanhueza, and any publications subsequent to the completion of this work will be co-authored with them.

Acknowledgements

First of all, I'd like to acknowledge my supervisor, Dr. Danielle Way. She not only taught me about plant physiology, but also exemplifies the scientist I'd like to become: passionate about the subject, meticulous in her work, inspiring in her teaching, and incredibly supportive as a mentor. She offered me opportunities and support to pursue my interest, learn new skills, and explore new projects. Above all, Dani was the voice of reassurance when I panicked, of encouragement when I doubted myself, and the laughter that reminded me to enjoy myself and my work.

It was also my honor to work with Drs. Carolina Sanhueza and León Bravo from Chile, whose expertise in Antarctic plant ecophysiology and plant specimens made this project possible. This thesis could not be completed without the support from my advisory committee, Drs. Norm Hüner and Hugh Henry, who provided patient guidance and valuable feedback. Dr. Richard Gardiner, Karen Nygard, and Bill Hancock from the Biotron Integrated Microscopy were also extremely supportive and patient, and I am grateful for the knowledge in microscopy they taught me.

I'd also like to thank the members of the Way lab, who have been there along my journey as a graduate student: Yulia Kroner, Joe Stinziano, Alejandra Rey, Elaine Liu, Nick Harris, Andre Duarte, Eric Dusenge, and Sasha Madhavji. Thank you, Joe, for always bringing the exemplary work ethic, your excellent advice, and your aeropress coffee to work. Thank you, Yulia, for being an amazing teacher on and off the bench, and Alejandra, for being the greatest undergraduate assistant and a lovely friend.

I also appreciate the wonderful friendship and support from fellow graduate students in BGS and beyond. Thank you, Susan Anthony (and Primrose), for the late-night company, Jantina Toxopeus, Jackie Lebenzon, Kurtis Turnbull, Tian Wu, Justin Croft, and Sarah McFarlane, for all the fun at lunch and trivia, and others, for the lovely memories.

Last but not least, I'm grateful to my family back home for their constant moral support. Bobby Chon, thank you for being my anchor; no words can express my appreciation of your unwavering love, countless sacrifices, and the support from your family.

Table of Contents

Abstract.....	ii
Keywords	ii
Co-Authorship Statement.....	iii
Acknowledgements	iv
Table of Contents	v
List of Tables.....	viii
List of Figures	ix
List of Appendices.....	xi
List of Abbreviations	xii
Chapter 1: Introduction.....	1
1.1 Climate change	1
1.2 Terrestrial environment in Antarctica	1
1.2.1 Physical conditions in Antarctica.....	1
1.2.2 Antarctic terrestrial biota	3
1.2.3 Warming trends.....	3
1.3 <i>Deschampsia antarctica</i> and <i>Colobanthus quitensis</i>	4
1.3.1 Ecology of the species	4
1.3.2 Adaptations to an extreme environment.....	6
1.4 Photosynthesis in C ₃ plants	7
1.4.1 Photosynthetic electron transport	8
1.4.2 The Calvin-Benson cycle.....	10
1.4.3 Modelling photosynthesis	11
1.4.4 CO ₂ diffusion	13
1.4.5 Chlorophyll fluorescence	14
1.5 Leaf anatomy	16
1.6 Photosynthetic and leaf anatomical responses to climate change parameters.....	18
1.6.1 Warming	18
1.6.1.1 Acute temperature responses.....	18
1.6.1.2 Acclimation to warmer growth temperature	20
1.6.1.3 Plant growth and leaf structural responses under warming	21

1.6.2	Elevated CO ₂	21
1.6.2.1	Acute response to elevated CO ₂	21
1.6.2.2	Acclimation to elevated growth CO ₂	22
1.6.2.3	Plant growth and leaf structural responses to elevated CO ₂	23
1.6.3	Warming and elevated CO ₂	23
1.7	Photosynthesis and leaf anatomy in <i>D. antarctica</i> and <i>C. quitensis</i>	24
1.7.1	Photosynthesis in <i>D. antarctica</i> and <i>C. quitensis</i>	24
1.7.2	Leaf anatomy of <i>D. antarctica</i> and <i>C. quitensis</i>	24
1.7.2.1	<i>D. antarctica</i>	24
1.7.2.2	<i>C. quitensis</i>	25
1.8	Objectives	26
Chapter 2: Material and Methods		28
2.1	Experimental design.....	28
2.2	Gas exchange measurements	29
2.3	Biomass and C/N analysis	30
2.4	Light microscopy	31
2.5	Aphid attack.....	34
2.6	Statistical analysis	34
Chapter 3: Results.....		35
3.1	Photosynthetic response to warming and elevated CO ₂	35
3.2	Leaf structure and biomass accumulation	54
3.3	Leaf anatomy	61
Chapter 4: Discussion.....		67
4.1	Photosynthesis in both species showed little acclimation.....	67
4.1.1	Neither species showed thermal acclimation of photosynthesis to an 8 °C increase in growth temperature	68
4.1.2	Photosynthetic performance at growth temperature was driven by direct response to measurement temperature.....	71
4.2	Enhanced photosynthesis at elevated CO ₂ was mostly due to the direct CO ₂ effect.....	72
4.2.1	Photosynthesis in both species was enhanced by direct CO ₂ response	72

4.2.2	Photosynthesis was down-regulated at elevated CO ₂ in <i>D. antarctica</i>	73
4.2.3	There was no acclimate to elevated CO ₂ in <i>C. quitensis</i>	74
4.3	Leaf anatomy showed little plasticity, except in <i>D. antarctica</i> stomatal grooves.	75
4.3.1	There were no major changes in leaf morphology in either species	75
4.3.2	Modified stomatal groove structure in <i>D. antarctica</i> suggests high moisture stress at high temperature	76
4.4	Leaf-level photosynthetic responses did not always translate to growth	77
4.4.1	Biomass accumulation was enhanced at elevated CO ₂ in both species.....	77
4.4.2	Warming did not consistently enhance growth.....	78
4.4.3	<i>D. antarctica</i> and <i>C. quitensis</i> performance in future climates	79
4.5	Future directions	81
4.6	Conclusions	82
	References	84
	Appendices.....	92
	Curriculum Vitae	95

List of Tables

Table 3.1. Mean \pm SE of maximal light-harvesting capacity of PSII (F_v/F_m) measured at leaf temperature of 16 °C and 400 ppm CO ₂	45
Table 3.2. Mean \pm SE of leaf carbon, nitrogen, and carbon to nitrogen ratio of <i>D. antarctica</i> and <i>C. quitensis</i>	60
Table 3.3. Proportion of cross-sectional images of <i>D. antarctica</i> and <i>C. quitensis</i> filled with mesophyll cells, intercellular air space, vascular bundles, and other non-photosynthetic tissues, as well as leaf thickness and width.	64

List of figures

Figure 1.1. a) Photosynthetic electron transport and b) the Calvin Benson cycle	9
Figure 1.2. A model of chlorophyll fluorescence.....	15
Figure 1.3. Cross section of a typical C ₃ leaf.....	17
Figure 1.4. CO ₂ assimilation rate in response to acute changes in leaf temperature and acclimation to an increased growth temperature.....	19
Figure 2.1. Images of <i>D. antarctica</i> and <i>C. quitensis</i>	31
Figure 2.2 Comparisons of random point estimates vs tracing individual tissues to estimate proportion of leaf cross-sectional area filled by a given tissue type in <i>D. antarctica</i> and <i>C. quitensis</i>	33
Figure 3.1. Average air temperature and atmospheric CO ₂ concentrations every two days in six treatments from November 2014 to May 2015.....	37
Figure. 3.2. Net CO ₂ assimilation rate (A_{net}) of <i>Deschampsia antarctica</i> at saturating light across treatments and different measurement conditions	38
Figure 3.3. Net CO ₂ assimilation rate (A_{net}) of <i>Colobanthus quitensis</i> at saturating light across treatments and different measurement conditions	39
Figure 3.4. Maximum Rubisco carboxylation rate (V_{cmax}), maximum electron transport rate (J_{max}), and $V_{cmax}:J_{max}$ ratio of <i>D. antarctica</i> across treatments and different measurement conditions	41
Figure 3.5. Maximum Rubisco carboxylation rate (V_{cmax}), maximum electron transport rate (J_{max}), and $V_{cmax}:J_{max}$ ratio of <i>C. quitensis</i> across treatments and different measurement conditions	43
Figure 3.6. Electron transport rate (ETR) of <i>D. antarctica</i> across treatments and different measurement conditions	48

Figure 3.7. Electron transport rate (ETR) of <i>C. quitensis</i> across treatments and different measurement conditions	49
Figure 3.8. Intercellular to atmospheric CO ₂ concentrations ratio (C _i /C _a) of <i>D. antarctica</i> across treatments and different measurement conditions	50
Figure 3.9. Intercellular to atmospheric CO ₂ concentrations ratio (C _i /C _a) of <i>C. quitensis</i> across treatments and different measurement conditions	51
Figure 3.10. Dark respiration rate (R _{dark}) of <i>D. antarctica</i> across treatments and different measurement conditions	52
Figure 3.11. Dark respiration rate (R _{dark}) of <i>C. quitensis</i> across treatments and different measurement conditions	53
Figure 3.12. Specific leaf area of <i>D. antarctica</i> and <i>C. quitensis</i>	55
Figure 3.13. Aboveground, belowground, total biomass, and root to shoot ratio of <i>D. antarctica</i> on a pot basis	56
Figure 3.14. Aboveground, belowground, total biomass, and root to shoot ratio of <i>C. quitensis</i> on a pot basis	58
Figure 3.15. Cross sections of <i>D. antarctica</i> and <i>C. quitensis</i>	63
Figure 3.16. a) Average stomatal groove width, b) depth, and c) area to perimeter ratio of <i>Deschampsia antarctica</i>	65

List of Appendices

Appendix A. Removed data from <i>C. quitensis</i> in treatment 12/AC.....	92
Appendix B. Permission to use images from copyright holders.....	93

List of Abbreviations

A	CO ₂ assimilation rate/ photosynthesis
AC	ambient CO ₂ concentration
A _{net}	net CO ₂ assimilation rate
ATP	adenosine triphosphate
C	carbon
Ca	atmospheric CO ₂ concentration
Ci	intercellular CO ₂ concentration
CO ₂	carbon dioxide
Cyt b6/f	cytochrome b6/f
EC	elevated CO ₂ concentration
ETR	electron transport rate
Fd	ferredoxin
F	steady-state fluorescence in light-incubated leaves
F _o	minimal fluorescence in dark-incubated leaves
F _m	maximal fluorescence in dark-incubated leaves
F' _m	maximal fluorescence in light-incubated leaves
F _v /F _m	maximum photochemical efficiency of PSII
Γ*	CO ₂ compensation point in the absence of mitochondrial respiration
g _s	stomatal conductance
J _{max}	maximum electron transport rate
K _c	Rubisco's Michaelis-Menten constant for carboxylation
K _m	Rubisco's Michaelis-Menten constant for carboxylation and oxygenation
K _o	Rubisco's Michaelis-Menten constant for oxygenation
N	nitrogen
NADPH	nicotinamide adenine dinucleotide phosphate
O ₂	oxygen
PC	plastocyanin
PFD	photon flux density

P_i	inorganic phosphate
PGA	3-phosphoglyceric acid
PQ	plastoquinone
Φ_{PSII}	quantum yield of PSII
PSII	photosystem II
R	respiration
R_{dark}	dark respiration rate
R_{light}	light respiration rate
SLA	specific leaf area
T_{opt}	optimal temperature
V_c	Rubisco carboxylation rate
V_{cmax}	maximum Rubisco carboxylation rate
V_o	Rubisco oxygenation rate
VPD	vapor pressure deficit

CHAPTER 1: INTRODUCTION

1.1 Climate change

Human activities since the Industrial Revolution, including burning of fossil fuels and land use change, have significantly increased atmospheric CO₂ concentration. As a result, atmospheric CO₂ concentration has risen from 280 ppm in the 19th century to 400 ppm in 2014, as 2000 Gt CO₂ from anthropogenic sources were released into the atmosphere during this period (IPCC 2014). The increases in atmospheric CO₂, as well as other greenhouse gases from anthropogenic sources, have resulted in a global rise in temperature. Global average temperature, integrated between land and sea, has risen by between 0.65 and 1.08 °C from 1880 to 2012. As a result, there have been significant declines in sea ice, and a rise in sea level, as well as other major changes in the climate system (IPCC 2014).

The Intergovernmental Panel on Climate Change (IPCC) has issued five assessment reports since 1990 to synthesize scientific research surrounding the evidence of climate change and predictions of future climates. Predictions are usually grouped into four emission scenarios, with the best case scenario predicting zero emissions of greenhouse gases globally before 2100, and the worst case scenario being “business-as-usual”. Because of the long residence time of CO₂ in the atmosphere, the warming trend is expected to continue, even under the zero emission scenario, due to cumulative past emissions (IPCC 2014). Under the business-as-usual emission scenario, by 2100, annual greenhouse gas emissions are expected to more than double the current level of emissions (IPCC 2014); in this worst-case scenario, global mean surface temperature will increase by over 4 °C by 2100. This trend of rising temperature and atmospheric CO₂ can have major implications for many biological systems.

1.2 Terrestrial environment in Antarctica

1.2.1 Physical conditions in Antarctica

Antarctica occupies one-tenth of the Earth's land surface, mostly south of the 60 °S latitude (Kennedy 1995). The continent consists of three main zones: the mainland south of the Antarctic Circle, the Maritime Antarctic (which includes the Antarctic Peninsula and its associated islands), and the sub-Antarctic islands north of the 60 °S latitude (Alberdi et al. 2002). The difference in climate among these three zones is the result of correlated variation in latitude, distance from the sea, day length, and thereby temperature and precipitation (Holdgate 1977). Antarctica experiences the coldest conditions on Earth. The climate on the continent varies greatly among the sub-Antarctic, Maritime Antarctic, and continental Antarctic, generally growing milder with decreasing latitude. Temperature can be above freezing for at least 6 months per year in the sub-Antarctic islands, above 0 °C in mid- austral summer and just above -15 °C in the Maritime Antarctic, or below freezing even in the austral summer and dropping well below -25 °C in the austral winter in the continental Antarctic (Holdgate 1977).

Despite holding 90% of the Earth's freshwater, Antarctica is the driest continent on Earth. Its climate ranges from arid to semiarid, and the continental Antarctic is considered a desert. This paradox exists because the vast majority of fresh water on the continent is either frozen or sporadic in distribution and transient in timing, mostly due to fluctuations in temperature between day and night and between austral summer and winter (Kennedy 1993). Annual precipitation ranges from 100-200 cm in the sub-Antarctic islands to insignificant amounts in the continental Antarctic (Holdgate 1977). While temperature might limit the distribution of species on a regional scale, moisture availability might determine the distribution of life forms at the microhabitat level (Kennedy 1993).

The extreme thermal and moisture conditions in 98% of Antarctica's land surface are too inhospitable for most terrestrial life forms, leaving approximately $2 \cdot 10^5$ km² of land available for colonization by vegetation, mostly in the Maritime Antarctic and on sub-Antarctic islands (Alberdi et al. 2002). Even in these regions, colonization is challenged by subsurface permafrost, and constrained by microclimate effects from wind speed, surface features, and moisture availability (Beyer et al. 2000). Soils in Antarctica have very low moisture, C:N ratios, and pH (Beyer et al. 2000).

1.2.2 Antarctic terrestrial biota

The harsh climate in Antarctica, as well as its isolation from other continents, results in extremely low biodiversity in the terrestrial biota compared to the same latitude in the Arctic (Convey 2010). The continent separated from the Gondwana landmass over 25 million years ago, carrying with it the terrestrial fauna and flora typical of the south temperate rainforests (Convey et al. 2008). Since then, several periods of climate cooling and glacial advances wiped out the majority of the terrestrial biota until the Last Glacial Maximum twenty thousand years ago (Ellis-Evans and Walton 1990, Convey et al. 2008). Additionally, the Antarctic Circumpolar Current creates a natural boundary at the Antarctic Polar Front Zone and prevents most terrestrial biota exchange between Antarctica and other continents. The isolation of Antarctica on a multi-million year timescale presents a major barrier for colonization, so the terrestrial biota consists of both relict species that survived the glacial periods in refugia, and a few colonizers that arrived after the Last Glacial Maximum (Convey et al. 2008, Convey 2010).

Generally, species richness and ecosystem complexity increase with decreasing latitude and proximity to the sea, but there is also a high level of regionalization within a given biogeographic region (Bergstrom and Chown 1999, Convey et al. 2008). Terrestrial flora in the Continental Antarctic consists of mostly lichens and mosses (Holdgate 1977). Maritime Antarctic and the sub-Antarctic islands, on the other hand, host a more diverse community of mosses, liverworts, lichens, and two species of vascular plants, Antarctic hair grass, *Deschampsia antarctica* Desv. (Poaceae) and Antarctic pearlwort, *Colobanthus quitensis* (Kunth) Bartl. (Caryophyllaceae).

1.2.3 Warming trends

Climate change has caused significant warming in Antarctica. Patterns of warming are highly regional; while some meteorological stations on the continent have not reported significant warming, others recorded a steep rate of increase in mean annual temperature, particularly over the second half of the 20th century (Vaughan et al. 2003). For example, the Faraday/Vernadsky Station in the Maritime Antarctic reported a 3.7 °C temperature increase per century since 1946 (Vaughan et al. 2003); Byrd Station on the Central West

of the Continental Antarctic also experienced a rapid rate of warming of 2.3 °C from 1958 to 2010 (Bromwich et al. 2012). Overall, data from across the continent demonstrates a trend of moderate warming despite large spatial and interannual variability, and more extreme warming in the austral winter than summer (Chapman and Walsh 2007).

Rising temperatures potentially alter thermal and moisture regimes, impacting both physical and biological systems on the continent. For example, aerial photographs from the British Antarctic Survey from 1940 to 1999 showed a steady loss of snow cover on the Antarctic Peninsula (Fox and Cooper 1998). Additionally, the warming trend results in a 74% increase in the number of days with temperature above 0 °C (Vaughan et al. 2003), and an expansion of ice-free areas (Fowbert and Smith 1994). The ice retreat not only alters the hydrology of the terrestrial ecosystem, but also exposes bare soils to colonization by bryophytes and lichens (Smith 1994). Similarly, there has been a subsequent increase in the population size of the two vascular plant species, *Deschampsia antarctica* and *Colobanthus quitensis*, on the Argentine Islands on the Antarctic Peninsula between 1964 and 1990, following a warming rate of 0.056 °C per year (Fowbert and Smith 1994). Monitoring the population of these two vascular species on Argentine and Signy Islands, Smith (1994) suggested they could be bioindicators of the thermal environment in the Maritime Antarctic.

1.3 *Deschampsia antarctica* and *Colobanthus quitensis*

1.3.1 Ecology of the species

Deschampsia antarctica Desv. (Poaceae) and *Colobanthus quitensis* (Kunth) Bartl. (Caryophyllaceae) are the only two vascular plant species found in Antarctica. Both species are distributed throughout the sub-Antarctic islands and the Maritime Antarctic to as far south as the Terra Firma Islands, approximately 68 ° 42 ' South, but do not enter the continental Antarctic (Komáková 1985). Outside Antarctica, *D. antarctica* can be found in Argentina, Chile, and Tierra del Fuego, while the range of *C. quitensis* extends to Mexico, Ecuador, Bolivia, Peru, Argentina, Chile, and Tierra del Fuego (Moore 1970).

Studies trying to unravel the “enigma” of why these are the only two successful vascular species on the continent suggested that they might be migratory relicts dispersed to the continent before Antarctica completely separated from the Gondwanan landmass. (Smith 2003, Parnikoza et al. 2007, 2011). The two species might have survived the glaciation periods in warmer refugia, and thrived and spread throughout the continent by bird dispersal once the glaciers retreated (Parnikoza et al. 2007).

The distributions of *D. antarctica* and *C. quitensis* are influenced more by climate than soil conditions (Parnikoza et al. 2011). The two species are most commonly found together in north-facing coastal areas, and at low altitude sites (Smith 2003). The microclimate of these sites insulates the plants under the snow during the austral winter and shelters them from the wind year-round (Smith 2003). Additionally, both species inhabit areas that receive maximal sunlight, creating radiation traps that capture irradiance and heat (Edwards 1972). Neither species are constrained by specific soil conditions; in fact, the vascular vegetation cover with a true root structure improves the organic carbon status of the soil (Beyer et al. 2000).

Deschampsia antarctica Desv. is a perennial grass, and is closely related to a number of species in the same genus in South America (Parnikoza et al. 2011). *D. antarctica* forms densely packed tufts; leaf blades are 0.5 to 1.5 mm wide, wiry, and frequently roll inwards (Moore 1970). The species spreads clonally through tillers, forming large colonies up to several hundred square meters, and disperses with the assistance of birds, as it can re-establish itself after being uprooted (Smith 2003). In harsher sites, the species invests instead in reproductive biomass, producing bisexual flowers that self-pollinate (Convey 1996a). The production of both inflorescence and seeds depends on photoperiod, but the rates of inflorescence production, seed production, and germination depend on temperature (Holtom and Greene 1967).

Colobanthus quitensis (Kunth) Bartl. is a perennial pearlwort that can live up to 35-40 years. The genus *Colobanthus* is distributed throughout the Southern Hemisphere, but even in the same species, there is a lot of variability in morphology among populations (Moore 1970). The plant consists of linear leaves growing into a rosette around a simple

stem, with a long taproot (Moore 1970). Individuals tend to form a compact, hemispherical cushion up to a few centimeters in diameter, which assists in the capture of heat (Smith 2003). In contrast to *D. antarctica*, *C. quitensis* is unable to reproduce vegetatively; instead, its sexual reproductive output is much higher than that of *D. antarctica* (Convey 1996a). Flowering in *C. quitensis* is not photoperiod-dependent, and can occur multiple times in the same season if favorable conditions persist. Seed production also increases in warmer summers (Convey 1996a), and germination success increases with seed age (Holtom and Greene 1967). As a result, warming experiments have shown increases in seed production that could account for the expanding population of *C. quitensis* as the climate warms (Fowbert and Smith 1994).

1.3.2 Adaptations to an extreme environment

Survival in Antarctica requires all life forms to have a strategy to cope with the below-freezing temperatures for most of the year. These cold-resistance strategies differ between the two species: *D. antarctica* tolerates freezing, while *C. quitensis* avoids freezing by supercooling (Bravo et al. 2001). *D. antarctica* individuals, after a period of cold hardening and long photoperiod, accumulate proline and sucrose (Bravo et al. 2001), as well as antifreeze proteins, which lower the freezing point of cells and slow down the rate of ice crystal formation (Bravo and Griffith 2005). *D. antarctica*, therefore, can survive freezing down to -26°C . *C. quitensis*, on the other hand, avoids freezing by accumulating sucrose and supercooling, and experiences freezing at -4°C (Bravo et al. 2001). *D. antarctica* and *C. quitensis* also rely on snow cover for insulation and their tufted or cushion-like growth forms to retain heat when exposed (Smith 1994).

Being able to tolerate extreme temperatures is a beneficial, but costly, strategy. As typical stress-adapted species, *D. antarctica* and *C. quitensis* have very slow growth rates (Convey et al. 1996b). The two species also have photosynthetic machinery typical of cold-acclimated plants. Both species are photosynthetically active at freezing temperatures, and the lower temperature compensation point, where photosynthesis is equivalent to respiration, is -3°C for *D. antarctica*, and -2°C for *C. quitensis* (Xiong et al. 1999). In addition, *D. antarctica* is very tolerant of high irradiance, allowing it to

efficiently photosynthesize during the short austral summer (Montiel et al. 1999); however, high temperature (above 20 °C) presents a challenge due to high respiration rates which consume the carbon fixed in photosynthesis (Xiong et al. 1999). *D. antarctica* also possesses high water use efficiency, with efficiency values well above other C₃ grasses and more comparable to a CAM (Crassulacean Acid Metabolism) species (Montiel et al. 1999).

A changing thermal environment is likely to have major implications for the growth and performance of *D. antarctica* and *C. quitensis*. The aforementioned expanding population size of both species is extensive, yet poorly understood. Populations of *D. antarctica* on the Argentine Islands archipelago increased by 25 times from 1964 to 1990, whereas *C. quitensis* more than quadrupled their population size over the same period (Fowbert and Smith 1994). The greater population expansion of *D. antarctica* could be attributed to its ability to reproduce vegetatively through tillers, and its tolerance of disturbed habitat: the grass is one of the first species to colonize a newly exposed area when the ice retreats (Fowbert and Smith 1994). *C. quitensis*, on the other hand, takes advantage of the increased number of days above freezing (Vaughan et al. 2003), which offers more favorable conditions for flowering and seed germination (Day et al. 1999). More recent surveys of these species have shown a stabilization in both populations from 1990 to 2008, attributed to a slower warming trend on the continent over this period and a lack of available habitat (Parnikoza et al. 2009). Hence, more information is needed to understand the mechanisms underlying past increased growth in *D. antarctica* and *C. quitensis* and to predict the performance of the two species in future climates.

1.4 Photosynthesis in C₃ plants

Photosynthesis is one of the most important processes on the planet, harvesting the energy from sunlight and fixing CO₂ into sugar molecules that fuel metabolism and growth. Photosynthesis occurs in the chloroplast, an organelle present in all photosynthetic eukaryotes. Photosynthesis involves two separate but interconnected phases, the photosynthetic electron transport and the Calvin-Benson cycle (Fig. 1.1). The

photosystems absorb light energy, and through an electron transport chain, energy (ATP) and reducing power (NADPH) are produced. This energy and reducing power then fuel the Calvin-Benson cycle, an enzyme-dependent process that fixes CO₂ and produces sugar (Fig. 1.1). (Hopkins and Hüner 2008).

1.4.1 Photosynthetic electron transport

The energy from light is absorbed by chlorophyll, a pigment that absorbs red and far-red light while reflecting green light, giving leaves and other photosynthetic tissues their green color. This pigment forms two pigment-protein complexes in the thylakoid membranes responsible for light harvesting, photosystems I and II (PSI and PSII) (Fig. 1.1). The two reaction centers at the center of each photosystem absorb light at slightly different wavelengths, with PSI absorption peaking at 700 nm, and PSII at 680 nm; the first electron donors of each photosystem, therefore, are named P700 and P680 (Anderson 1986).

Photosynthesis begins when the light energy from a photon is gathered by the antennae and light harvesting complexes, and funneled to the chlorophyll molecules in the reaction center of PSII. This energy causes a charge separation, oxidizing P680 in PSII to P680⁺, and raises the energy level of an electron in this molecule to an excited state (Hopkins and Hüner 2008). This electron is unstable, and can be either used to fuel photochemistry, emitted as fluorescence, or dissipated as heat (Maxwell and Johnson 2000). In photochemistry, the excited electron is passed from PSII through a series of redox reactions along the transport chain to PSI through the plastoquinone pool (PQ), a cytochrome complex (b6f), and plastocyanin (PC) (Fig. 1.1). The last electron acceptor at PSI is ferredoxin (Fd), which reduces NADP⁺ to NADPH. At PSII, water is also oxidized, releasing O₂ and generating electrons to reduce P680⁺ to P680, opening the reaction center for the next photochemical reaction. Meanwhile, the thylakoid lumen is also acidified with the H⁺ produced from the PQ pool and the oxidation of water. The difference in pH between the two sides of the thylakoid membrane allows the production of ATP from ADP, facilitated by the ATP-synthase coupling factor (Hopkins and Hüner 2008) (Fig. 1.1).

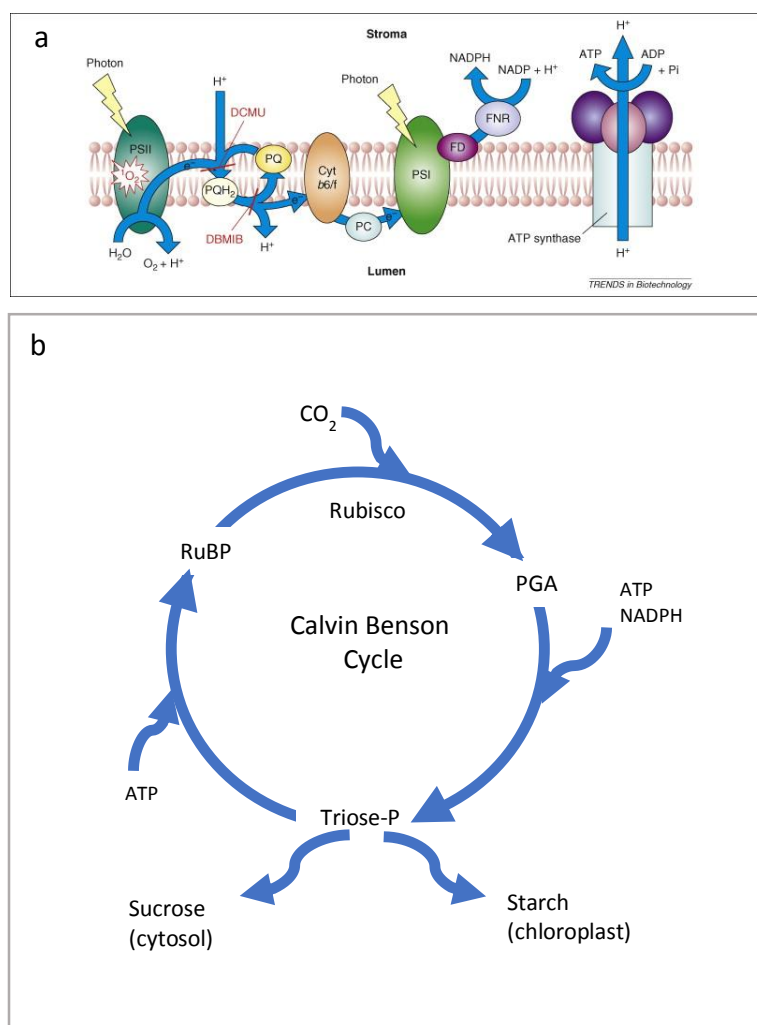


Figure 1.1 A model of photosynthesis. The light reactions harvest lights and produces ATP and NADPH from the photosynthetic electron transport chain (a). In the thylakoid membranes are two photosystems (PSII and PSI), a cytochrome complex (Cytochrome b6-f), and an ATP synthase. Energy from light excites an electron, which is passed from PSII to the plastoquinone pool (PQ), Cytochrome b6-f, plastocyanin (PC), and PSI. Finally, ferredoxin (Fd) reduces $NADP^+$ to generate NADPH in the stroma. The proton gradient created by the cycling of the plastoquinone pool and oxidation of water at PSII is used to generate ATP at the ATPase. The Calvin-Benson cycle (b) includes CO_2 fixation by enzyme Rubisco, the production of sugar and starch, and the regeneration of RuBP using ATP and NADPH produced from the photosynthetic electron transport chain. Image a) was taken from Lamers et al. 2008 with permission from Elsevier.

1.4.2 The Calvin-Benson cycle

The energy and reducing power produced from the light reactions, in the form of ATP and NADPH, is then used in the Calvin-Benson cycle, which occurs in the stroma of the chloroplast. The fixation of CO₂ using the substrate RuBP (Ribulose-1,5-biphosphate) is catalyzed by the enzyme Rubisco (Ribulose-1,5-biphosphate carboxylase oxygenase). Rubisco is the key enzyme in the Calvin-Benson cycle, and represents the most abundant protein on earth. The CO₂ fixation reaction produces phosphoglyceric acid (PGA), which is then reduced, using ATP and NADPH from the light reaction, into triose-phosphate (triose-P). The pool of triose-P is split among the production of sucrose and other metabolites, the synthesis of starch, and the regeneration of RuBP (Farquhar et al. 1980) (Fig. 1.1). Sucrose and other metabolites are usually exported into the cytosol, and loaded into the phloem for transport to the rest of the plant to fuel metabolism and growth, while starch tends to be stored in the chloroplast. The process of regenerating RuBP completes the Calvin-Benson cycle (Farquhar et al. 1980).

Rubisco is activated by light, as are other enzymes in the Calvin-Benson cycle. Rubisco perceives the increase in pH and Mg²⁺ concentration in the stroma due to the proton gradient generated across the thylakoid membranes from the photosynthetic electron transport (Salvucci and Ogren 1996). Additionally, CO₂ acts as an activator of the enzyme, in addition to its direct role as a substrate. However, full activation of Rubisco *in vivo* requires Rubisco activase, an enzyme that makes the active site on Rubisco available for CO₂ fixation (Salvucci and Ogren 1996).

Rubisco is a dual-function enzyme that has the capacity to fix O₂ instead of CO₂ in a process called photorespiration. When O₂ is fixed by Rubisco, it produces the toxic molecule phosphoglycolate, which needs to be transported to the peroxisome and then mitochondria, and finally back to the chloroplast as glycerate to produce PGA. Photorespiration consumes ATP and NADPH, and releases previously fixed CO₂. Rubisco's affinity for CO₂ compared to O₂ depends on temperature and the relative concentration of the two gases (Farquhar et al. 1980).

1.4.3 Modelling photosynthesis

Because photosynthesis ultimately draws CO₂ from the atmosphere, plant physiologists measure the exchange of CO₂ flux in leaves to assess net photosynthetic rates, using infrared gas analyzers (Field et al. 1982). A common parameter used to assess photosynthetic performance is net CO₂ assimilation rate (A_{net}), measured at standard conditions of saturating light, a leaf temperature of 25 °C, ambient CO₂ concentration, and constant humidity. A_{net} accounts for CO₂ fluxes at the leaf-level deriving mainly from photosynthesis, mitochondrial respiration and photorespiration.

In 1980, Farquhar, von Caemmerer, and Berry developed a model for CO₂ assimilation based on the biochemical components of photosynthesis (Farquhar et al. 1980). The model synthesizes knowledge of the enzyme kinetics of Rubisco, taking into account its carboxylation and oxygenation capacity. From this model, physiologists can derive a number of photosynthetic parameters from a series of measurements of A_{net} across a range of intercellular CO₂ concentrations (C_i), producing an A- C_i curve. They defined three main limitations to net photosynthesis at the chloroplast: Rubisco carboxylation, which depends on the quantity and activity of Rubisco; RuBP regeneration, which depends on the rate of photosynthetic electron transport and its ability to produce ATP and NADPH; and inorganic phosphate (P_i) regeneration, which depends on the consumption rate of products of photosynthesis to release P_i (Farquhar et al. 1980).

The Farquhar et al. model (1980) parameterizes A_{net} as the balance between the rate of carboxylation (V_c) and oxygenation (V_o) of Rubisco, and mitochondrial respiration in the light (R_{light}), with one molecule of CO₂ produced for every molecule of O₂ oxygenated, producing Equation (1):

$$A_{net} = V_c - 0.5V_o - R_{light} \quad (1)$$

The rates of carboxylation and oxygenation can be described by Michaelis-Menten kinetics, with K_c and K_o being the Michaelis-Menten constants for carboxylation and oxygenation, respectively. However, when both substrates are present, they compete with each other to bind to Rubisco. The specificity of Rubisco, K_m , therefore, takes into

account the concentration of oxygen (O), following Equation (2):

$$K_m = K_c \left(1 + \frac{O}{K_o} \right) \quad (2)$$

For a given quantity of activated Rubisco, the model identified two types of limitations: Rubisco-limitation, when CO₂ concentrations relative to O₂ are low, and RuBP-limitation, when Rubisco is CO₂-saturated but photosynthesis is limited by RuBP regeneration, or the rate of electron transport producing ATP and NADPH. When CO₂ is limited, the rate of carboxylation depends on the competition between carboxylation and oxygenation, and the specificity of Rubisco for CO₂ vs O₂. Equation (1), therefore, becomes Equation (3):

$$A_{net} = V_{cmax} \cdot \frac{C - \Gamma^*}{C + K_m} - R_{light} \quad (3)$$

where V_{cmax} describes the maximum carboxylation rate of Rubisco, C and O are the partial pressures of CO₂ and O₂ at the site of carboxylation or oxygenation, respectively, and Γ^* is the CO₂ compensation point when photosynthesis is equivalent to photorespiration in the absence of mitochondrial respiration.

Alternatively, when Rubisco is CO₂-saturated and RuBP limited, the rate of electron transport is maximal and constant (J_{max}), assuming CO₂ is the only electron sink. Assuming four electrons are required for each carboxylation and oxygenation reaction, Equation (1) becomes Equation (4):

$$A_{net} = J_{max} \cdot \frac{C - \Gamma^*}{4(C + 2\Gamma^*)} - R_{light} \quad (4)$$

Using this model, plant physiologists can measure leaf-level gas exchange, specifically A-C_i curves, to derive meaningful parameters such as maximum Rubisco carboxylation rates (V_{cmax}) and maximum electron transport rates (J_{max}) from different regions of the A-C_i curve using Equations (3) and (4) (Sharkey et al. 2007). These parameters are commonly used to assess photosynthetic capacity.

1.4.4 CO₂ diffusion

The Farquhar et al. (1980) model describes the biochemical demand of photosynthesis under varying intercellular CO₂ concentration (C_i). Whether this demand is met depends on the diffusion of CO₂ from the atmosphere, which is regulated by stomata. While being key to the CO₂ supply for photosynthesis, stomata are also the site of evaporative plant water loss; as a result, changes to the stomatal conductance influence both CO₂ diffusion into the leaf for carbon gain, and water out of the leaf through transpiration. Stomata close when vapor pressure deficit (VPD) increases to avoid water loss, or close upon receiving signals of low soil water potential in the form of abscisic acid (Turner et al. 1984, Farquhar and Sharkey 1982). How stomatal conductance is regulated to balance the trade-off between water loss and carbon gain, however, continues to be under study. Therefore, assessments of photosynthesis should also include CO₂ diffusion limitations, which can be altered by changes to the growth environment.

Most infrared gas exchange systems used to evaluate photosynthesis can also assess stomatal conductance (g_s), although values of g_s are highly transient (Field et al. 1982). Another commonly used measure of stomatal behavior is the C_i/C_a ratio. This parameter measures the ratio of intercellular (C_i) to atmospheric CO₂ concentrations (C_a), and reflects the balance between CO₂ demand and supply (Sage 1994). It integrates both the ability of CO₂ to diffuse from the atmosphere to the intercellular air space, and the usage of this internal CO₂ concentration in photosynthesis. Combined A_{net} , the C_i/C_a ratio can inform of any physical limitations hindering CO₂ diffusion, and the mechanisms determining changes in photosynthesis in a new growth environment.

Another resistance in the CO₂ diffusion pathway is at the mesophyll level. The Farquhar et al. (1980) model assumes the CO₂ diffusion from the intercellular air space to the chloroplast is large enough to not affect photosynthesis. As a result, the chloroplast CO₂ concentration (C_c) is presumably equivalent to the CO₂ concentration at the intercellular air space (C_i). However, Bernacchi et al. (2002) demonstrated that this diffusion pathway is, in fact, significant. Termed mesophyll conductance, CO₂ diffusion along this pathway is influenced by the leaf cell density, the diffusion of CO₂ at aqueous phase, the transport

through aquaporins, and the conversion to HCO_3^- by carbonic anhydrase (Bernacchi et al. 2002). Mesophyll conductance responds to changes in environmental conditions, and can therefore affect photosynthesis.

1.4.5 Chlorophyll fluorescence

As previously mentioned, when a photon is absorbed by chlorophyll and excites an electron, this energy can be passed on to other molecules to fuel photochemistry, be dissipated as heat, or be emitted at a longer wavelength as fluorescence. Plant physiologists use the fluorescent property of chlorophyll to evaluate the photochemical performance of photosystem II (PSII) (Maxwell and Johnson 2000). When a leaf is incubated in darkness for a sufficient period of time (> 20 minutes), all the reaction centers are open, and ready to accept the energy of a new photon (Fig. 1.2). When measured with a low-intensity red light, a leaf at this state returns a stable minimal fluorescence level (F_o), indicating all reaction centers are open and ready for photochemistry. Then, upon exposure to a saturating pulse of light, the fluorescence emitted rises to a maximal level (F_m), as all reaction centers close (Fig. 1.2). The ratio of the difference between F_m and F_o to F_m , also known as F_v/F_m (Equation 5), is used to assess the maximal photochemical efficiency of PSII.

$$F_v/F_m = \frac{F_m - F_o}{F_m} \quad (5)$$

The F_v/F_m in a healthy leaf ranges between 0.75 and 0.82, and lower F_v/F_m ratios indicate some form of stress affecting the photochemical efficiency of PSII (Maxwell and Johnson 2000).

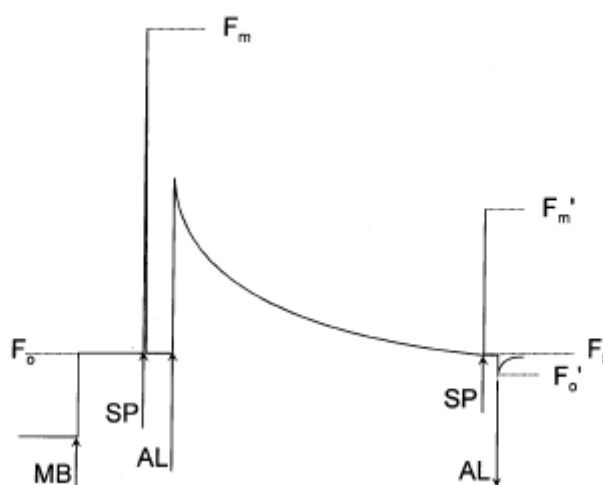


Figure 1.2 Chlorophyll fluorescence trace. Dark-incubated leaves yield minimum fluorescence (F_o) under a measuring light (MB), and after a saturating pulse (SP), give a maximal fluorescence value (F_m). After a period of time under actinic light (AL), the fluorescence signal stabilizes at F_t , and the same saturating flash (SP) will result in a fluorescence F_m' lower than F_m . Under this condition, exposure to a brief dark period (AL off) will yield a minimal fluorescence (F_o') higher than F_o . Figure was taken from Maxwell and Johnson 2000, with permission from Oxford University Press.

When the leaf has been exposed to its natural light environment, however, the fluorescence signal gradually reaches a steady state (F_t) (Fig. 1.2). This steady state of fluorescence is higher than the minimal fluorescence, because under an actinic light, not all reaction centers are open. At this point, the same exposure to a pulse of high intensity light will not result in a maximal fluorescence as high as F_m , but instead reaches F_m' level (Fig. 1.2). This is because under steady-state photosynthesis, the electron transport chain and the consumption of ATP and NADPH in the Calvin-Benson cycle operate at a much lower rate than PSII (Hopkins and Hüner 2008). Not all photons absorbed can be used in photochemistry, and instead can be partially dissipated as heat. The ratio of the difference between maximal and baseline fluorescence to the baseline fluorescence level is calculated as the realized photochemical efficiency of PSII, or photochemical quantum yield of PSII, (Φ_{PSII} , Equation 6):

$$\Phi_{PSII} = \frac{F_{m'} - F_t}{F_{m'}} \quad (6)$$

Because the quantum yield of PSII positively correlates with electron transport rate (ETR), the latter can be calculated from the former (Equation 7), with a known absorbed photon flux density (PFDa) and the partitioning of absorbed photons between PSII and PSI (often assumed to be 0.5) (Maxwell and Johnson 2000):

$$ETR = \Phi_{PSII} * PFDa * 0.5 \quad (7)$$

1.5 Leaf anatomy

Leaves are the main photosynthetic and transpiratory organ in plants; therefore, their structure is optimized for harvesting light and absorbing CO₂ while preventing excessive water loss. A leaf is bound by the upper (adaxial) and lower (abaxial) epidermis (Fig. 1.3). Embedded within the epidermal layers are stomata, which are pores that allow gas exchange between the leaf and the environment. A transverse section of the leaf reveals a number of typical tissue types (Fig. 1.3). Between the epidermis lies the mesophyll cells, which are the main photosynthetic tissues and occupy the largest proportion of the leaf cross-sectional area (Fig. 1.3). The arrangement of mesophyll cells allows CO₂ to diffuse to the site of carboxylation from the stomata through the intercellular air space. In many species, the mesophyll cells are differentiated into palisade mesophyll and spongy mesophyll. Mesophyll cells also need to be in the proximity of the vascular bundle, which includes xylem, which supplies water to the rest of the tissues, and phloem, which transport products of photosynthesis to the rest of the plant (Fig. 1.3) (Lambers et al. 2008).

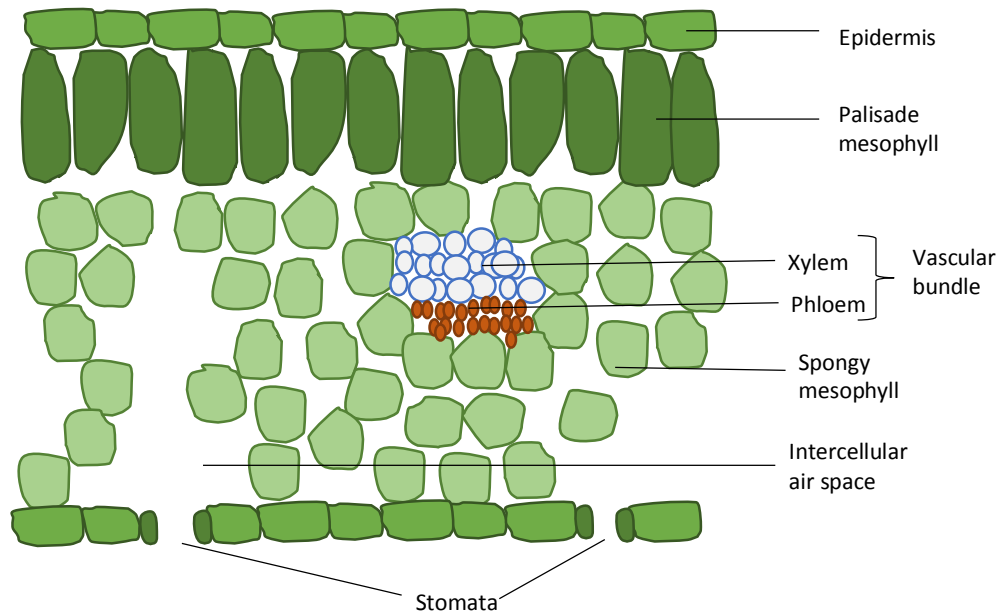


Figure 1.3 Cross section of a typical C_3 leaf reveals an upper and lower epidermis, palisade and spongy mesophyll, stomata, intercellular air space, and vascular bundle (comprised of xylem and phloem).

In grasses and other monocotyledon plants, leaves tend to be long, narrow and linear, with parallel veins. Additionally, grasses from dry habitats tend to be inwardly folded towards the adaxial side. In these arid-adapted grass species, the adaxial epidermis consists of ribs where the vascular bundles occur, and furrows between these ribs. Stomata occur on the adaxial side of the leaf, and along the wall of these furrows, forming stomatal grooves (Ellis 1976). The in-rolling of the leaf blade along these grooves is facilitated by the shrinking of bulliform cells, very thin-walled cells along the epidermis that easily lose water from turgor loss. When these cells shrink due to dry conditions, the leaf folds. This xeromorphic feature produces an additional air pocket with higher humidity compared to the ambient atmosphere, lowering water loss.

1.6 Photosynthetic and leaf anatomical responses to climate change parameters

1.6.1 Warming

1.6.1.1 Acute temperature responses

Net CO₂ assimilation rates (A_{net}), when measured across a range of leaf temperatures, typically show an increase up to an optimum temperature (T_{opt}) followed by a decrease above the optimal temperature (Fig. 1.4). This response is because components of photosynthesis, including the maximum Rubisco carboxylation rate (V_{cmax}), maximum electron transport rate (J_{max}), photorespiration, and respiration, increase exponentially with increasing leaf temperature, peak at an optimal temperature, and then decline. These responses follow an Arrhenius function, which describes the temperature dependence of enzyme reaction rates (Medlyn et al. 2002). V_{cmax} tends to be more responsive to temperature changes compared to J_{max} , due to the temperature sensitive parameters used to derive V_{cmax} , including the Michaelis constant for carboxylation (K_m) and CO₂ compensation point (Γ^*) (see Equation 3) (Medlyn et al. 2002).

Temperature affects both Rubisco carboxylation and oxygenation: at higher temperature, Rubisco's specificity for CO₂ relative to O₂ decreases, and the solubility of CO₂ decreases more rapidly than that of O₂ (Jordan and Ogren 1984). As a result, greater photorespiration at high leaf temperatures increases the CO₂ compensation point in the absence of light respiration (Γ^*), raising the cost of carboxylation. At non-saturating CO₂ concentrations, therefore, an increase in V_{cmax} at warmer leaf temperature is offset by the increase in oxygenation rate (V_{omax}), resulting in little change in net CO₂ assimilation rate (Sage and Kubien 2007).

J_{max} is less sensitive to acute increases in temperature, and reaches a lower temperature optimum, than V_{cmax} (Medlyn et al. 2002). The positive response of J_{max} to leaf temperature is commonly attributed to a stimulated energy or electron flow through PSII, PSI, or the cytochrome b6/f complex (Sage and Kubien 2007), which is also reflected in an increase in Φ_{PSII} with increasing leaf temperature (Bernacchi et al. 2003). The stability of PSII (F_v/F_m), on the other hand, is not affected by leaf temperature, except at very high leaf temperature (above 40 °C) (Bernacchi et al. 2003).

The higher photosynthetic capacity (V_{cmax} and J_{max}) that occurs at warmer leaf temperatures does not always translate to an increase in A_{net} . Most capacity measurements are done at conditions that maximize diffusion of CO_2 to the chloroplast (such as moderate relative humidity), which is not always the case in the natural growth environment. An increase in air temperature with constant humidity generates an increase in vapor pressure deficit (VPD), which can cause stomata to close to conserve water (Berry and Bjorkman 1980). Similarly, high respiration and photorespiration rates at high leaf temperatures will also decrease A_{net} .

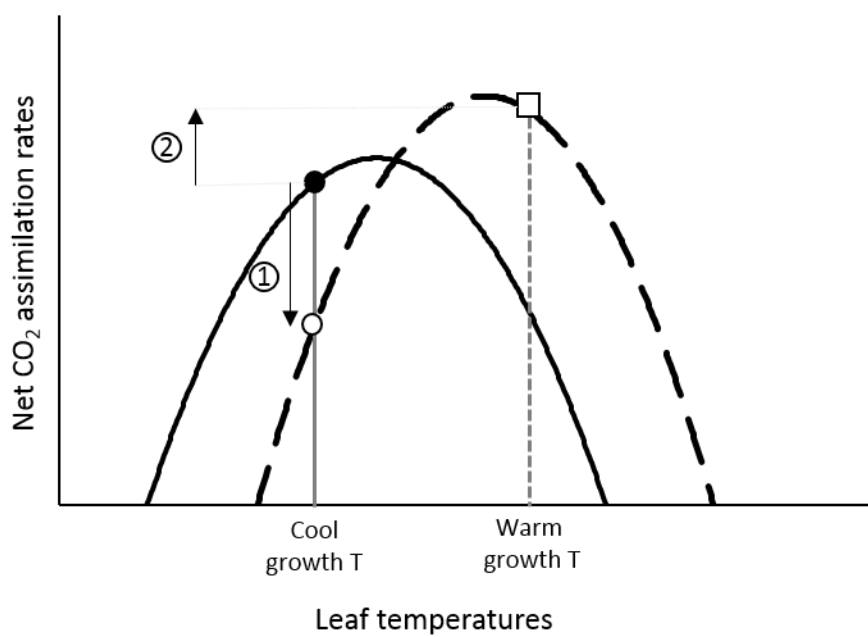


Figure 1.4 Net CO_2 assimilation rate (A_{net}) in response to acute changes in leaf temperature. The two curves represent a plant grown at a cooler growth temperature (solid curve) and one acclimated to a warmer growth temperature (long dashed curve). Two vertical lines indicate the cooler (solid line) and warmer growth temperature (short dash). Thermal acclimation of photosynthesis from a cooler grown plant to a warmer grown individual could include a shift in A_{net} at a common measurement temperature (1) or an increase in A_{net} at the respective growth temperatures (2). Filled symbols represent A_{net} from a cool-grown plant, and empty symbols from a warm-grown plant. Circles represent A_{net} measured at a common, cool temperature. Figure was modified from Way and Yamori (2013).

1.6.1.2 Acclimation to warmer growth temperature

Long-term exposure to a new growth conditions, including warmer temperatures, can result in adjustments in the photosynthetic apparatus. However, these thermal adjustments of photosynthesis do not always result in improved plant performance at the new growth condition. Berry and Bjorkman (1980), in their well-cited review, defined acclimation of photosynthesis as adjustments in the photosynthetic machinery that enhances performance at the new growth temperature. More recently, Way and Yamori (2013) outlined a number of ways to assess thermal adjustments, and demonstrated that thermal adjustments of photosynthesis can be constructive (i.e. increasing A_{net} at the new growth condition, as seen in Fig. 1.4) or detractive (i.e. reducing A_{net} at the new growth temperature). In addition to changes in mechanistic parameters such as V_{cmax} and J_{max} at a common basal temperature (usually 25 °C), thermal adjustment of photosynthesis usually results in the shift in temperature response curve of photosynthesis towards the new growth temperature (Fig. 1.4). The assessment of thermal acclimation of photosynthesis, therefore, include both the adjustments in the photosynthetic apparatus, assessed at a common set of conditions (A_{net} at a common leaf temperature, (1) in Fig. 1.4), and photosynthetic performance at the growth conditions (A_{net} at the respective growth temperature, (2) in Fig. 1.4), when the direct effects of leaf temperature are also included. In this study, the term acclimation refers to any adjustments in photosynthesis under a new suite of growth conditions, and is assessed by measuring A_{net} and photosynthetic capacity (V_{cmax} , J_{max}) under a common set of conditions and again at the growth conditions.

Both V_{cmax} and J_{max} have the capacity to acclimate to warmer growth temperature, as evidenced by an upward shift in the T_{opt} of both parameters in 36 plant species (Kattge and Knorr 2007). Acclimation to a warmer growth temperature usually involves an increase in electron transport capacity to supply the greater capacity of the dark reactions, and the production of a more heat-stable isoform of Rubisco activase in some species (Sage and Kubien 2007). When measured at, or extrapolated to, a leaf temperature of 25 °C, however, V_{cmax} and J_{max} in warm-grown plants do not always show an increase compared to cool-grown counterparts (Kattge and Knorr 2007, Way and Oren 2010, Way

and Yamori 2013). Meanwhile, there is little evidence of F_v/F_m , Φ_{PSII} , and ETR acclimating to increases in growth temperature (Bernacchi et al. 2003).

1.6.1.3 Plant growth and leaf structural responses to warming

Another challenge in plant physiology is scaling leaf-level fluxes to whole-plant carbon gain. All else being equal, biomass accumulation is the difference between the carbon gained from whole-canopy CO_2 assimilation and the carbon lost through respiration, photorespiration, root exudation, and volatile organic compounds. However, leaf-level photosynthesis, respiration, and transpiration also influence biomass allocation, plant water status, and canopy structure, among other processes, all of which can in turn affect the whole-plant growth pattern and act as feedbacks to leaf-level processes (Reynolds et al. 1993). A new growth condition can alter leaf-level processes and these interactions differently, causing a discrepancy between measurements of leaf-level photosynthesis and whole-plant biomass accumulation.

An example of the link between leaf-level and whole-plant performance is the response to growth at warmer temperatures. For example, warmer temperatures can stimulate leaf-level photosynthesis, but a lack of acclimation in respiration means higher respiratory losses could offset the increased carbon gain (Atkin et al. 2007). Warming experiments tend to have a positive effect on growth in deciduous species, although little change has been seen in biomass allocation in evergreen species (Way and Oren 2010). However, severe warming usually decreases total biomass due to the larger respiratory losses that occurs at high temperatures (Atkin et al. 2007). In terms of leaf morphology, while acclimation to low temperature results in thicker leaves, or a decrease in specific leaf area (SLA), warming has little effect on SLA, or any other leaf structural parameters (Poorter et al. 2009).

1.6.2 Elevated CO_2

1.6.2.1 Acute response to elevated CO_2

An increase in CO_2 concentration significantly stimulates photosynthesis for two reasons. First, elevated atmospheric CO_2 raises the intercellular CO_2 concentration, increasing the

supply of substrate for photosynthesis, which, under current ambient conditions, operates under CO₂ limitation. Thus, high CO₂ increases the rate of carboxylation, thereby increasing photosynthesis (Ainsworth and Rogers 2007). Secondly, an increase in CO₂ concentration also alters the relative concentrations of CO₂ and O₂, which inhibits photorespiration and further enhances A_{net} (Ainsworth and Rogers 2007). Exposure to elevated CO₂, therefore, tends to stimulate photosynthesis.

1.6.2.2. Acclimation to elevated growth CO₂

Longer-term exposure of plants to elevated CO₂ (weeks or longer) can result in an acclimation response (Curtis and Wang 1998). The stimulation of photosynthesis at high CO₂ generates a buildup of carbohydrates, which elicits a feedback inhibition that down-regulates photosynthesis (Arp 1991). Since CO₂ enrichment shifts the limitation of photosynthesis away from Rubisco, fewer resources, particularly N, are invested in Rubisco, resulting in a decrease in V_{cmax} (Medlyn et al. 2001). Overall, despite this down-regulation, the direct stimulation of photosynthesis under CO₂ enrichment via increases in substrate supply and suppressed photorespiration rates usually increases A_{net}, and therefore growth, although the magnitude of the stimulation varies among functional groups (Ainsworth and Long 2005). The acclimation response of photosynthesis is more pronounced in small-pot experiments (Arp 1991), or when N is limited (Ainsworth and Long 2005). In both cases, photosynthetic sink capacity is limited, eliciting a stronger feedback inhibition.

A decrease in stomatal conductance is also frequently observed in plants grown at elevated CO₂. Stomatal behavior is regulated by the CO₂ concentration in the intercellular air space; as a result, direct exposure to elevated CO₂ decreases stomatal opening (Ainsworth and Roger 2007). In addition, plants grown under elevated CO₂ may develop fewer stomata, decreasing stomatal conductance further. Thus, at elevated CO₂, water loss is reduced, and instantaneous water use efficiency (photosynthesis/transpiration) improves (Ainsworth and Long 2004).

1.6.2.3 Plant growth and leaf structural responses to elevated CO₂

Growth is commonly stimulated in plants grown under elevated CO₂, and this response can be sustained over multiple years (Ainsworth and Long 2005). Biomass allocation also shifts to belowground, increasing the root: shoot ratio (Curtis and Wang 1998), and leaf nitrogen concentrations decrease (Curtis 1996). Since the CO₂ diffusion limitation is reduced at high CO₂, leaves generally become thicker from either more starch accumulation or thicker mesophyll tissues (Arp 1991). As a result, SLA is usually reduced in leaves that develop under elevated CO₂ (Ainsworth and Long 2005).

1.6.3 Warming and elevated CO₂

Based on our separate understanding of photosynthetic response to warming and elevated CO₂, theoretically, the combination of the two factors is expected to stimulate photosynthesis. While high temperatures increase the rate of Rubisco oxygenation relative to carboxylation and increase photorespiration, elevated CO₂ alleviates this effect by increasing the concentration of CO₂. This interaction potentially modifies the response of photosynthesis to temperature, including increasing T_{opt} of net photosynthesis and A_{net} itself (Long 1991). Even when the down-regulation of A_{net} to elevated CO₂ is taken into account, a combination of increased growth temperature and elevated CO₂ is expected to result in higher photosynthetic rates. In addition, because sink capacity increases at warmer temperatures, the feedback inhibition that down-regulates photosynthesis at elevated CO₂ is reduced (Morison and Lawlor 1999). In a meta-analysis by Wang et al. (2012), A_{net} was indeed higher in plants grown at warmer temperature and elevated CO₂; however, the magnitude of this response was variable among plant functional groups.

It is difficult to generalize whole-plant growth responses to high temperature and elevated CO₂ from leaf-level photosynthesis. Stomatal behavior, whole-plant respiration rates, plant developmental stage, and partitioning of carbohydrates can influence biomass accumulation in plants grown under warming and elevated CO₂ (Morison and Lawlor 1999). The interactive effect of temperature and CO₂ on these processes, therefore, is not often characterized in meta-analyses (Morison and Lawlor 1999, Wang et al. 2012).

1.7 Photosynthesis and leaf anatomy in *D. antarctica* and *C. quitensis*

1.7.1 Photosynthesis in *D. antarctica* and *C. quitensis*

Studies of photosynthesis in the two Antarctic vascular plant species began only recently. Overall, these studies highlight the two species' ability to operate at sub-zero temperatures and their poor performance at temperatures above 20 °C. Xiong et al. (1999) demonstrated that both *D. antarctica* and *C. quitensis* could carry out photosynthesis at 0 °C, and that they had a temperature compensation point below freezing. Long-term exposure (60-85 days) to either sub-optimal (7 °C), near-optimal (12 °C), or supra-optimal (20 °C) temperatures produced no shift in the T_{opt} of A_{net} , although A_{net} in plants grown at 20 °C was suppressed compared to plants grown at 12 °C (Xiong et al. 2000). The direct stimulation of photosynthesis by increasing leaf temperature, as well as the full thermal acclimation of dark respiration, resulted in an increase in biomass and leaf production at warmer temperatures in both species (Xiong et al. 2000). However, both species performed poorly, with negligible A_{net} on warm, sunny days when air temperature was above 20 °C (Xiong et al. 1999).

Antarctica is directly affected by ozone depletion and increased UV radiation; therefore, many studies have investigated the effects of UV-A and UV-B on photosynthesis in *D. antarctica* and *C. quitensis* (Rozema et al. 2005). These studies found decreased growth under UV-B, but no direct effect on A_{net} (Day et al. 1999, Montiel et al. 1999, Ruhland and Day 2000, Xiong and Day 2001). In response to the damage on PSII of the upper mesophyll cells from UV-B, Antarctic plants produce thicker, denser leaves to maintain the same A_{net} for the same leaf area (Xiong and Day 2001).

1.7.2 Leaf anatomy of *D. antarctica* and *C. quitensis*

1.7.2.1 *D. antarctica*

The leaf epidermal structure of *D. antarctica* is very typical of xerophytic plants from polar regions, with a thick cuticle layer on the abaxial (outside) epidermis, small epidermal cells, and high stomatal density (Romero et al. 1999). Stomata concentrate in stomatal grooves, sunken areas between ribs that run along the length of the leaf blade. Leaves of *D. antarctica* are usually inwardly folded towards the adaxial, or inner,

epidermis. The folding is also typical of grasses grown in dry habitats, and facilitated by large bulliform cells on the adaxial epidermis. Cross sections of leaves reveal high cell density, and two layers of cells surrounding the vascular bundle. Above the abaxial epidermis are bundles of sclerenchymatic fibers, which are small cells with thick cell walls (Romero et al. 1999, Gielwanowska and Szczuka 2005).

D. antarctica leaf morphology and anatomy vary with changes in habitat, despite a lack of genetic variation, indicating a high degree of plasticity (Chwedorzewska et al. 2008). Comparisons of leaf structure among plants from different habitats, either naturally-occurring or in experiments, show plasticity in leaf shape, thickness, size, cell shapes and density. For example, bulliform cells are smaller or completely absent in plants from drier habitats, and this is directly associated with more folded leaf blades (Gielwanowska et al. 2005, Chwedorzewska et al. 2008). Very dry conditions result in a smaller leaf surface, smaller and denser epidermal cells, the absence of the second layer around the vascular bundle, and thicker leaves with denser mesophyll cells (Romero et al. 1999). The leaf ultrastructure also shows plasticity with environmental factors, including the organization and shape of the chloroplast, mitochondria, and endoplasmic reticulum inside mesophyll cells (Gielwanowska et al. 2005).

1.7.2.2 *C. quitensis*

C. quitensis leaves are thick and anatomically typical of dicotyledon leaves. Stomata occur on both sides of the leaves, but are more prevalent on the adaxial side. Underneath the adaxial epidermis are rectangular palisade mesophyll cells, arranged into rows with extensive intercellular air space to facilitate CO₂ diffusion through the stomata to mesophyll cells. Stomata on the abaxial side are mostly close to the leaf margins. Unlike *D. antarctica*, *C. quitensis* shows little sign of xeromorphy, with no wax layer on the epidermis and no tight enclosure of the vascular bundle (Mantovani and Vieira 2000). The cushion-like growth form of *C. quitensis* potentially moderates the cold and dry growth conditions, alleviating the pressure to develop xeromorphic leaf structures (Gianoli et al. 2004). In addition, the leaf structure of *C. quitensis* is under stronger genetic control, with plants forming different ecotypes in Antarctica compared to the

Andes. Plants collected from Antarctica have shorter and wider leaves, thicker mesophyll, and larger chloroplasts compared to plants from the Andes when both are grown in the same conditions (Gianoli et al. 2004, Bascuñán-Godoy et al. 2010).

1.8 Objectives

Deschampsia antarctica and *Colobanthus quitensis* are the only vascular plant species native to Antarctica, and they have existed in a very stable climate since the Last Glacial Maximum. The recent rise in temperature is correlated with a positive effect on growth in both species, and Smith (1994) suggests using these species as bioindicators of the abiotic changes on the continent. However, the mechanisms underlying the positive effect of climate change on both species are still not fully understood, and certainly not enough to predict future performance of the two species as temperatures and atmospheric CO₂ concentrations continue to rise.

In addition, the growing population size of these species has been mostly attributed to warming, with little consideration of the rise in atmospheric CO₂ over the same time period. There have been no studies to date investigating the effect of elevated CO₂ on photosynthesis and growth of *D. antarctica* or *C. quitensis*. Since CO₂ enrichment can also stimulate photosynthesis, understanding the response of these two species to elevated CO₂, as well as the interaction between warming and elevated CO₂, can provide useful insights into the plasticity of the photosynthetic apparatus of the two species. In addition, this knowledge could strengthen our understanding of the mechanisms underlying the improved performance of the two species in the field, and improve predictions of their performance in future climates.

Commonly found in the same area, *D. antarctica* and *C. quitensis* possess some similar strategies to survive the harsh conditions of Antarctica. However, each species still differs in growth form, cold resistant strategies, leaf morphological structure, and other traits that could potentially influence its response to future climates. Therefore, comparing and contrasting the responses of the two species to elevated temperatures and CO₂ will also inform predictions of their relative success, the success of non-native

species introduced to the continent, and potential shifts in the terrestrial ecosystem of Antarctica.

My thesis investigates the responses of *D. antarctica* and *C. quitensis* to warming and elevated CO₂, including the acclimation potential of photosynthesis, leaf-level photosynthetic performance, as well as modifications in leaf structure under a range of future growth conditions. I aim to answer two key questions:

- 1) How does photosynthesis of *D. antarctica* and *C. quitensis* respond to elevated growth temperature and CO₂?
- 2) How does leaf anatomy of *D. antarctica* and *C. quitensis* respond to elevated growth temperature and CO₂?

The literature regarding the acclimation potential of photosynthesis and leaf anatomy in *D. antarctica* and *C. quitensis* to changes in the growth conditions does not provide enough background to predict the response of these two species to warming and elevated CO₂.

CHAPTER 2: MATERIAL AND METHODS

2.1 Experimental design

Three hundred individual plants of each of two species, *Deschampsia antarctica* Desv. (Antarctic hairgrass) and *Colobanthus quitensis* (Kunth) Bartl. (Antarctic pearlwort), were initially collected from King George Island (62 ° 09 ' S; 58 ° 28 ' W), where average austral summer and winter temperatures are 1.09 °C and -7 °C, respectively (Ferron et al. 2004). Collected plant specimens were maintained in growth chambers at the Universidad de la Frontera, in Temuco, Chile before being transported to the University of Western Ontario in November 2014. Plants were wrapped in moist paper towels, sealed in Ziploc bags, and transported in Styrofoam boxes kept cool with ice packs. Leaves from *D. antarctica* individuals were trimmed at 1 cm above the base to facilitate leaf regrowth, and individuals from both species were weighed for pre-treatment mass. Plants were then transplanted into 20-cm diameter pots (2.42 L) (20 individuals of one species per pot) in a medium made of 3:1:1 (v:v:v) black loam: peat moss: vermiculite. Plants were kept in a walk-in growth chamber (Environmental Growth Chambers, Chagrin Falls, OH) at 12 °C and 350 $\mu\text{mol photons m}^{-2} \text{s}^{-1}$ and 10-hour daylight to establish under conditions that minimized the stress incurred during the transport and handling period.

One week later, five individuals of each species were planted into 10-cm diameter pots (0.5 L) with a medium of 3:1:1 (v:v:v) black loam: peat moss: perlite. Ten pots of each species were placed in one of six experimental rooftop greenhouses in the Biotron Center for Experimental Climate Change Research (Fig. 2.1). The experiment was a full-factorial design with three target temperatures (11.5 °C, 15.5 °C, and 19.5 °C, referred to as 12 °C, 16 °C, or 20 °C treatments) in combination with either an ambient (400 ppm CO₂, referred to as AC) or elevated (750 ppm CO₂, referred to as EC) atmospheric CO₂ concentrations. The six treatments are referred to from now on as 12/AC, 16/AC, 20/AC, 12/EC, 16/EC, and 20/EC. The humidity was maintained between 60 and 80%, facilitated by misters. The greenhouses received natural light, with a set of curtains that engaged from 10 am to 2 pm daily, reducing light intensity by 50-80% compared to outside to maintain temperature control. Therefore, light levels reached a maximum of 2450 μmol

photons $\text{m}^{-2} \text{s}^{-1}$ during April, with an average midday light levels of $650 \mu\text{mol photons m}^{-2} \text{s}^{-1}$ over the six-month period. Temperature, CO_2 concentrations, and humidity were controlled and monitored by an Argus Control System (Argus Control System Ltd, Surrey, BC), and measured every minute. Pots were placed in a net box built with a wooden frame and white net to prevent insect attack. The netting reduced the light intensity by 16%. Plants were watered as needed to maintain a moist medium, and fertilized with half-strength Hoagland's solution once a week.

2.2 Gas exchange measurements

After six months in the experimental conditions, gas exchange measurements were performed on new, fully expanded leaves of both species using a LI-6400 XT portable photosynthesis system (LiCor, Lincoln, NE). Net CO_2 assimilation rate (A_{net}) was measured across a range of intercellular CO_2 concentrations (C_i) (producing an A- C_i curve) at a saturating light level of $1000 \mu\text{mol photons m}^{-2} \text{s}^{-1}$, and a vapor pressure deficit between 1.2 and 1.6 kPa. Measurements were sequentially made at the following CO_2 concentrations: 400, 300, 200, 100, 50, 400, 750, 900, 1200, 1500, 2000, and 2200 ppm. For each species in each treatment, six A- C_i curves were measured at 16°C , and in the case of the 12°C and 20°C treatments, another six A- C_i curves were assessed at their growth temperatures (12°C or 20°C , respectively). This allowed gas exchange parameters to be assessed across treatments both at a common temperature of 16°C (to determine the degree of acclimation) and at the growth temperature (to determine performance in the growth environment).

During the A- C_i measurements, A_{net} was recorded at each CO_2 concentration, and a high-intensity short flash of irradiance was applied to the leaf to measure light-adapted chlorophyll fluorescence. At the end of each A- C_i curve, the leaf material was kept in the dark at 400 ppm CO_2 to minimize post-illumination bursts of CO_2 release (Atkin et al. 1998). After 20 minutes, dark-adapted chlorophyll fluorescence and dark respiration rates were assessed at 400 ppm CO_2 , then again at 750 ppm CO_2 . After the gas exchange measurements were complete, the leaf material in the gas exchange cuvette was harvested, images of the leaves laid out on a white surface were taken, and leaf samples

were dried at 60 °C until they reached a constant mass for assessment of dry mass. The leaf images were analyzed using ImageJ software (US National Institutes of Health, Bethesda, MD) for leaf area. Specific leaf area (SLA, leaf area/ leaf dry mass) was also calculated.

Measured A_{net} values were corrected for diffusion due to differences in the CO_2 concentration between the ambient atmosphere and inside the cuvette (as per Bruhn et al. 2002). A- C_i curves were used to derive maximum Rubisco carboxylation rates (V_{cmax}) and maximum electron transport rates (J_{max}) using the Farquhar et al. (1980) photosynthetic model. The model assumed infinite mesophyll conductance and used the Michaelis-Menten constants for Rubisco carboxylation (K_c) and oxygenation (K_o) and the CO_2 compensation point in the absence of mitochondrial respiration (Γ^*) from tobacco (von Caemmerer et al. 1994); these parameters were adjusted for leaf temperature based on the equations of Bernacchi et al. (2002).

A_{net} values at 400 ppm CO_2 and growth CO_2 were also extracted from the gas exchange. Using the chlorophyll fluorescence data, the maximal efficiency of photosystem II (F_v/F_m), photochemical quantum yield of photosystem II (Φ_{PSII}), and electron transport rate (ETR) were determined at both 400 and 750 ppm CO_2 to allow a comparison of these parameters at a common CO_2 concentration of 400 ppm and at the growth CO_2 concentration. Dark respiration rates (R_{dark}) are only reported at 400 ppm CO_2 , as short-term changes in CO_2 concentration do not affect R_{dark} (Amthor 2000), and diffusion artifacts in measurements made at elevated CO_2 conditions resulted in unrealistic values.

2.3 Biomass and C/N analysis

At the end of the measurement campaign, all plant material was harvested. Since the cushion-like growth form of *C. quitensis* did not allow for distinguishing individual plants from each other, aboveground and belowground biomass were harvested, dried at 60 °C to a constant mass and weighed for each individual pot. For *D. antarctica*, aboveground biomass was obtained for individual plants, but belowground biomass was assessed per pot because the root biomass could not be allocated to individual plants.

Biomass analysis was pooled on a pot basis for both species, because analysis of *D. antarctica* biomass on an individual plant basis yielded the same results as the pot level aggregated data (data not shown).

Dried leaves from five plants per species per treatment were sampled for carbon and nitrogen analysis. Leaf samples were ground with a Wiley mill (Thomas Scientific, Swedesboro, NJ), weighed, and sent to Duke Environmental Stable Isotope Laboratory to obtain foliar percentage of carbon (C) and nitrogen (N) using a Carlo Erba NA 1500 Elemental Analyzer (CE Elantech, Inc., Lakewood, NJ). Leaf C:N ratios were then calculated.



Figure 2.1. Images of *Deschampsia antarctica* (left) and *Colobanthus quitensis* (right) in the experiment. Lines at bottom right indicate 1 cm.

2.4 Light microscopy

Fresh leaf samples were collected in May 2015 for light microscopy from five plants per species per treatment. For *D. antarctica*, 1 cm sections of the leaf blade from the middle

of the leaf length were collected; for *C. quitensis*, entire, fully developed leaves were harvested. Leaf samples were fixed in 90:5:5 (v:v:v) FAA (formaldehyde: acetic acid: alcohol) for 48 hours, washed in Sorensen's phosphate buffer (0.1 M, pH 7.2), and stored in 70% ethanol. Once ready for processing, samples were rehydrated through a series of solutions with decreasing ethanol concentrations. Individual leaf sections were placed in a plastic mold with 1% agarose to help orient the samples in a paraffin mold. Each sample was cut into 2-3 mm sections, placed in paraffin cassettes submerged in 70% ethanol, and embedded in paraffin wax.

After being paraffin-embedded and sectioned with a rotating microtome, sections were mounted on slides, deparaffinized with xylene, rehydrated to water, and stained with 0.05% toluidine blue O. After briefly dehydrating in ethanol and clearing in xylene, stained slides were mounted with Permount™ mounting medium. Slides were then viewed under a light microscope (Nikon Eclipse Ci, Melville, NY), and images captured with a digital camera (Nikon DS Ri2, Melville, NY) and analyzed using ImageJ software (US National Institutes of Health, Bethesda, MD).

Images were analyzed for the proportional area of the leaf cross-section accounted for by mesophyll cells, vascular bundles, abaxial and adaxial epidermal cells, and intercellular air space. These proportional measurements were performed using a system of randomly generated points projected onto the captured image. The proportion of points falling on each type of tissue corresponds to the proportion of area in the cross-section occupied by the type of tissue (Parkhurst 1982). In order to verify the accuracy of the random point method, a subset of six images per species was also analyzed by tracing out and measuring the area of each tissue type on the cross-sectional area. Fig. 2.2 illustrates the comparison between measurements from the random point method and those taken from manually tracing each tissue type. Because the random point method produced similar estimates to the traced proportion above 579 points/mm² in *D. antarctica*, and above 434 points/mm² in *C. quitensis* (Fig. 2.2), images of *D. antarctica* cross-sections were analyzed at 600 points/mm², and *C. quitensis* images at 450 points/mm².

In addition to the proportional estimates of the tissue types, each image from both species was measured for leaf thickness, width, and thickness to width ratio. On images of *D.*

antarctica, stomatal grooves were also characterized. Stomatal grooves are sunken areas on the leaf surface that run longitudinally along the length of the grass blade and contain a high concentration of stomata. They serve to reduce water loss by increasing the tortuosity of the diffusion path for water from the intercellular airspaces into the air outside the leaf boundary layer. Each stomatal groove was measured for the width of the opening, groove depth, and the ratios of groove area to groove perimeter were calculated, assuming each groove is a half-ellipse with groove depth being the major axis, and width the minor axis.

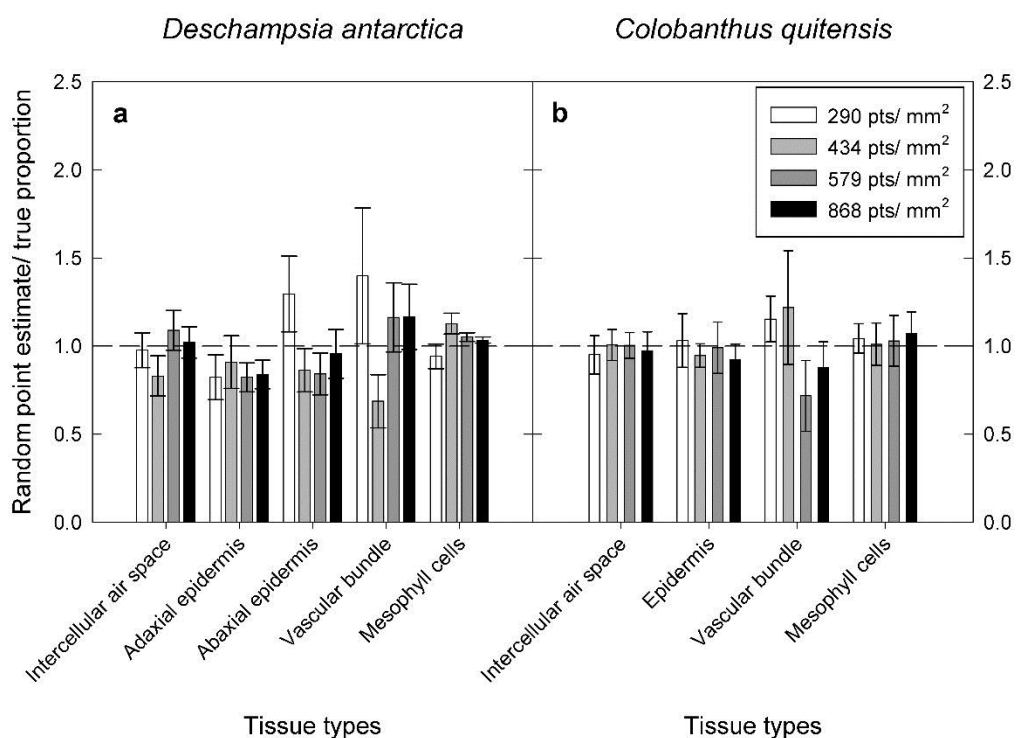


Figure 2.2. Ratios of random point proportional estimates of leaf cross-sectional area filled by a given tissue type to the true proportion taken from tracing individual tissues in a) *Deschampsia antarctica* and b) *Colobanthus quitensis*. Data reported are ratios of proportional estimates of each tissue type using random point method to their individually traced proportions. Bars depict means \pm SE, N = 6. Different bar colors indicate different point densities. Dashed line indicates a ratio of 1, where the two

methods yield the same results. Based on these data, image analyses were done using 600 points/mm² for *D. antarctica*, and 450 points/mm² for *C. quitensis*.

2.5 Aphid attack

In late March 2014, an aphid outbreak occurred in the 12/AC greenhouse. The aphids specifically targeted *C. quitensis*, and a pyrethrin-based insecticide was used to control the outbreak (Schultz Houseplant and Garden Insecticide, Spectrum Brands, Madison, WI). However, by the time gas exchange measurements were performed, *C. quitensis* individuals from this treatment still looked unhealthy, and gas exchange measurements showed 40-50% higher photosynthetic capacities (V_{cmax} , J_{max} , Φ_{PSII} , ETR) than the remaining treatments. This appears to be a compensatory response common in plants under insect attack, rather than a treatment response. Remaining leaves of plants attacked by insects show greater photosynthetic capacity as a result of changes in the source-sink balance (Trumble et al. 1993; Thomson et al. 2003; Franzen et al. 2007). As a result, all data of *C. quitensis* from the 12/AC treatment were removed from the rest of the analysis.

2.5 Statistical analysis

For each species, two-way ANOVAs were performed on individual variables of interest against temperature, CO₂, and the interaction of temperature and CO₂. A Tukey's HSD posthoc test was performed when there was a significant treatment effect. In the case of *C. quitensis*, the elimination of one treatment resulted in an unbalanced design, so the two-way ANOVAs were run using Type II sum of square calculations. Statistical analyses were performed using R software.

CHAPTER 3: RESULTS

Fig. 3.1 shows the air temperature and CO₂ concentrations recorded in the six treatment chambers over the experimental period. From November 2014 to April 2015, temperature control in each treatment was consistently within 7% of the target temperature, except for the 12 °C treatments, where temperature was slightly more variable (Fig. 3.1a). CO₂ control in the ambient CO₂ (AC) and elevated CO₂ (EC) treatments remained consistently within 15% of the target CO₂ concentration, except for a brief period in early January when CO₂ control failed in all EC treatments (Fig. 3.1b).

3.1 Photosynthetic response to warming and elevated CO₂

Net CO₂ assimilation rates at saturating light (A_{net}) were used as a proxy for photosynthetic rate, and were measured under various combinations of conditions (data shown in Fig. 3.2) to assess *D. antarctica*'s photosynthetic performance. First, A_{net} measured at a common temperature of 16 °C and CO₂ concentration of 400 ppm (Fig. 3.2a) allows assessment of acclimation of photosynthesis to the treatment conditions through any statistically significant response to growth temperature or CO₂. A_{net} in *D. antarctica* measured at this set of conditions showed a 25.6% decrease in response to elevated growth CO₂ ($p = 0.009$) and no response to growth temperature ($p = 0.61$, Fig. 3.2a), suggesting a down-regulation of photosynthesis at elevated CO₂, but no thermal acclimation. The significant response to elevated CO₂, however, did not manifest in the Tukey's HSD post-hoc test due to the smaller sample size of the individual treatments compared to that used to evaluate treatment effects. The interpretation of the treatments effects in this chapter, therefore, will focus on the temperature or CO₂ response from the ANOVA, and the Tukey's post-hoc test will be highlighted when a significant interaction is identified.

Because A_{net} was also expected to respond to direct changes in measurement temperature, the response of A_{net} measured at the growth temperature and a common CO₂ concentration demonstrated the combined effects of acclimation to growth temperature and the direct response to leaf temperature. Fig. 3.2b showed a marginally significant

effect of temperature on A_{net} in *D. antarctica* ($p = 0.06$) due to the stimulation of photosynthesis at high leaf temperature alone, as A_{net} showed no acclimation to growth temperature ($p = 0.61$, Fig. 3.2a). Likewise, A_{net} is known to also respond to measurement CO_2 ; therefore, comparing treatment effects, especially the CO_2 response of photosynthesis, among plants measured at a common temperature of $16\text{ }^\circ\text{C}$ and their growth CO_2 concentration allowed evaluation of the combined effects of acclimation to growth CO_2 and the direct response to high measurement CO_2 on A_{net} . This comparison showed that the down-regulation of A_{net} in EC treatments (Fig. 3.2a) was overwhelmed by the direct stimulatory effect of high measurement CO_2 on photosynthesis, resulting in a 54% increase in A_{net} in leaves grown and measured at EC treatments compared to AC ($p < 0.001$, Fig. 3.2c). Finally, all plants could be measured at their growth temperature and growth CO_2 to assess their actual performance in the treatment conditions. In their growth environment, A_{net} was stimulated by 57.7% at elevated growth CO_2 ($p < 0.001$), mostly due to the direct CO_2 effects on photosynthesis, in addition to a positive temperature response that was due to high measurement temperature ($p = 0.014$, Fig. 3.2d). The same pattern is used to summarize the trends in A_{net} , V_{cmax} , J_{max} , and ETR in both species.

In *C. quitensis*, A_{net} measured at a common condition of $16\text{ }^\circ\text{C}$ and 400 ppm CO_2 showed a small degree of acclimation to growth temperature ($p = 0.027$) and no acclimation to growth CO_2 ($p = 0.13$, Fig. 3.3a). The acclimation to growth temperature in A_{net} resulted in $16\text{ }^\circ\text{C}$ treatments having the highest A_{net} (Fig. 3.3a). However, this response was offset by the positive response of A_{net} to increasing measurement temperature, as there were no longer temperature effects in A_{net} measured at the growth temperature ($p = 0.14$, Fig. 3.3b). In contrast, the direct effect of high CO_2 concentration led to a 46% stimulation of A_{net} in EC treatments measured at their growth CO_2 ($p = 0.012$, Fig. 3.3c). As a result, when all treatments were measured at their growth temperature and CO_2 , A_{net} significantly increased in EC plants as a result of the direct CO_2 effect on photosynthesis ($p < 0.001$, Fig. 3.3d).

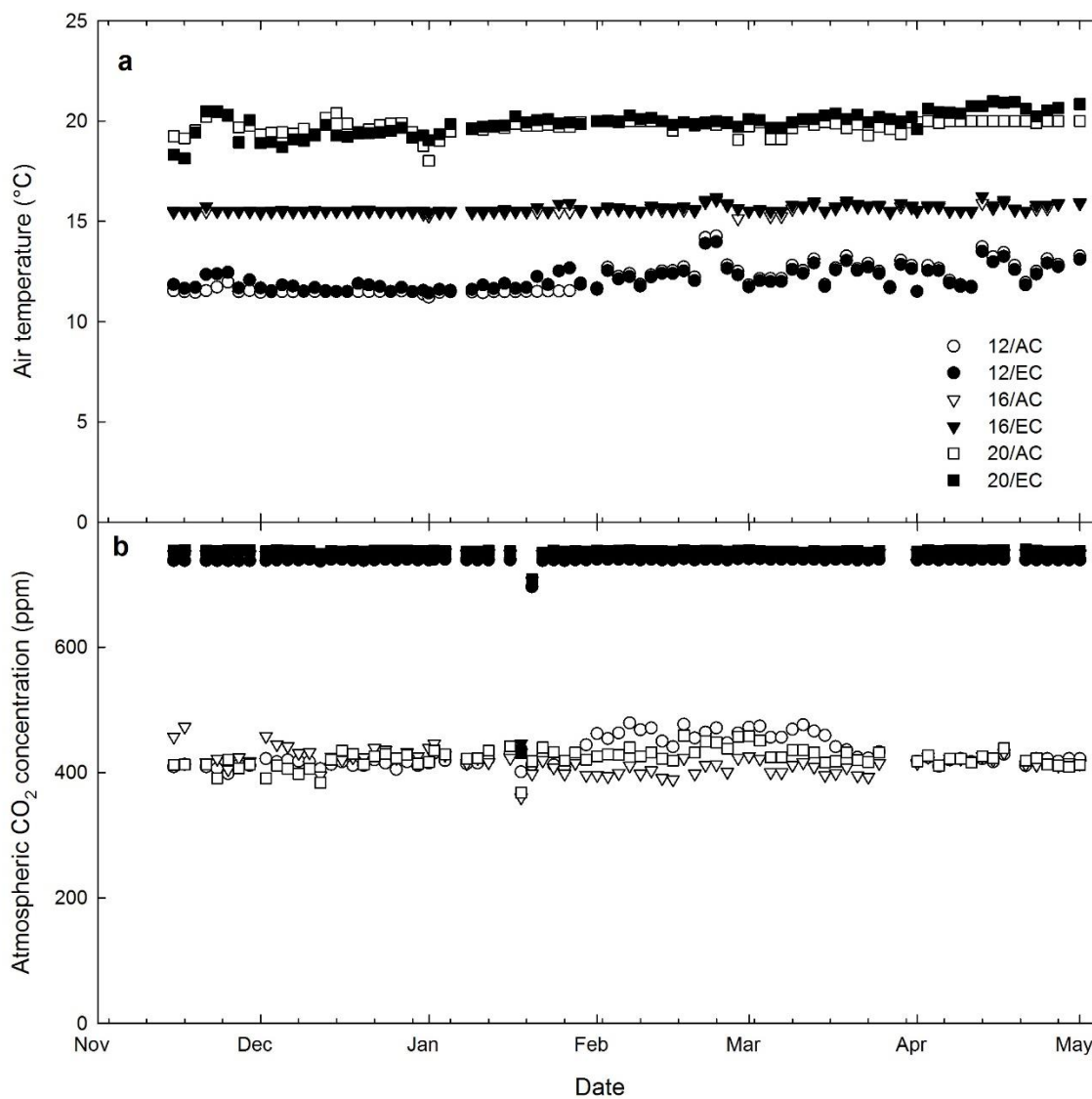


Figure 3.1 Average a) air temperature and b) atmospheric CO₂ concentrations every two days in six treatments from November 2014 to May 2015. Circles represent 12 °C treatments, triangles represent 16 °C treatments, and squares represent 20 °C treatments (20). Empty symbols represent treatments experiencing ambient CO₂ concentration (400 ppm, AC), and filled symbols represent elevated CO₂ concentration (750 ppm, EC).

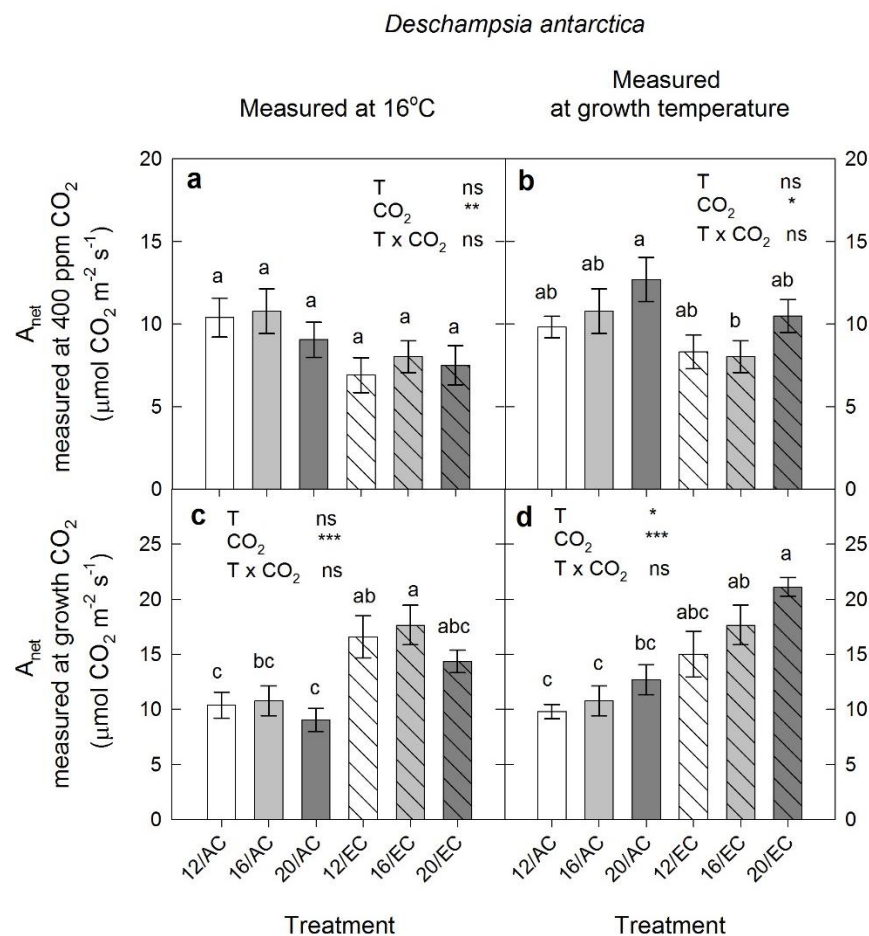


Figure 3.2 Net CO₂ assimilation rate (A_{net}) of *Deschampsia antarctica* at saturating light measured at: a) 400 ppm CO₂ and leaf temperature of 16 °C; b) 400 ppm CO₂ and growth temperature; c) growth CO₂ concentration and leaf temperature of 16 °C; and d) growth CO₂ concentration and growth temperature. Bars depict means \pm SE, N = 6. White bars represent growth temperature of 12 °C, grey bars represent growth temperature of 16 °C, and dark grey bars represent growth temperature of 20 °C. Empty bars represent ambient growth CO₂ (400 ppm CO₂, AC) and hashed bars represent elevated growth CO₂ (750 ppm CO₂, EC). For each graph, the effect of growth temperature (T), growth CO₂ (CO₂) and the interaction of temperature and CO₂ (T x CO₂) is shown: ns indicates no significant difference, * indicates $p < 0.05$, ** indicates $p < 0.01$, and *** indicates $p < 0.001$. Means with different letters are significantly different (Tukey's HSD, $p < 0.05$).

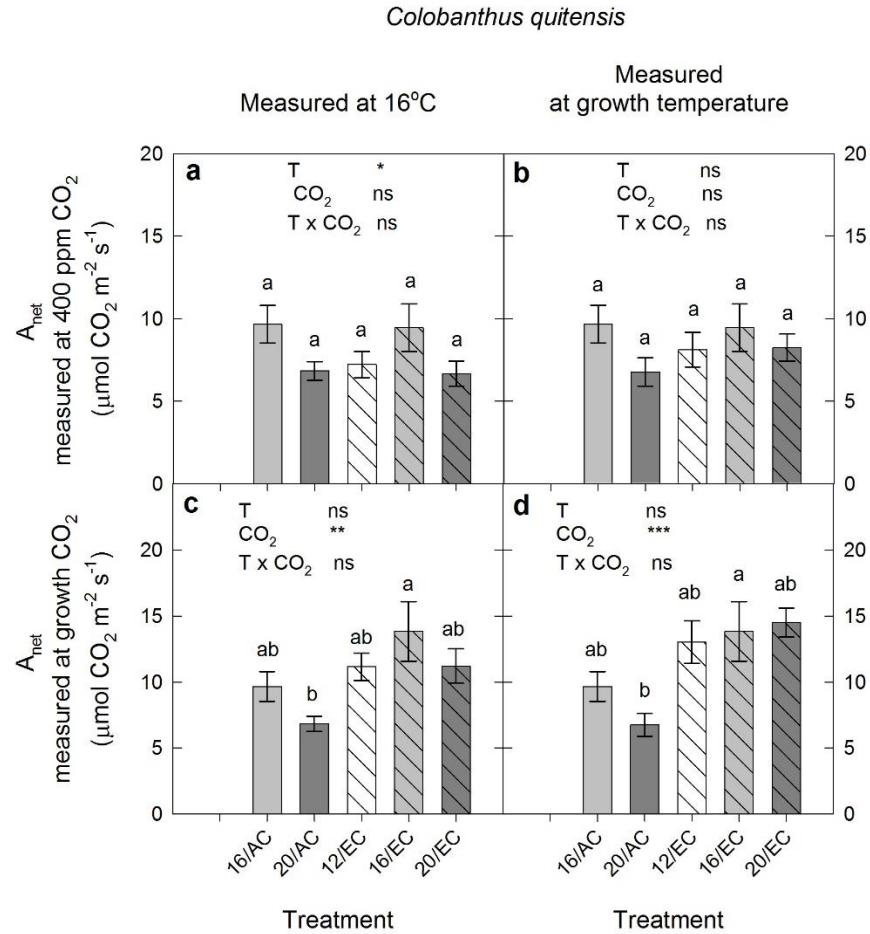


Figure 3.3 Net CO₂ assimilation rate (A_{net}) of *Colobanthus quitensis* at saturating light measured at: a) 400 ppm CO₂ and 16 °C; b) 400 ppm CO₂ and growth temperature; c) growth CO₂ and 16 °C; and d) growth CO₂ and growth temperature. Bars depict means \pm SE, N = 6. White bars represent growth temperature of 12 °C, grey bars represent growth temperature of 16 °C, and dark grey bars represent growth temperature of 20 °C. Empty bars represent ambient growth CO₂ (400 ppm CO₂, AC) and hashed bars represent elevated growth CO₂ (750 ppm CO₂, EC). For each graph, the effect of growth temperature (T), growth CO₂ (CO₂) and the interaction of temperature and CO₂ (T x CO₂) is shown: ns indicates no significant difference, * indicates $p < 0.05$, ** indicates $p < 0.01$, and *** indicates $p < 0.001$. Means with different letters are significantly different (Tukey's HSD, $p < 0.05$).

Maximum Rubisco carboxylation rates (V_{cmax}) and maximum electron transport rates (J_{max}) were derived over a range of CO_2 concentrations to highlight changes in either carboxylation or RuBP regeneration capacities under the new growth environment. In *D. antarctica*, neither V_{cmax} nor J_{max} acclimated to growth temperature ($p > 0.35$ for both) or growth CO_2 ($p = 0.5$ for both), as assessed at a common temperature (Figs. 3.4a, c). The ratio of these two highly correlated parameters (the $V_{\text{cmax}}:J_{\text{max}}$ ratio), on the other hand, gives insights into the balance between carboxylation and RuBP regeneration. The $V_{\text{cmax}}:J_{\text{max}}$ ratios did not acclimate to either growth temperature ($p = 0.57$) or growth CO_2 ($p = 0.90$, Fig. 3.4e). However, growth temperature stimulated both V_{cmax} ($p < 0.001$) and J_{max} ($p = 0.006$), implying a direct effect of measurement temperature on photosynthetic capacity (Figs. 3.4b, d). The $V_{\text{cmax}}:J_{\text{max}}$ ratio increased with increasing measurement temperature ($p = 0.004$, Fig. 3.4f), due to the larger magnitude of the response in V_{cmax} (103.5%) than J_{max} (72.5%) across an 8 °C change in measurement temperature.

Photosynthetic capacity in *C. quitensis* also showed no acclimation to growth temperature or CO_2 in V_{cmax} ($p > 0.61$ for both, Fig. 3.5a), J_{max} ($p > 0.67$ for both, Fig. 3.5c), the $V_{\text{cmax}}:J_{\text{max}}$ ratio ($p > 0.11$ for both, Fig. 3.5e). There was no direct effect of growth temperature on V_{cmax} or J_{max} ($p > 0.27$ for both, Figs. 3.5b, d); however, $V_{\text{cmax}}:J_{\text{max}}$ responded positively to growth temperature ($p = 0.019$), implying V_{cmax} responded to increasing leaf temperature to a greater extent than did J_{max} (Fig. 3.5f).

The maximal photochemical efficiency of PSII (F_v/F_m) was obtained from chlorophyll fluorescence measurements of dark-incubated leaves. F_v/F_m values between 0.76 and 0.82 indicate healthy leaves, and values below this range suggest leaves under stress (Maxwell and Johnson 2000). *D. antarctica* showed no effect of growth temperature ($p = 0.39$) or growth CO_2 ($p = 0.25$) on the maximal photochemical efficiency (Table 3.1). The values of F_v/F_m , however, were between 0.70 and 0.77, suggesting that photochemical efficiency of PSII generally operated at less-than optimal levels, but was not affected by the treatment conditions (Table 3.1). In *C. quitensis*, F_v/F_m values were significantly lower in the 20/EC treatment, resulting in a significant interaction between growth temperature and CO_2 ($p = 0.001$), but all F_v/F_m values were still within the range of healthy leaves (Table 3.1). The variations, therefore, likely had no biological significance.

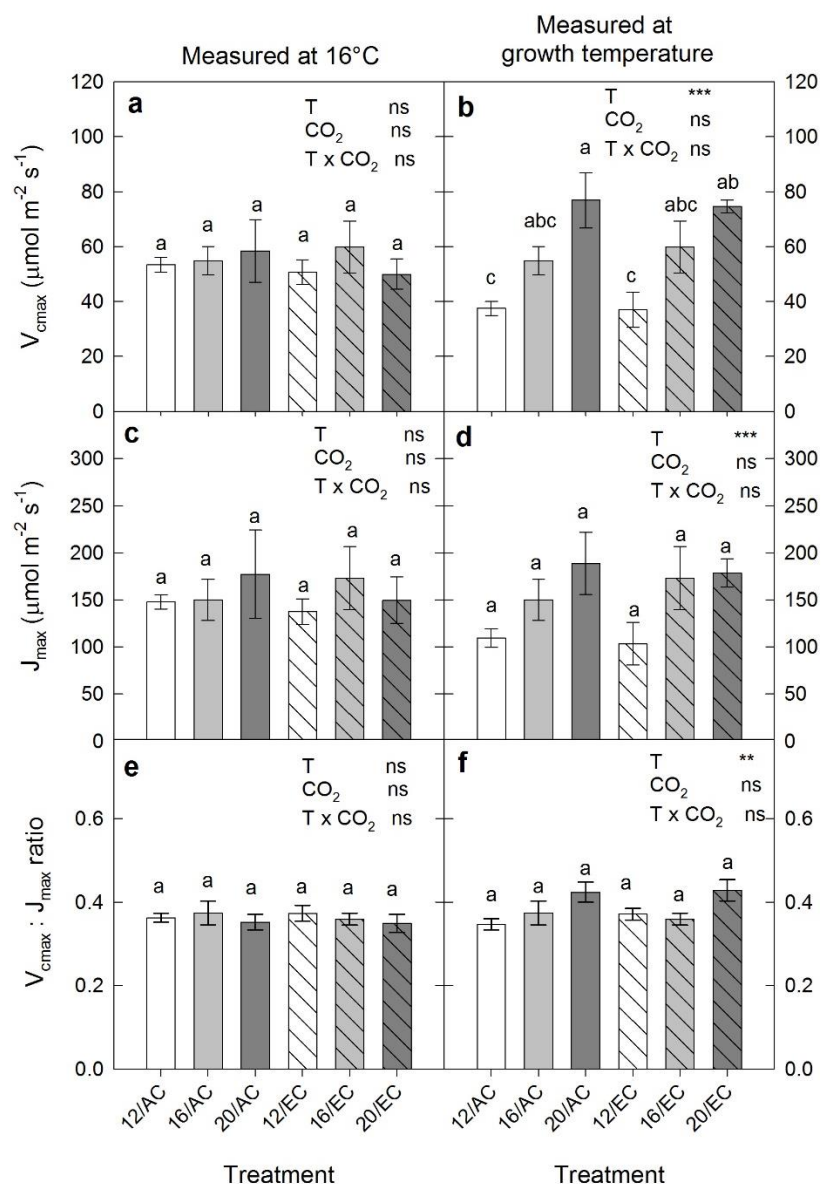
Deschampsia antarctica

Figure 3.4 a-b) Maximum Rubisco carboxylation rate (V_{cmax}), c-d) maximum electron transport rate (J_{max}), and e-f) V_{cmax} to J_{max} ratio of *D. antarctica* measured at leaf temperature of 16 °C (a, c, e) and growth temperature (b, d, f). Bars depict means \pm SE, N = 6, except for 12/EC (N = 5), and 16/AC (N = 4). White bars represent growth temperature of 12 °C, grey bars represent growth temperature of 16 °C, and dark grey bars represent growth temperature of 20 °C. Empty bars represent ambient growth CO₂ (400 ppm CO₂, AC) and hashed bars represent elevated growth CO₂ (750 ppm CO₂, EC).

For each graph, the effect of growth temperature (T), growth CO₂ (CO₂) and the interaction of temperature and CO₂ (T x CO₂) is shown: ns indicates no significant difference, * indicates $p < 0.05$, ** indicates $p < 0.01$, and *** indicates $p < 0.001$. Means with different letters are significantly different (Tukey's HSD, $p < 0.05$).

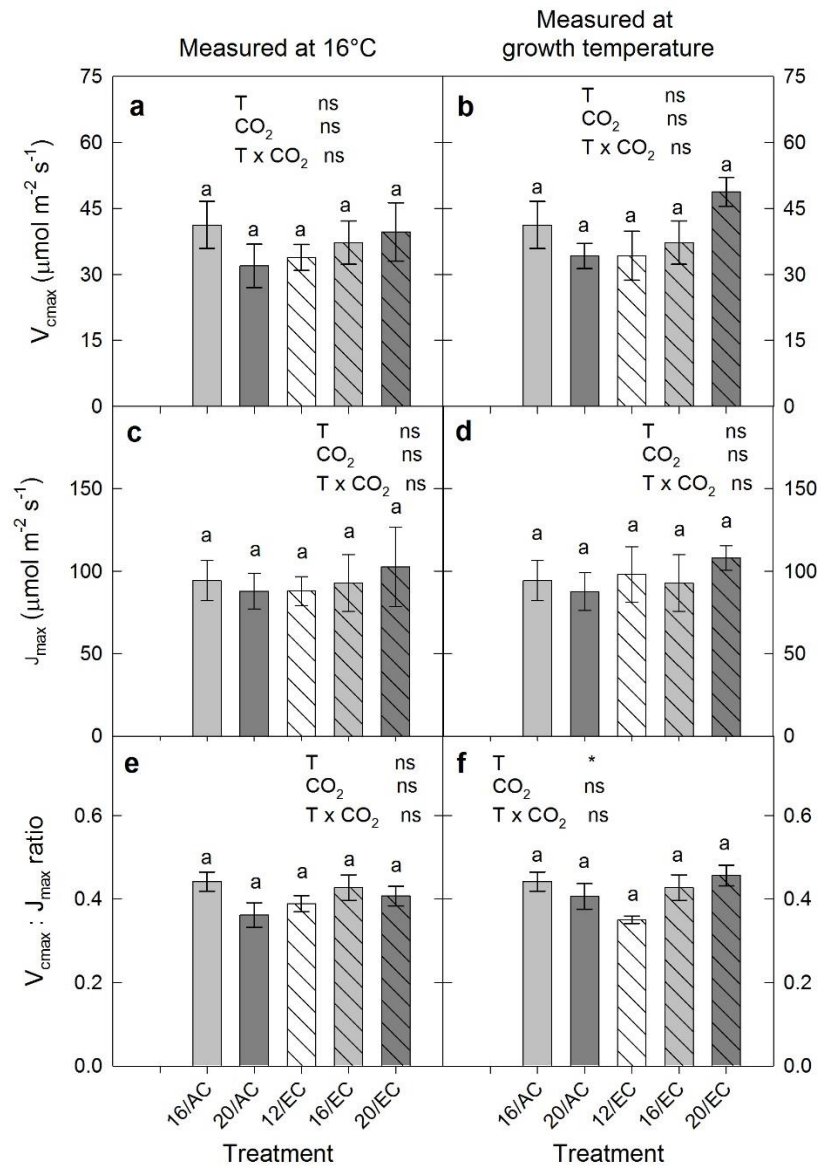
Colobanthus quitensis

Figure 3.5 a-b) Maximum Rubisco carboxylation rate (V_{cmax}), c-d) maximum electron transport rate (J_{max}), and e-f) V_{cmax} to J_{max} ratio of *C. quitensis* measured at leaf temperature of 16 °C (a, c, e) and growth temperature (b, d, f). Bars depict means \pm SE, N = 6. White bars represent growth temperature of 12 °C, grey bars represent growth temperature of 16 °C, and dark grey bars represent growth temperature of 20 °C. Empty bars represent ambient growth CO_2 (400 ppm CO_2 , AC) and hashed bars represent elevated growth CO_2 (750 ppm CO_2 , EC). For each graph, the effect of growth temperature (T), growth CO_2 (CO_2) and the interaction of temperature and CO_2 (T x CO_2)

is shown: ns indicates no significant difference, * indicates $p < 0.05$, ** indicates $p < 0.01$, and *** indicates $p < 0.001$. Means with different letters are significantly different (Tukey's HSD, $p < 0.05$).

Table 3.1 Mean \pm SE of maximal photochemical capacity of PSII (F_v/F_m) measured at leaf temperature of 16 °C and 400 ppm CO₂ (N = 6). The last 3 rows denote treatment effect from growth temperature (T), CO₂ concentration (CO₂), and their interaction (T x CO₂): ns indicates no significant difference, * indicates $p < 0.05$, ** indicates $p < 0.01$, and *** indicates $p < 0.001$. Different letters in brackets suggest significant differences between treatments within a species (Tukey's HSD, $p < 0.05$).

<i>Treatment</i>	<i>D. antarctica</i>	<i>C. quitensis</i>
12/AC	0.70 \pm 0.028 (a)	
16/AC	0.73 \pm 0.018 (a)	0.78 \pm 0.003 (ab)
20/AC	0.71 \pm 0.024 (a)	0.80 \pm 0.005 (a)
12/EC	0.77 \pm 0.006 (a)	0.79 \pm 0.006 (ab)
16/EC	0.74 \pm 0.022 (a)	0.79 \pm 0.004 (ab)
20/EC	0.70 \pm 0.026 (a)	0.77 \pm 0.005 (b)
T	ns	ns
CO₂	ns	ns
T x CO₂	ns	***

The electron transport rate measured with chlorophyll fluorescence (ETR) demonstrated the performance of the electron transport chain independent of the Calvin-Benson cycle. This parameter was calculated from measurements of quantum yield of PSII (Φ_{PSII}), the trends in both ETR and Φ_{PSII} were therefore very similar, and only data for the former were presented. In *D. antarctica*, ETR showed evidence of a weak down-regulation in response to increased growth temperature ($p = 0.04$) and elevated growth CO_2 ($p = 0.04$) when measured at a common leaf temperature and CO_2 concentration (Fig. 3.6a). ETR, therefore, decreased at higher growth temperatures and CO_2 . The down-regulation under higher temperatures, however, was fully compensated for by the positive effect of increasing leaf temperature on ETR, because there was no longer a significant temperature effect when ETR was measured at the growth temperature ($p = 0.30$, Fig. 3.6b). On the other hand, measurements at growth CO_2 showed a small but significant positive CO_2 effect, suggesting that the direct effect of higher CO_2 concentrations on ETR overwhelmed the down-regulation of ETR at elevated CO_2 ($p = 0.016$, Fig. 3.6c). Consequently, when measured at the growth conditions (growth temperature and growth CO_2), ETR in *D. antarctica* leaves showed no response to either temperature ($p = 0.40$) or CO_2 ($p = 0.13$, Fig. 3.6d).

In *C. quitensis*, measurements at a leaf temperature of 16 °C and CO_2 concentration of 400 ppm indicated a 14% down-regulation in ETR ($p = 0.008$, Fig. 3.7a) in the 20 °C treatments. The effect, however, was more than offset by the direct effect of higher leaf temperature, as ETR in the warmest treatments was 18% greater ($p = 0.02$, Fig. 3.7b) than the 12 °C treatment when both were assessed at the growth temperatures. Measurements at a common leaf temperature and CO_2 concentration did not show any acclimation to growth CO_2 ($p = 0.44$), but direct exposure to high measurement CO_2 resulted in a small increase in ETR ($p = 0.013$, Fig. 3.7c). The ETR of *C. quitensis* measured at the growth conditions was, therefore, stimulated under warming ($p = 0.003$) and elevated CO_2 treatments ($p = 0.011$, Fig. 3.7d), mostly due to the direct effects of higher leaf temperature and CO_2 level.

The ratios of intercellular to atmospheric CO_2 concentrations (C_i/C_a) can inform us of the stomatal behavior in response to both acute temperature and CO_2 effects and long-term

acclimation to the new growth temperature or CO₂ level. In *D. antarctica*, C_i/C_a measured at a common temperature and CO₂ concentration showed no acclimation to growth temperature (p = 0.22), but there was an increased ratio in plants grown in elevated CO₂ (p = 0.021, Fig. 3.8a). When the ratio in each treatment was evaluated at the respective growth temperature, there was no response to growth temperature (p = 0.64, Fig. 3.8b), implying that the C_i/C_a ratio was not affected by acute temperature changes. When measured at the growth CO₂, C_i/C_a was significantly higher in elevated CO₂ treatments (p = 0.018, Fig. 3.8c), suggesting that increasing the measurement CO₂ concentration did not alter stomatal behavior of *D. antarctica* leaves grown at elevated CO₂. Under the growth temperature and CO₂, the C_i/C_a ratio in *D. antarctica* showed no CO₂ response (p = 0.22), but a significant temperature effect (p = 0.025), with decreasing ratios at higher temperatures (Fig. 3.8d).

In *C. quitensis*, C_i/C_a ratios generally followed the same trends as in *D. antarctica*. Under a common leaf temperature of 16 °C and CO₂ concentration of 400 ppm, C_i/C_a was higher in plants grown under elevated CO₂ (p = 0.012, Fig. 3.9a). Measured under the same CO₂ concentration and the growth temperatures, the C_i/C_a ratio decreased as leaf temperature increased (p = 0.034, Fig. 3.9b). The increased C_i/C_a ratio under elevated CO₂ was magnified when plants were measured at their growth CO₂ (p < 0.001, Fig. 3.9c), as a strong CO₂ effect was found. When all plants were measured at their growth temperature and CO₂, the CO₂ response was no longer observed (p = 0.14); instead, the C_i/C_a ratio decreased with rising growth temperatures (p = 0.04) and was particularly low in the 20/EC treatment (Fig. 3.9d).

Dark respiration (R_{dark}) offered an estimate of the CO₂ released from leaf mitochondrial metabolism. In *D. antarctica*, R_{dark} assessed at a common measurement temperature showed no response to either growth temperature (p = 0.32) or growth CO₂ (p = 0.26, Fig. 3.10a), nor did R_{dark} measurements at growth temperature show any response to temperature (p = 0.21) or CO₂ (p = 0.66) (Fig. 3.10b). However, the variance between individuals and among measurements was high. Similarly, R_{dark} in *C. quitensis* showed neither acclimation to growth temperature or CO₂ (p > 0.19 for both, Fig. 3.11a) nor did it respond to changes in leaf measurement temperature (p > 0.16 for both, Fig. 3.11b).

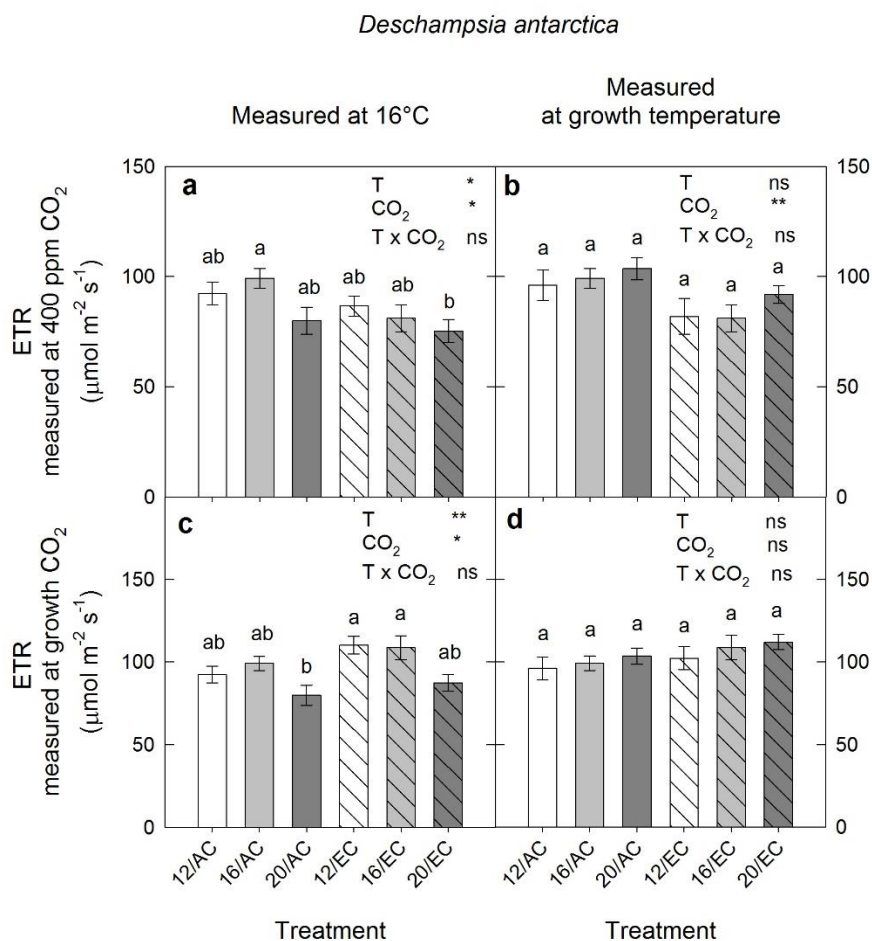


Figure 3.6 Electron transport rate (ETR) of *D. antarctica* measured at: a) 400 ppm CO₂ and leaf temperature of 16 °C; b) 400 ppm CO₂ and growth temperature; c) growth CO₂ concentration and leaf temperature of 16°C; and d) growth CO₂ concentration and growth temperature. Bars depict means ± SE, N = 6. White bars represent growth temperature of 12 °C, grey bars represent growth temperature of 16 °C, and dark grey bars represent growth temperature of 20 °C. Empty bars represent ambient growth CO₂ (400 ppm CO₂, AC) and hashed bars represent elevated growth CO₂ (750 ppm CO₂, EC). For each graph, the effect of growth temperature (T), growth CO₂ (CO₂) and the interaction of temperature and CO₂ (T x CO₂) is shown: ns indicates no significant difference, * indicates p < 0.05, ** indicates p < 0.01, and *** indicates p < 0.001. Means with different letters are significantly different (Tukey's HSD, p < 0.05).

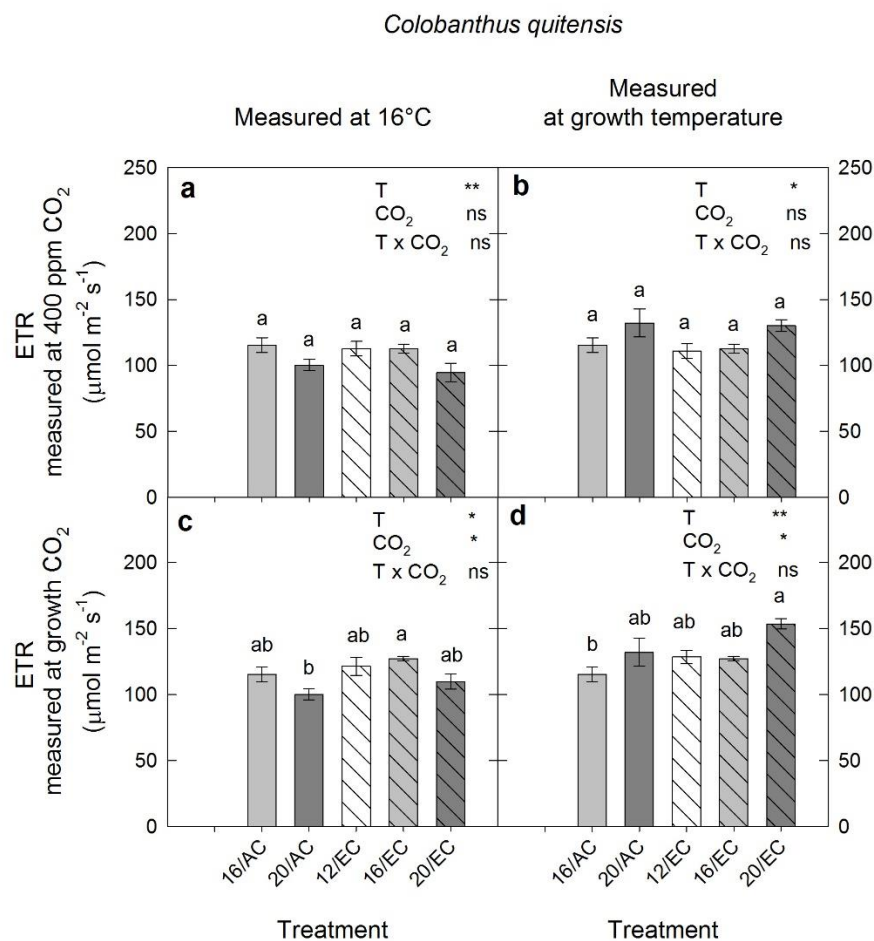


Figure 3.7 Electron transport rate (ETR) of *C. quitensis* measured at: a) 400 ppm CO₂ and leaf temperature of 16 °C; b) 400 ppm CO₂ and growth temperature; c) growth CO₂ concentration and leaf temperature of 16°C; and d) growth CO₂ concentration and growth temperature. Bars depict means \pm SE, N = 6. White bars represent growth temperature of 12 °C, grey bars represent growth temperature of 16 °C, and dark grey bars represent growth temperature of 20 °C. Empty bars represent ambient growth CO₂ (400 ppm CO₂, AC) and hashed bars represent elevated growth CO₂ (750 ppm CO₂, EC). For each graph, the effect of growth temperature (T), growth CO₂ (CO₂) and the interaction of temperature and CO₂ (T x CO₂) is shown: ns indicates no significant difference, * indicates $p < 0.05$, ** indicates $p < 0.01$, and *** indicates $p < 0.001$. Means with different letters are significantly different (Tukey's HSD, $p < 0.05$).

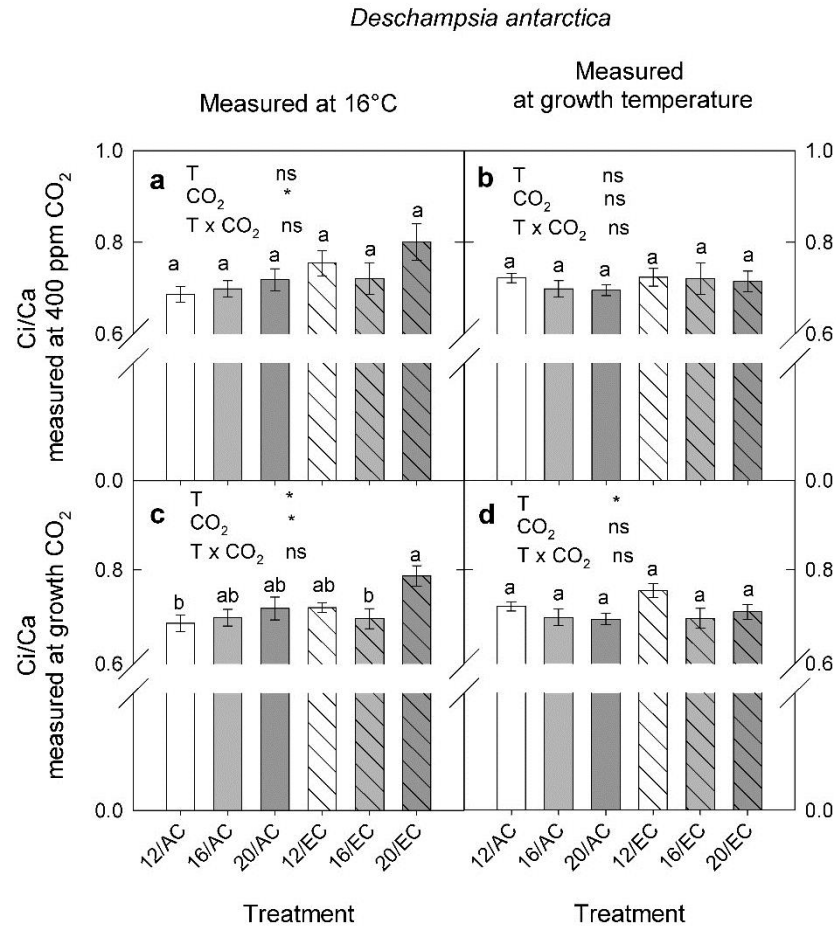


Figure 3.8 Intercellular (C_i) to atmospheric (C_a) CO₂ concentrations ratio (C_i/C_a) of *D. antarctica* measured at: a) 400 ppm CO₂ and leaf temperature of 16 °C; b) 400 ppm CO₂ and growth temperature; c) growth CO₂ concentration and leaf temperature of 16 °C; and d) growth CO₂ concentration and growth temperature. Bars depict means \pm SE, N = 6. White bars represent growth temperature of 12 °C, grey bars represent growth temperature of 16 °C, and dark grey bars represent growth temperature of 20 °C. Empty bars represent ambient growth CO₂ (400 ppm CO₂, AC) and hashed bars represent elevated growth CO₂ (750 ppm CO₂, EC). For each graph, the effect of growth temperature (T), growth CO₂ (CO₂) and the interaction of temperature and CO₂ (T x CO₂) is shown: ns indicates no significant difference, * indicates $p < 0.05$, ** indicates $p < 0.01$, and *** indicates $p < 0.001$. Means with different letters are significantly different (Tukey's HSD, $p < 0.05$).

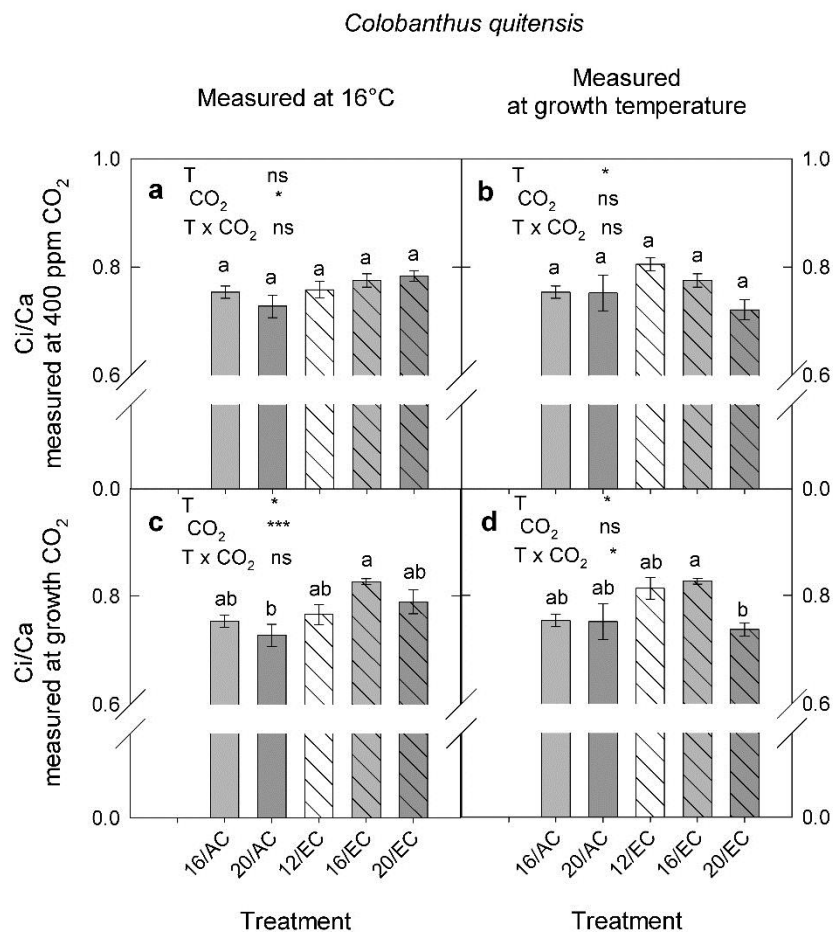


Figure 3.9 Intercellular to atmospheric CO₂ concentrations ratio (C_i/C_a) of *C. quitensis* measured at: a) 400 ppm CO₂ and leaf temperature of 16 °C; b) 400 ppm CO₂ and growth temperature; c) growth CO₂ concentration and leaf temperature of 16 °C; and d) growth CO₂ concentration and growth temperature. Bars depict means \pm SE, N = 6. White bars represent growth temperature of 12 °C, grey bars represent growth temperature of 16 °C, and dark grey bars represent growth temperature of 20 °C. Empty bars represent ambient growth CO₂ (400 ppm CO₂, AC) and hashed bars represent elevated growth CO₂ (750 ppm CO₂, EC). For each graph, the effect of growth temperature (T), growth CO₂ (CO₂) and the interaction of temperature and CO₂ (T x CO₂) is shown: ns indicates no significant difference, * indicates $p < 0.05$, ** indicates $p < 0.01$, and *** indicates $p < 0.001$. Means with different letters are significantly different (Tukey's HSD, $p < 0.05$).

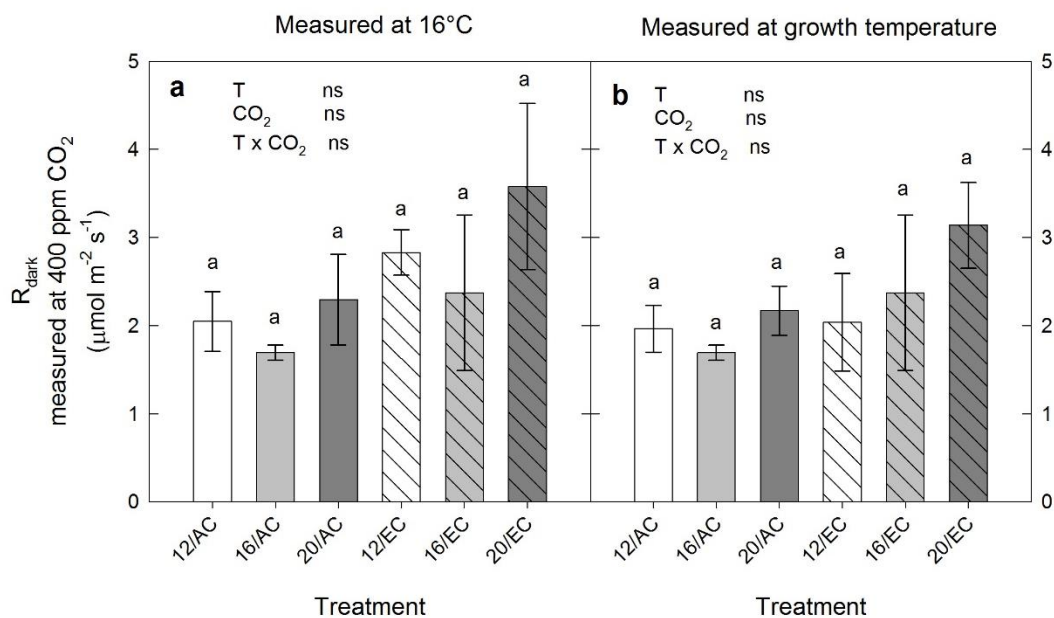
Deschampsia antarctica

Figure 3.10 Dark respiration rate (R_{dark}) of *D. antarctica* measured at: a) 400 ppm CO_2 and leaf temperature of 16 °C and b) 400 ppm CO_2 and growth temperature. Bars depict means \pm SE, N = 6. White bars represent growth temperature of 12 °C, grey bars represent growth temperature of 16 °C, and dark grey bars represent growth temperature of 20 °C. Empty bars represent ambient growth CO_2 (400 ppm CO_2 , AC) and hashed bars represent elevated growth CO_2 (750 ppm CO_2 , EC). For each graph, the effect of growth temperature (T), growth CO_2 (CO_2) and the interaction of temperature and CO_2 (T x CO_2) is shown: ns indicates no significant difference, * indicates $p < 0.05$, ** indicates $p < 0.01$, and *** indicates $p < 0.001$. Means with different letters are significantly different (Tukey's HSD, $p < 0.05$).

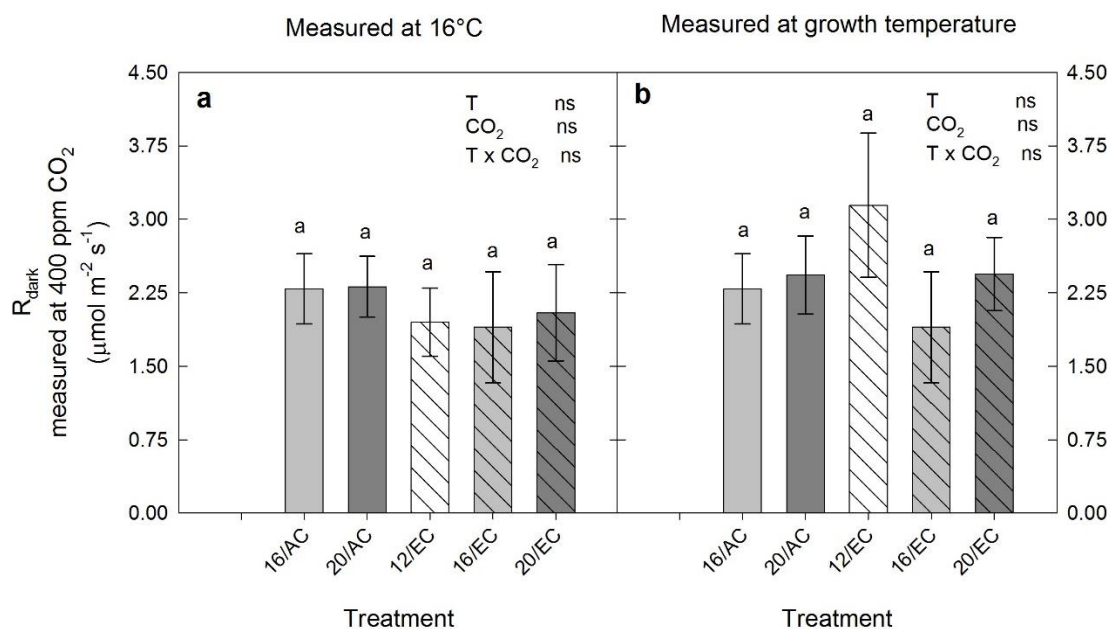
Colobanthus quitensis

Figure 3.11 Dark respiration rate (R_{dark}) of *C. quitensis* measured at: a) 400 ppm CO_2 and leaf temperature of 16 °C and b) 400 ppm CO_2 and growth temperature. Bars depict means \pm SE, N = 6. White bars represent growth temperature of 12 °C, grey bars represent growth temperature of 16 °C, and dark grey bars represent growth temperature of 20 °C. Empty bars represent ambient growth CO_2 (400 ppm CO_2 , AC) and hashed bars represent elevated growth CO_2 (750 ppm CO_2 , EC). For each graph, the effect of growth temperature (T), growth CO_2 (CO_2) and the interaction of temperature and CO_2 (T x CO_2) is shown: ns indicates no significant difference, * indicates $p < 0.05$, ** indicates $p < 0.01$, and *** indicates $p < 0.001$. Means with different letters are significantly different (Tukey's HSD, $p < 0.05$).

3.2 Leaf structure and biomass accumulation

Specific leaf area (SLA) is the ratio of leaf area to dry mass, and reflects the structural investment of plants in photosynthetic tissue, with a lower SLA suggesting thicker leaves. The SLA in *D. antarctica* was higher as growth temperature increased ($p = 0.020$), and lower at higher growth CO_2 ($p = 0.020$), although the magnitude of the change was small (Fig. 3.12a). *C. quitensis*, in contrast, showed no significant treatment effects on SLA ($p > 0.11$ for temperature and CO_2 , Fig. 3.12b).

Biomass of both *D. antarctica* and *C. quitensis* was affected by the treatments (Figs. 3.13-14). In *D. antarctica*, aboveground and belowground biomass increased by 46.2% under elevated growth CO_2 ($p < 0.001$, Figs. 3.13a-c). Growth was also enhanced at higher growth temperatures ($p < 0.001$, Figs. 3.13a-c), but only under moderate warming (from 12 to 16 °C), since the biomass in 20 °C treatments was equivalent to that in the coolest treatment. The direction and magnitude of the growth response to temperature and CO_2 were consistent between aboveground and belowground biomass, therefore, there were no treatment effects on the root:shoot ratios in *D. antarctica* ($p > 0.10$ for both, Fig. 3.13d). Similar to *D. antarctica*, CO_2 stimulated root and shoot growth in *C. quitensis* ($p < 0.001$, Figs. 3.14a-c). In contrast, increasing temperature negatively affected biomass accumulation at both CO_2 levels ($p < 0.001$, Figs. 3.14a-c). Root to shoot ratios were not affected by growth temperature ($p = 0.75$), but elevated CO_2 tended to promote root growth more than shoot growth in *C. quitensis* ($p = 0.04$, Fig. 3.14d).

Across all treatments, *D. antarctica* showed a consistent leaf carbon content of 40% ($p > 0.16$ for both temperature and CO_2 , Table 3.2). Foliar nitrogen, however, was lower in plants grown at elevated CO_2 ($p = 0.001$), although there was no growth temperature effect ($p = 0.32$, Table 3.2). The C:N ratio, therefore, was reflective of the treatment response to nitrogen, i.e higher C:N ratios in elevated CO_2 -grown plants ($p < 0.001$, Table 3.2). *C. quitensis* leaves grown at the warmer treatments had a lower percentage of carbon than cool-grown plants, but the effect was small ($p = 0.010$, Table 3.2). Elevated CO_2 , on the other hand, reduced foliar N in *C. quitensis* leaves by 11.5% ($p = 0.046$, Table 3.2), resulting in an increase in the C:N ratio in elevated CO_2 -grown plants ($p = 0.041$, Table 3.2).

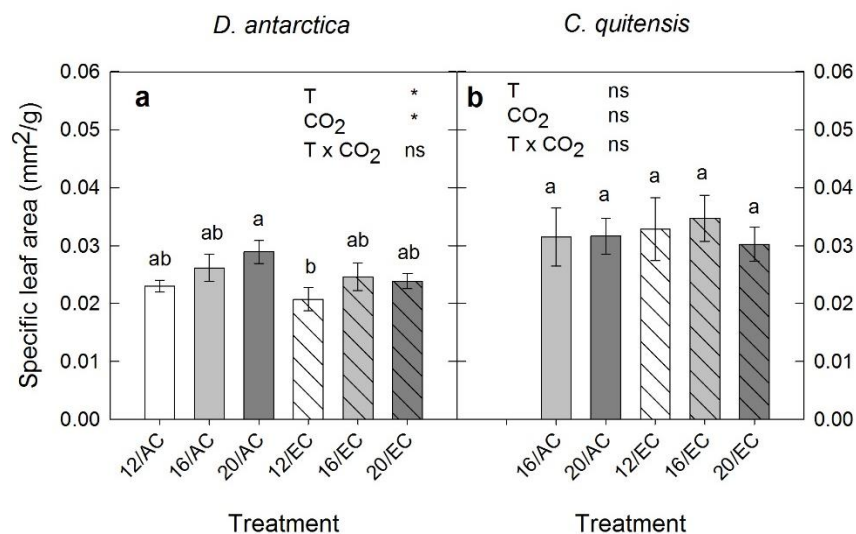


Figure 3.12 Specific leaf area of a) *D. antarctica* and b) *C. quitensis*. Bars depict mean \pm SE, N = 12, except for 16/AC and 16/EC (N = 6). White bars represent growth temperature of 12 °C, grey bars represent growth temperature of 16 °C, and dark grey bars represent growth temperature of 20 °C. Empty bars represent ambient growth CO₂ (400 ppm CO₂, AC) and hashed bars represent elevated growth CO₂ (750 ppm CO₂, EC). For each graph, the effect of growth temperature (T), growth CO₂ (CO₂) and the interaction of temperature and CO₂ (T x CO₂) is shown: ns indicates no significant difference, * indicates p < 0.05, ** indicates p < 0.01, and *** indicates p < 0.001. Means with different letters are significantly different (Tukey's HSD, p < 0.05).

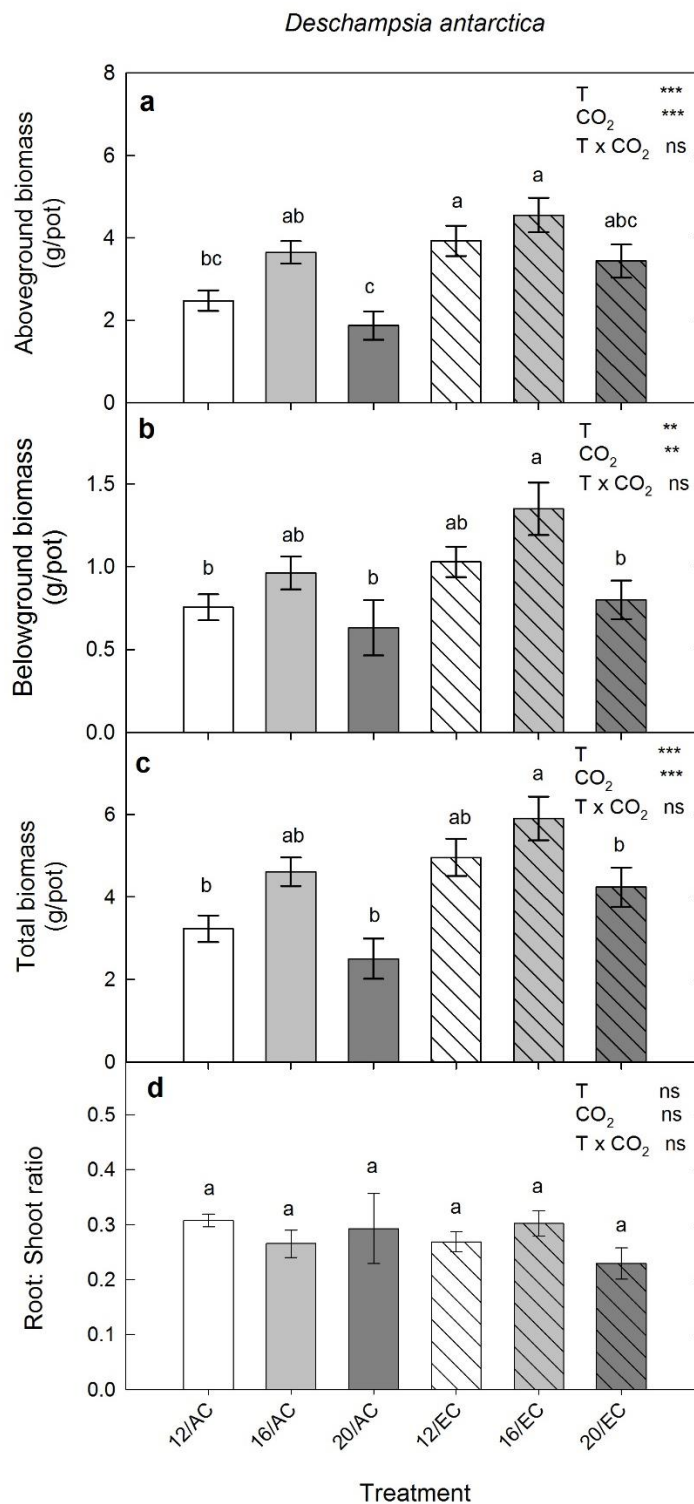


Figure 3.13 a) Aboveground biomass, b) belowground biomass, c) total biomass, and d) root to shoot ratio of *D. antarctica* on a pot basis. Bars depict means \pm SE, N = 10, except for 20/AC (N = 8) and 20/EC (N = 9). White bars represent growth temperature of 12 °C,

grey bars represent growth temperature of 16 °C, and dark grey bars represent growth temperature of 20 °C. Empty bars represent ambient growth CO₂ (400 ppm CO₂, AC) and hashed bars represent elevated growth CO₂ (750 ppm CO₂, EC). For each graph, the effect of growth temperature (T), growth CO₂ (CO₂) and the interaction of temperature and CO₂ (T x CO₂) is shown: ns indicates no significant difference, * indicates $p < 0.05$, ** indicates $p < 0.01$, and *** indicates $p < 0.001$. Means with different letters are significantly different (Tukey's HSD, $p < 0.05$).

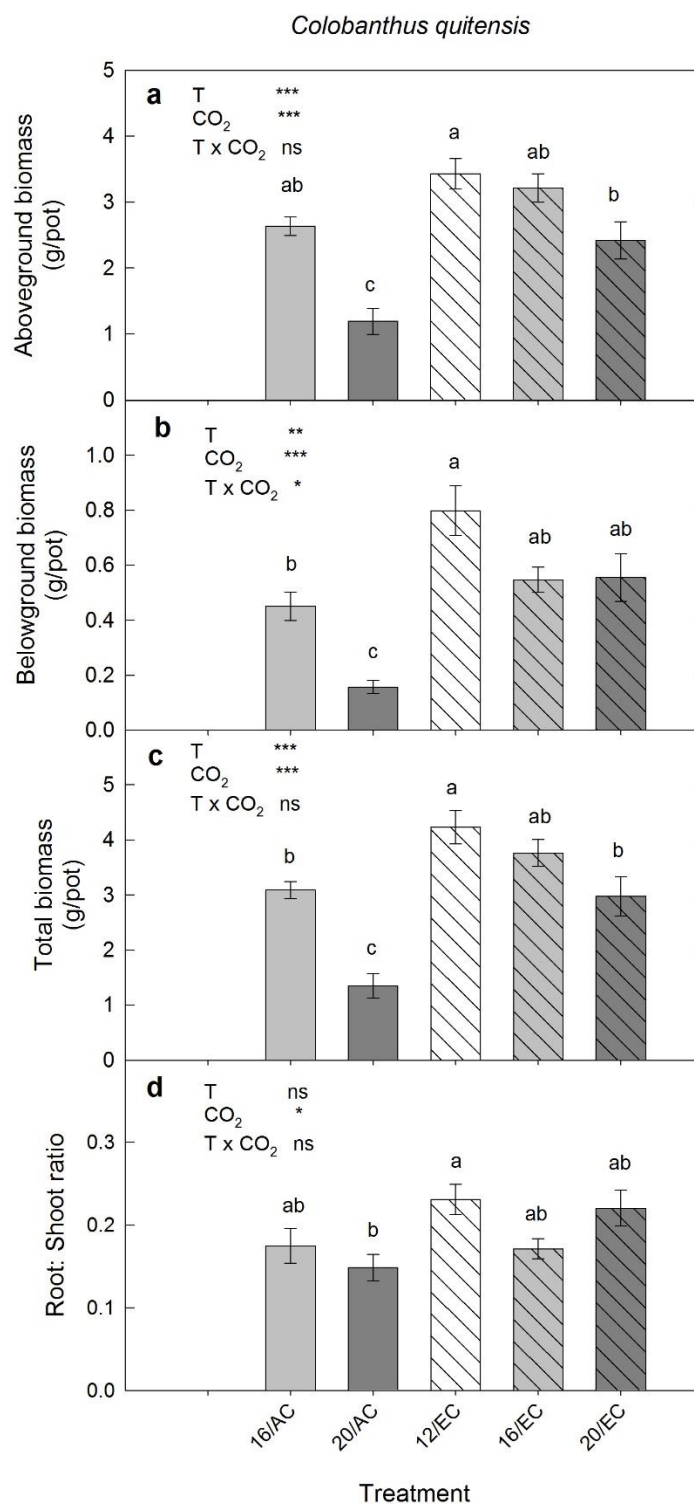


Figure 3.14 a) Aboveground biomass, b) belowground biomass, c) total biomass, and d) root to shoot ratio of *C. quitensis* on a pot basis. Bars depict means \pm SE, N = 10. White

bars represent growth temperature of 12 °C, grey bars represent growth temperature of 16 °C, and dark grey bars represent growth temperature of 20 °C. Empty bars represent ambient growth CO₂ (400 ppm CO₂, AC) and hashed bars represent elevated growth CO₂ (750 ppm CO₂, EC). For each graph, the effect of growth temperature (T), growth CO₂ (CO₂) and the interaction of temperature and CO₂ (T x CO₂) is shown: ns indicates no significant difference, * indicates $p < 0.05$, ** indicates $p < 0.01$, and *** indicates $p < 0.001$. Means with different letters are significantly different (Tukey's HSD, $p < 0.05$).

Table 3.2 Mean \pm SE of leaf carbon, nitrogen, and carbon to nitrogen ratio of *D. antarctica* and *C. quitensis* (N = 5). The last 3 rows denote treatment effects from growth temperature (T), CO₂ concentration (CO₂), and their interaction (T x CO₂): ns indicates no significant difference, * indicates $p < 0.05$, ** indicates $p < 0.01$, and *** indicates $p < 0.001$. Different letters in brackets suggest significant differences between treatments within a species (Tukey's HSD, $p < 0.05$).

Treatment	<i>D. antarctica</i>			<i>C. quitensis</i>		
	%C	%N	C:N	%C	%N	C:N
12/AC	40.93 \pm 0.24 (a)	2.74 \pm 0.15 (a)	15.14 \pm 0.88 (b)			
16/AC	41.44 \pm 0.25 (a)	2.42 \pm 0.17 (ab)	17.44 \pm 1.14 (b)	36.98 \pm 0.40 (ab)	2.56 \pm 0.18 (a)	14.77 \pm 1.14 (a)
20/AC	41.36 \pm 0.25 (a)	2.63 \pm 0.21 (a)	16.12 \pm 1.32 (b)	35.60 \pm 0.19 (b)	2.81 \pm 0.12 (a)	12.77 \pm 0.62 (a)
12/EC	40.84 \pm 0.30 (a)	1.75 \pm 0.10 (b)	23.53 \pm 1.05 (a)	38.93 \pm 0.16 (a)	2.49 \pm 0.16 (a)	15.87 \pm 0.92 (a)
16/EC	41.47 \pm 0.47 (a)	2.15 \pm 0.21 (ab)	19.87 \pm 1.43 (ab)	37.46 \pm 1.08 (ab)	2.33 \pm 0.24 (a)	16.89 \pm 2.07 (a)
20/EC	40.59 \pm 0.25 (a)	2.34 \pm 0.16 (ab)	17.65 \pm 1.20 (b)	36.59 \pm 0.46 (ab)	2.30 \pm 0.14 (a)	16.15 \pm 1.05 (a)
T	ns	ns	ns	*	ns	ns
CO₂	ns	**	***	ns	*	*
T x CO₂	ns	ns	*	ns	ns	ns

3.3 Leaf anatomy

Analysis of leaf anatomy provides an additional method to assess acclimation to the new growth environments. While modifications in the mesophyll cells, the main photosynthetic tissue, could help explain thermal or CO₂ acclimation of photosynthesis, other structures revealed by the cross-sectional analysis, such as stomata, vascular bundles, and epidermis, can also inform of the plant water status and allocation of resources that contribute to photosynthetic performance.

All 30 samples of leaf cross-sections across treatments of *D. antarctica* showed a leaf blade folded towards the adaxial epidermis (Fig. 3.15a). Leaves from all treatments had a thick-walled abaxial epidermis and a thinner-walled adaxial side (Fig. 3.15a). Vascular bundles were well-differentiated, and wrapped inside a layer of mesothyme with thick internal walls. The number of vascular bundles ranged from 3 to 5, resulting in 3 to 5 stomatal grooves, where most stomata occurred. Bulliform cells, which are usually located at the bottom of each stomatal groove to facilitate leaf folding or unfolding, were missing in all treatments. Mesophyll cells were undifferentiated, and did not follow any particular arrangements.

Transverse sections of *C. quitensis* were typical of dicotyledon plants. Stomata occurred on both sides of the leaf, but there were significantly more stomata on the adaxial side, and only near the leaf margin on the abaxial side (Fig. 3.15b). Mesophyll cells were differentiated into palisade mesophyll on the adaxial side and spongy mesophyll on the abaxial side. There was one main vascular bundle at the center of the cross-section where the central vein was, in addition to three to four smaller vascular bundles surrounded by a sheath of cells without chlorophyll (Fig. 3.15b).

D. antarctica cross-sectional images showed no significant treatment responses in leaf thickness ($p > 0.48$ for temperature and CO₂, Table 3.3) or width ($p > 0.43$ for temperature and CO₂, Table 3.3). *C. quitensis* leaf thickness also did not vary among treatments ($p > 0.10$ for temperature and CO₂, Table 3.3). However, leaf width in *C. quitensis* decreased by up to 39% as temperature increased at ambient growth CO₂ ($p = 0.001$), and this response to temperature was much less pronounced in the elevated CO₂ treatments ($p = 0.03$, Table 3.3). Analyses of the cross-sectional areas occupied by

different types of tissue showed that intercellular air space in *D. antarctica* was significantly reduced at 16 °C growth temperature ($p = 0.042$, Table 3.3). There was no treatment response in the cross-sectional areas filled by mesophyll cells, vascular bundles, or any other non-photosynthetic tissues in *D. antarctica* ($p > 0.13$ for all, Table 3.3). The same analyses on *C. quitensis* showed no significant treatment effects in any tissue types ($p > 0.13$ for all, Table 3.3).

Stomatal grooves, a unique anatomical feature in grasses, were characterized in *D. antarctica* in terms of width, depth, area, and perimeter, assuming a half-ellipse shape (Fig. 3.16). Groove width was smallest in plants grown at 20/AC, but the groove significantly widened at higher growth CO₂ ($p = 0.37$ for temperature, $p = 0.005$ for CO₂, $p = 0.012$ for the interaction, Fig. 3.16a). Grooves also became shallower as growth temperature increased ($p = 0.030$), with no CO₂ effect on groove depth ($p = 0.40$, Fig. 3.16b). Analysis of groove area to perimeter ratio allowed an estimate of the balance between the size of the diffusion surface (perimeter) and the pocket of air with high humidity (area). Most notably, the perimeter to area ratio of the stomatal groove was lowest in the warmest treatment at ambient CO₂ concentration (20/AC), but significantly increased in the same growth temperature at elevated CO₂ ($p = 0.005$ for CO₂, $p = 0.014$ for the interaction, Fig. 3.16c). This suggested that very high evaporative demand at the 20/AC treatment resulted in a groove structure that minimized diffusion to prevent water loss, and that elevated CO₂ concentrations alleviated the negative effect of high temperature.

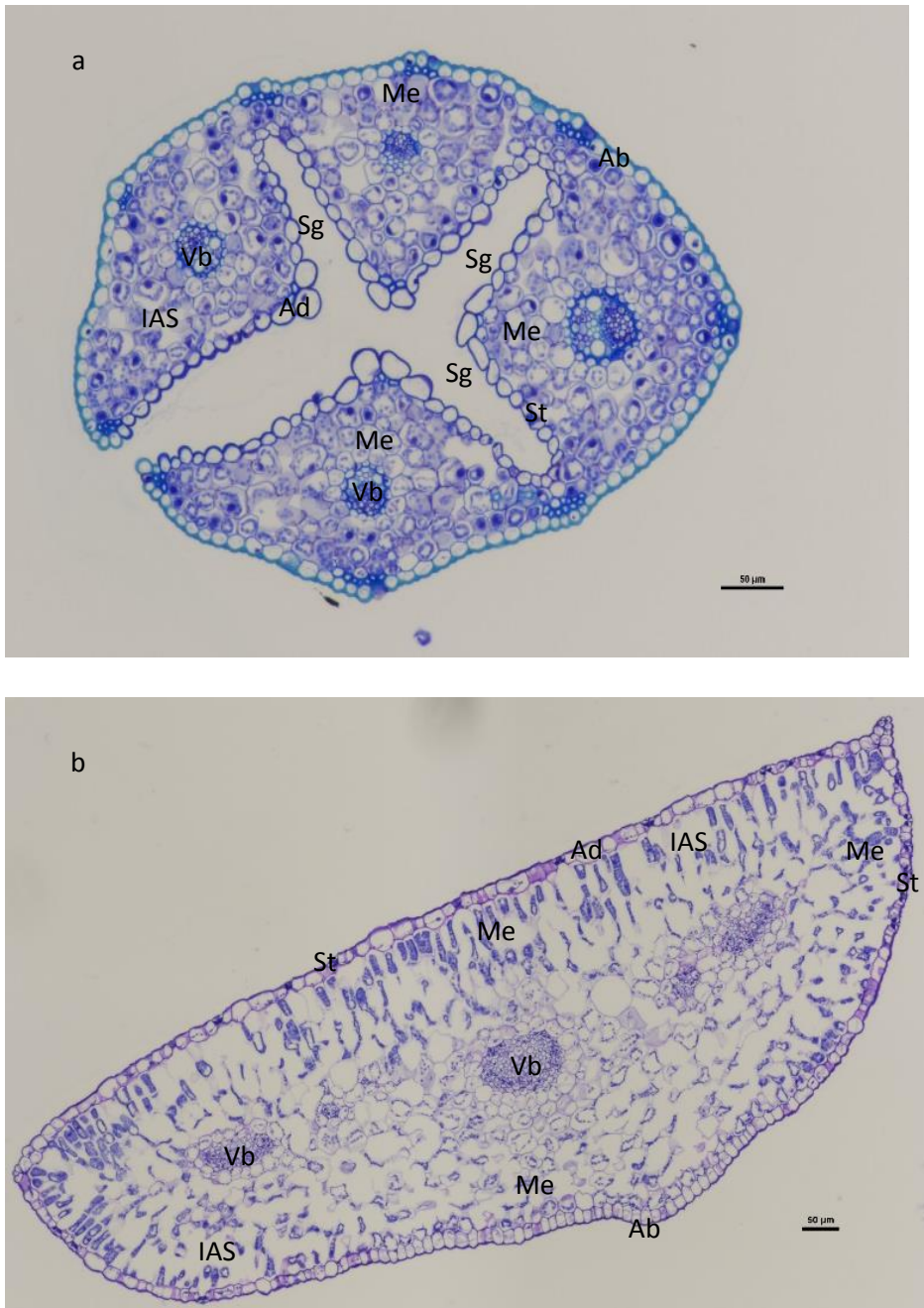


Figure 3.15 Cross sections of a) *D. antarctica* and b) *C. quitensis* stained with Toluidine blue O. Tissue types shown include mesophyll cells (Me), vascular bundles (Vb), intercellular air space (IAS), stomata (St), abaxial epidermis (Ab), adaxial epidermis (Ad), and stomatal groove (Sg). Scale bars indicate 50 µm.

Table 3.3 Proportion of cross-sectional images of *D. antarctica* and *C. quitensis* filled with mesophyll cells, intercellular air space, vascular bundles, and other non-photosynthetic tissues (abaxial and adaxial epidermis, fiber bundles), as well as leaf thickness and width. Data are means \pm SE, N = 5. The last 3 rows denote treatment effects from growth temperature (T), CO₂ concentration (CO₂), and their interaction (T x CO₂): ns indicates no significant difference, * indicates $p < 0.05$, ** indicates $p < 0.01$, and *** indicates $p < 0.001$. Different letters in brackets suggest significant differences between treatments within a species (Tukey's HSD, $p < 0.05$).

	Treat- ment	Mesophyll cells	Inter- cellular air space	Vascular bundles	Other tissues	Thickness (μ m)	Width (μ m)
<i>D. antarctica</i>	12/AC	0.50 \pm 0.043 (a)	0.16 \pm 0.013 (a)	0.049 \pm 0.004 (a)	0.29 \pm 0.032 (a)	202.8 \pm 13.8 (a)	1487.9 \pm 129.0 (a)
	16/AC	0.58 \pm 0.024 (a)	0.07 \pm 0.025 (a)	0.047 \pm 0.010 (a)	0.29 \pm 0.017 (a)	213.1 \pm 11.1 (a)	1542.7 \pm 126.2 (a)
	20/AC	0.49 \pm 0.040 (a)	0.14 \pm 0.032 (a)	0.072 \pm 0.017 (a)	0.30 \pm 0.026 (a)	196.0 \pm 7.2 (a)	1272.2 \pm 92.5 (a)
	12/EC	0.57 \pm 0.030 (a)	0.11 \pm 0.028 (a)	0.061 \pm 0.020 (a)	0.26 \pm 0.045 (a)	197.0 \pm 12.3 (a)	1448.7 \pm 150.9 (a)
	16/EC	0.58 \pm 0.025 (a)	0.07 \pm 0.025 (a)	0.040 \pm 0.013 (a)	0.30 \pm 0.029 (a)	213.0 \pm 9.3 (a)	1524.2 \pm 123.8 (a)
	20/EC	0.53 \pm 0.043 (a)	0.14 \pm 0.030 (a)	0.056 \pm 0.010 (a)	0.26 \pm 0.034 (a)	219.9 \pm 20.5 (a)	1447.4 \pm 151.9 (a)
	T	ns	*	ns	ns	ns	ns
	CO ₂	ns	ns	ns	ns	ns	ns
	T x CO ₂	ns	ns	ns	ns	ns	ns
<i>C. quitensis</i>	12/AC	0.44 \pm 0.049 (a)	0.31 \pm 0.052 (a)	0.017 \pm 0.005 (a)	0.23 \pm 0.051 (a)	412.7 \pm 39.7 (a)	1362.6 \pm 160.5 (a)
	16/AC	0.47 \pm 0.019 (a)	0.21 \pm 0.026 (a)	0.064 \pm 0.020 (a)	0.25 \pm 0.024 (a)	345.1 \pm 21.5 (a)	829.3 \pm 76.8 (b)
	20/AC	0.49 \pm 0.034 (a)	0.27 \pm 0.048 (a)	0.026 \pm 0.012 (a)	0.22 \pm 0.021 (a)	352.9 \pm 36.6 (a)	872.2 \pm 35.5 (b)
	12/EC	0.45 \pm 0.033 (a)	0.28 \pm 0.028 (a)	0.066 \pm 0.021 (a)	0.21 \pm 0.020 (a)	355.2 \pm 25.6 (a)	1123.9 \pm 32.4 (ab)
	16/EC	0.52 \pm 0.050 (a)	0.22 \pm 0.027 (a)	0.059 \pm 0.030 (a)	0.20 \pm 0.026 (a)	349.1 \pm 18.6 (a)	980.7 \pm 66.7 (b)
	20/EC	0.52 \pm 0.028 (a)	0.22 \pm 0.031 (a)	0.023 \pm 0.007 (a)	0.24 \pm 0.019 (a)	299.1 \pm 16.0 (a)	1066.2 \pm 54.5 (ab)
	T	ns	ns	ns	ns	ns	**
	CO ₂	ns	ns	ns	ns	ns	ns
	T x CO ₂	ns	ns	ns	ns	ns	*

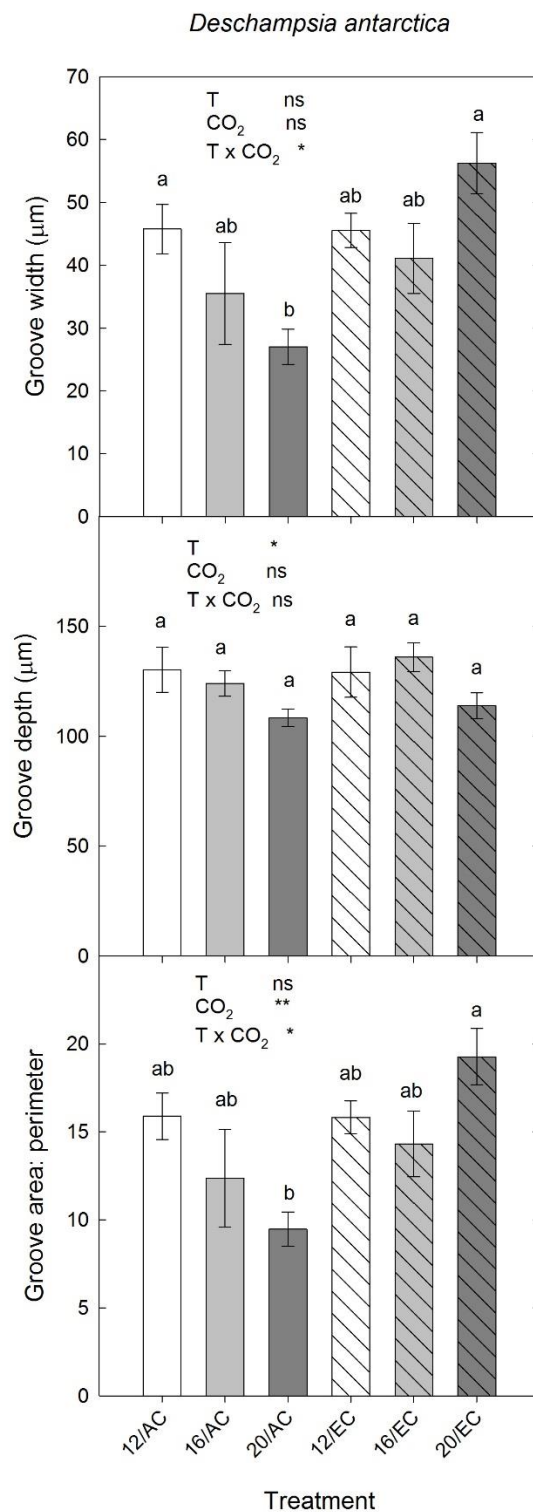


Figure 3.16 a) Average stomatal groove width, b) depth, and c) area to perimeter ratio of *Deschampsia antarctica*. Bars depict means \pm SE, N = 5, except for 12/AC (N = 4). White bars represent growth temperature of 12 °C, grey bars represent growth

temperature of 16 °C, and dark grey bars represent growth temperature of 20 °C. Empty bars represent ambient growth CO₂ (400 ppm CO₂, AC) and hashed bars represent elevated growth CO₂ (750 ppm CO₂, EC). For each graph, the effect of growth temperature (T), growth CO₂ (CO₂) and the interaction of temperature and CO₂ (T x CO₂) is shown, with ns indicates no significant difference, * indicates $p < 0.05$, ** indicates $p < 0.01$, and *** indicates $p < 0.001$. Means with different letters are significantly different (Tukey's HSD, $p < 0.05$).

CHAPTER 4: DISCUSSION

This study set out to investigate the effects of warming and elevated CO₂ concentration on the two species of vascular plants in Antarctica, *Deschampsia antarctica* and *Colobanthus quitensis*. Both species were assessed in terms of the capacity of the photosynthetic apparatus to acclimate to the new growth conditions, as well as any modifications in leaf morphology and biomass in response to the treatments. Overall, both species showed very little plasticity in the photosynthetic apparatus under different growth conditions. Maximum Rubisco carboxylation rates (V_{cmax}), maximum electron transport rates (J_{max}), and net CO₂ assimilation rates (A_{net}) did not show thermal acclimation to an 8 °C increase in growth temperatures in either *D. antarctica* or *C. quitensis*. In contrast, *D. antarctica* displayed a 25% down-regulation of A_{net} at elevated growth CO₂, while *C. quitensis* did not. Photosynthesis in both species was stimulated by higher CO₂ concentration, but in *D. antarctica* A_{net} was more responsive to increasing measurement temperatures than was *C. quitensis*. There was evidence of adjustments in leaf morphology of *D. antarctica* to the treatments, specifically a narrowing of the stomatal groove, to conserve water loss at very high temperatures, which could introduce CO₂ diffusion limitations under severe warming. However, similar to photosynthesis, leaf anatomy in both species also showed very little plasticity under a range of growth conditions. At the whole-plant level, elevated CO₂ stimulated growth in both species, while warming promoted growth only in *D. antarctica* at the moderate warming treatments (16 °C). Biomass accumulation decreased in the warmest treatments in *D. antarctica*, and in all warming treatments in *C. quitensis*.

4.1 Photosynthesis in both species showed little thermal acclimation

Thermal acclimation of photosynthesis is often defined as adjustments in the photosynthetic machinery that result in an enhanced performance at the new growth temperature (Berry and Bjorkman 1980). Additionally, both photosynthesis and respiration are known to respond to a direct increase in measurement temperatures, which, once combined with the photosynthetic and respiratory adjustments, can result in either an enhancement or a reduction in performance at the new growth conditions

(termed constructive or detractive acclimation by Way and Yamori (2013)). Therefore, this experiment evaluated thermal acclimation of photosynthesis by assessing photosynthetic parameters (A_{net} , V_{cmax} , J_{max} , and ETR) across treatments at both a common leaf temperature (16 °C) and at the growth temperature. One of the most prominent findings of my work is the lack of photosynthetic acclimation to an 8 °C increase in growth temperature in both *D. antarctica* and *C. quitensis*. The direct temperature response varied between species, and was ultimately responsible for the increased performance in their growth environment.

4.1.1 Neither species showed thermal acclimation of photosynthesis across an 8 °C increase in growth temperature

Photosynthetic performance, evaluated by the net CO₂ assimilation rate (A_{net}), showed no acclimation to growth temperatures in either *D. antarctica* or *C. quitensis*: measurements at a common set of conditions showed no significant temperature response. This is coupled with a lack of acclimation in both maximum Rubisco carboxylation rate (V_{cmax}) and the maximum electron transport rate (J_{max}) to growth temperature. Photosynthetic capacity (V_{cmax} and J_{max}) and the balance between carboxylation and RuBP regeneration ($V_{\text{cmax}}:J_{\text{max}}$ ratio) are usually responsible for thermal acclimation of photosynthesis (Hikosaka et al. 2006); therefore, the consistent response of these three parameters to the 8 °C range in growth temperature all pointed towards minimal plasticity in photosynthetic capacity in both species.

A lack of thermal adjustment in photosynthesis has been previously documented in these two species by Xiong et al. (2000). When grown at 7, 12, or 20 °C, neither *D. antarctica* nor *C. quitensis* showed a shift in the thermal optimum of photosynthesis, despite the demonstrated full thermal acclimation of respiration. The lack of photosynthetic plasticity in an Antarctic population of *C. quitensis* has been demonstrated (Sierra-Almeida et al. 2007). A change in growth temperature from 4 to 15 °C resulted in a much larger shift in the thermal optimum (T_{opt}) of photosynthesis in *C. quitensis* from the Andes, where temperature is both higher and more variable, compared to the population from the Maritime Antarctic. Additionally, the lower plasticity in the Antarctic population also

suggests that the evolutionary history on the continent (i.e. a cold but stable climate) might contribute to the lack of acclimation potential of photosynthesis in both species.

Measurements of A_{net} include photosynthesis, photorespiration, and mitochondrial respiration. The thermal acclimation of respiration could therefore influence the acclimatory response, or lack thereof, of A_{net} to growth temperature. Xiong et al. (1999), for example, demonstrated that on sunny and warm days (average temperature above 20 °C), it was the high respiratory losses that resulted in poor net carbon gain in both *D. antarctica* and *C. quitensis*. In my experiment, dark respiration rates (R_{dark}) did not acclimate to increasing growth temperature or show a direct increase in response to measurement temperature; the treatment response of A_{net} , therefore, is not caused by respiratory shifts.

Many studies find respiration acclimates more readily to a change in growth temperature than does photosynthesis, and the positive response of R_{dark} to increasing measurement temperature is well established (Atkins and Tjoelker 2003, Way and Oren 2010). Therefore, the lack of acclimation of R_{dark} in my experiment was unexpected. This could be either a result of large variability in the data, or a true lack of plasticity in respiration of the two species. Regarding the first point, given the small absolute value of the respiration rates (approximately 1-3 $\mu\text{mol CO}_2 \text{ m}^{-2} \text{ s}^{-1}$), the magnitude of the variability inherent to the gas exchange system (approximately 1 $\mu\text{mol CO}_2 \text{ m}^{-2} \text{ s}^{-1}$), and the sample size of six, the values produced would be much more variable. In fact, Xiong et al. (2000) conducted gas exchange measurements on the whole canopy, which produced larger fluxes, found full thermal acclimation of R_{dark} in both species. On the other hand, Larigauderie and Körner (1995), Loveys et al. (2003), and Atkin et al. (2006) all found large variations in the degree of thermal acclimation of respiration among species. Specifically, both Larigauderie and Körner (1995) and Atkin et al. (2006) found alpine plants to possess much less plasticity in both respiration and photosynthesis when grown under warmer conditions compared to lowland species, and it is likely that the same applies to *D. antarctica* and *C. quitensis*, which are adapted to cold, extreme conditions. Thermal acclimation of Rubisco carboxylation (V_{cmax}) and RuBP regeneration (J_{max}) is often considered the mechanism of thermal acclimation in photosynthesis (Hikosaka et al.

2006), and thus is often used to evaluate thermal acclimation of photosynthesis (Way and Yamori 2013). Thermal acclimation of V_{cmax} and J_{max} usually includes an upward shift in the thermal optima of these two parameters (Kattge and Knorr 2007), as well as a shift in the $V_{\text{cmax}}:J_{\text{max}}$ ratio when both are extrapolated to (or measured at) a common temperature (Hikosaka et al. 2006). In this study, neither *D. antarctica* or *C. quitensis* showed a change in V_{cmax} or J_{max} when measured at a common temperature, providing further evidence supporting the lack of thermal plasticity in both Antarctic species.

Even though this experiment was not set up to evaluate the thermostability of the thylakoid membranes, measurements of the maximal photochemical efficiency (F_v/F_m), PSII quantum yield (Φ_{PSII}) and electron transport rate (ETR) from chlorophyll fluorescence could inform us of the performance of PSII photochemistry and electron transport. F_v/F_m did not show any biologically meaningful changes across treatments in either species. Meanwhile, ETR was down-regulated at high growth temperatures in both species, which, once combined with the positive effect of measurement temperature, resulted in either the same (in *D. antarctica*) or improved ETR (in *C. quitensis*) under the growth temperature. This trend suggests the ability of PSII electron transport in *D. antarctica* to acclimate to changes in growth temperature.

Mawson and Cummins (1989), Yamasaki et al. (2002), and Xu and Zhou (2006) have suggested that the thermal acclimation of ETR and Φ_{PSII} could contribute to the acclimation of A_{net} to changes in growth temperature. However, this experiment saw an uncoupling of these two processes: there was thermal acclimation of ETR without an accompanying trend in A_{net} in either species. J_{max} , derived from gas exchange measurements, reveals electron transport rate assuming CO_2 is the only acceptor, while ETR, measured with chlorophyll fluorescence, reflects electron transport from PSII, which could be used in CO_2 fixation or other alternative sinks. The thermal acclimation of ETR in both *D. antarctica* and *C. quitensis* without an accompanied acclimatory response in J_{max} suggests that while PSII electron transport had the capacity to acclimate to a higher growth temperature, the rate of electron transport to CO_2 was largely unaffected by growth temperature.

The lack of thermal acclimation of photosynthesis in both Antarctic vascular plant species was a surprising, but not irregular, finding. The potential of photosynthesis to thermally acclimate greatly varies among species (Yamori et al. 2014). Cool-adapted plants are thought to have much less thermal acclimation potential in photosynthesis compared to warmer-adapted species. For example, Atkin et al. (2006) demonstrated that the alpine *Plantago euryphylla* showed little thermal acclimation of photosynthesis and respiration compared to two lowland congeners when grown under warm temperatures. Similarly, while desert clones of *Atriplex lentiformis* fully acclimated and had enhanced photosynthetic performance at high temperature, their coastal counterparts did not show any plasticity to temperature and suffered thermal damage (Pearcy 1977). In this case, neither *D. antarctica* or *C. quitensis* specimens collected from Antarctica showed thermal plasticity of photosynthesis, while there has been evidence that populations living outside of Antarctica have a larger acclimation potential (Sierra-Almeida et al. 2007). Hence, one could postulate that the long evolutionary history of the Antarctic ecotype in the stable and thermally extreme environment of Antarctica largely contributes to the limited plasticity in photosynthesis when both species is grown in a new environment.

4.1.2 Photosynthetic performance at growth temperature was driven by direct responses to measurement temperature

Direct temperature response of photosynthetic parameters has been well established: net CO₂ assimilation rate (A_{net}), maximum Rubisco carboxylation rate (V_{cmax}), and maximum electron transport rate (J_{max}) all respond positively to rising measurement temperature (Berry and Bjorkman 1980, Medlyn et al. 2002, Way and Oren 2010). The thermal optimum of A_{net} tends to be lower than that of V_{cmax} or J_{max} , and correlates with the growth temperature of the species (Medlyn et al. 2002, Yamori et al. 2014). The positive response of these parameters to measurement temperature is expected, and needs to be considered when evaluating photosynthetic performance across treatments.

In *D. antarctica*, net CO₂ assimilation rates (A_{net}) increased linearly with measurement temperature, which correlated with a direct temperature stimulation of the maximum Rubisco carboxylation rates (V_{cmax}) and maximum electron transport rates (J_{max}). The linear rise in A_{net} with rising leaf temperature suggested that 12, 16, and 20 °C all fell

below the thermal optimum of A_{net} . While this finding contradicts the findings by Xiong et al. (2000), who reported an optimal temperature for photosynthesis of approximately 10 °C in *D. antarctica*, it matches the temperature response curve data from the same experimental plants (Sanhueza et al., unpublished data). Overall, the lack of thermal acclimation and the strong response to measurement temperature resulted in an enhanced photosynthetic performance at elevated growth temperatures.

In contrast with *D. antarctica*, *C. quitensis* photosynthesis showed no response to increasing measurement temperature. Neither V_{cmax} nor J_{max} showed any temperature sensitivity and, as a result, A_{net} did not respond to increases in measurement temperature. This lack of response is uncommon, and may not reflect a true lack of temperature sensitivity in the species. Instead, the missing 12/AC treatment, the low sample size, or the narrow range of temperature exposure could make it difficult to detect small but significant temperature response. The temperature response curve of A_{net} from the same experiment saw very little change in A_{net} between 12 and 20 °C (Sanhueza et al., unpublished data), although a positive response to measurement temperatures from 5 to 35 °C still existed. Additionally, limitations in CO₂ diffusion could offer another explanation. In *C. quitensis*, the C_i/C_a ratio, an indicator of CO₂ diffusion from the atmosphere to the intercellular air space, showed a decline at high leaf temperatures, suggesting that CO₂ uptake was limited at high measurement temperature, potentially due to stomatal closure. Overall, photosynthesis in *C. quitensis* did not acclimate to warmer growth temperature, and demonstrated little response to increasing measurement temperature; consequently, *C. quitensis* photosynthetic performance remained fairly constant across the temperature changes in this experiment.

4.2 Enhanced photosynthesis at elevated CO₂ is mostly due to the direct CO₂ effect

4.2.1 Photosynthesis in both species was enhanced by direct exposure to elevated CO₂

Because CO₂ is the main substrate for photosynthesis, increasing CO₂ concentrations lead to higher net CO₂ assimilation rates (A_{net}) by providing more substrate for carboxylation. Additionally, a higher internal CO₂ concentration also inhibits photorespiration, further enhancing the efficiency of Rubisco (Drake et al. 1997). This short-term response has

been well-established when plants are exposed to elevated CO₂ concentrations, although the magnitude of the response might vary (Ainsworth and Roger 2007). In fact, under elevated atmospheric CO₂ (a higher C_a), both *D. antarctica* and *C. quitensis* saw an increase in C_i/C_a ratio, which suggests the CO₂ supply for carboxylation was enhanced. As a result, the increased A_{net} in both *D. antarctica* and *C. quitensis* when exposed to their growth CO₂ is expected.

4.2.2 Photosynthesis was down-regulated at elevated CO₂ in *D. antarctica*

After longer exposure to elevated CO₂, the stimulation of photosynthesis results in a larger quantity of carbohydrates synthesized through the Calvin cycle. The buildup of carbohydrates in the leaf elicits a sink feedback inhibition that down-regulates photosynthesis, a common response in plants grown at elevated CO₂. The down-regulation of photosynthesis at elevated growth CO₂ is usually manifested as a decrease in A_{net} when measured under a common CO₂ concentration. In fact, *D. antarctica* grown under elevated CO₂ did show a 25% down-regulation in A_{net}, but *C. quitensis* did not.

The down-regulation of photosynthesis at elevated CO₂ is usually attributed to a reduction in Rubisco activation state, Rubisco content, or leaf nitrogen allocated to Rubisco (Ainsworth and Rogers 2007). These responses are not mutually exclusive, but ultimately result in a decrease in maximum Rubisco carboxylation rate (V_{cmax}). A decrease in V_{cmax}, however, was not observed in *D. antarctica*. Stitt (1991) discussed the possibility of a direct feedback inhibition of photosynthesis from accumulation of carbohydrates and inorganic phosphate (P_i) limitation, instead of a regulation through Rubisco. Additionally, excess accumulation of starch could also damage the chloroplast and decrease CO₂ assimilation rates (Stitt 1991). However, evidence for these responses in the literature is rare, and data from my study do not allow for such interpretation. Meanwhile, in *D. antarctica*, the acclimation of stomatal conductance to elevated CO₂ was unlikely to cause the decrease in A_{net}. The C_i/C_a ratio in *D. antarctica* was higher in elevated CO₂ plants when measured at a common CO₂ concentration, which suggests that there was sufficient CO₂ in the intercellular air space, and that the decrease in A_{net} is a response of a lower CO₂ assimilation rate itself.

Additionally, CO₂ diffusion from the intercellular air space to the chloroplast could potentially account for the lack of V_{cmax} and J_{max} responses. My photosynthetic model assumed no resistance along this pathway in the calculation of apparent V_{cmax} and J_{max}. However, this assumption might not always hold, as mesophyll conductance has been demonstrated to decrease with elevated CO₂ as leaves become thicker and denser (Luo et al. 1994). Anatomically, there was no change in the density of mesophyll cells or intercellular air space in *D. antarctica* under elevated CO₂ that could suggest any physical changes to the diffusion pathway. Nevertheless, mesophyll conductance could also change via shifts in biochemistry, such as the diffusion of CO₂ in the aqueous phase, transport through aquaporins, or conversion by carbonic anhydrase (Bernacchi et al. 2002), none of which could be estimated in this experiment.

While there was no decrease in V_{cmax}, *D. antarctica* still had other responses typical of plants grown under elevated CO₂, including a decrease in leaf nitrogen (N) and specific leaf area (SLA), which could have implications for photosynthesis. The decrease in leaf N content was likely a result of N dilution through increasing leaf mass. As plants grown at elevated CO₂ accumulate more carbohydrates, their SLA decreases as leaf mass increases; as a result, the same amount of N is now expressed against a larger leaf dry mass, leading to lower leaf N content (Luo et al. 1994).

4.2.3 There was no CO₂ acclimation in *C. quitensis*

Elevated CO₂ directly stimulated A_{net} in *C. quitensis*, but no down-regulation was observed in A_{net}, V_{cmax}, or J_{max}. Additionally, the C_i/C_a ratio was higher in elevated CO₂ plants when measured at a common ambient CO₂ level, implying no diffusion limitations as a result of an acclimatory decline in stomatal conductance. In fact, with a higher C_i/C_a ratio at a common measurement CO₂, one would expect the observed direct stimulation of A_{net} by elevated CO₂. The lack of acclimation to elevated CO₂ in *C. quitensis* is therefore less likely an idiosyncratic response, and more likely suggests the presence of alternate carbohydrate sinks.

As previously mentioned, a down-regulation of photosynthesis at elevated CO₂ usually originates from an imbalance between production and consumption of carbohydrates (Drake et al. 1997). While A_{net} in *C. quitensis* was enhanced under elevated growth CO₂,

which suggests a larger capacity to produce carbohydrates, there was no change in SLA in plants grown under elevated CO₂, implying the excess photosynthates were not stored in the leaf. It can be postulated that consumption of carbohydrates could be enhanced elsewhere in the plant, removing the source-sink imbalance that would otherwise down-regulate photosynthesis. One possible explanation is the observed presence of flowers in *C. quitensis* during the measurement period: flower production could be one of the additional carbohydrate sinks that increased carbohydrate consumption. In fact, Lewis et al. (2002) also found no photosynthetic down-regulation in the period leading up to flowering and during fruit production in *Xanthium strumarium*.

Overall, *D. antarctica* exhibited an approximately 25% down-regulation of photosynthesis in plants grown at elevated CO₂, while no acclimation was observed in *C. quitensis*. Photosynthesis in both species, on the other hand, responded positively to high CO₂ levels. Together, under elevated growth CO₂, the direct CO₂ effect overwhelmed any down-regulation of photosynthesis, if any, and resulted in a higher capacity to assimilate CO₂ in both species. Ultimately, the enhancement of photosynthesis at elevated CO₂ had significant implications for the growth and performance of both *D. antarctica* and *C. quitensis*.

4.3 Leaf anatomy showed little plasticity, except in *D. antarctica* stomatal grooves

4.3.1 There were no major changes in leaf morphology in either species

While photosynthetic parameters are very sensitive to measurement conditions, leaf anatomy directly reflects effects of the growth conditions. In this experiment, there were no changes in the proportions of measured tissues in the leaf cross-sections in either *D. antarctica* or *C. quitensis* under the various treatments, which offers additional evidence for the small degree of acclimation of photosynthesis to variations in growth conditions. The general lack of acclimation to warming and elevated CO₂ in photosynthetic parameters was coupled with a lack of change in the quantity of the photosynthetic tissues. Furthermore, the aphid attack resulted in the loss of the 12/AC treatment in all comparisons of photosynthetic parameters. Here, because leaf structure of *C. quitensis* in 12/AC likely remained the same despite the aphid attack, the lack of structural response

across all six treatments further reinforced the conclusion that little acclimation occurred in *C. quitensis* under either warming or elevated CO₂.

4.3.2 Modified stomatal groove structure in *D. antarctica* suggests high moisture stress at high temperature

Anatomical features in *D. antarctica* leaves mostly reflect their growth environment, regardless of the level of genetic diversity (Chwedorzewska et al. 2008). The most prominent change in leaf anatomy was the modifications in stomatal groove structure in *D. antarctica*. Grass blades of *D. antarctica* tended to roll inward towards the adaxial side, creating stomatal grooves. This is where a high concentration of stomata occur, supposedly creating an air pocket with high humidity and preventing water loss (Ellis 1976). At warmer growth temperatures, both stomatal groove depth and width decreased as a direct response to the larger evaporative demand in warmer treatments. This study, like most warming experiments, did not control for vapor pressure deficit; therefore, at constant relative humidity, VPD increased with temperature, resulting in larger evaporative demand (Oishi et al. 2010). Therefore, the shift in the stomatal groove towards a more xeromorphic structure in warmer treatments served to recapture water lost through transpiration, likely limiting water loss to the atmosphere. This morphological acclimation came with a trade-off, however. A more tightly packed groove, while preventing water from escaping the leaf, also prevented CO₂ from diffusing into the intercellular air space, evidenced by a significant decrease in C_i/C_a ratio when measured at the growth conditions.

Qualitatively, leaf cross-sections also showed an absence of bulliform cells in *D. antarctica*. Bulliform cells are very large, thin-walled cells located on the epidermis at the bottom of the stomatal grooves to facilitate the folding and unfolding of the leaf blade through changes in stomatal groove width (Fig. 4.1). These cells lose water easily under dry conditions, and as they do, stomatal grooves shrink in size, the leaf blade folds, and water loss is minimized. The loss of this tissue has been previously observed in *D. antarctica* grown at a drier habitat compared to those developing at a coastal site in Antarctica (Chwedorzewska et al. 2008), as well as in greenhouse plants grown at 16-18 °C, compared to those grown at 2 °C or 13 °C (Romero et al. 1999, Gielwanowska et

al. 2005). The lack of bulliform cells in *D. antarctica* plants shown here suggests leaf unrolling was not regulated in their growth environment, and that the dry conditions in my experiment forced the leaf blades to stay constantly rolled. The absence of bulliform cells in the *D. antarctica* specimen in this experiment further supports a previous interpretation of the stomatal groove dimensions: without bulliform cells to facilitate leaf rolling or unrolling, stomatal groove dimensions were developmentally set. Hence, stomatal groove depth and width reflect the effects of the long-term exposure to the experimental growth conditions rather than the transient condition at the time of sample collection.

4.4 Leaf-level photosynthetic responses did not always translate to growth

While neither *D. antarctica* and *C. quitensis* displayed thermal acclimation of photosynthesis, and both showed some degree of acclimation to elevated CO₂, photosynthesis in both species was stimulated by a direct effect of high temperature and high CO₂. These measurements also allow an assessment of *D. antarctica* and *C. quitensis* photosynthetic performance in their treatment conditions that, when extrapolated to the whole-plant level, should correlate with the trends in biomass accumulation. A mismatch between leaf-level photosynthesis and whole-plant growth response can reveal either patterns in the partitioning of photosynthates towards other sinks, or changing variables and processes under the new growth environment.

4.4.1 Biomass accumulation was enhanced at elevated CO₂ in both species

In both species, photosynthesis was stimulated by elevated CO₂ in the growth environment, even when the down-regulatory response was accounted for. This trend directly translated to larger aboveground and belowground biomass in both *D. antarctica* and *C. quitensis*. This response is quite common (Ainsworth and Long 2005): while the magnitude of the stimulation of growth under elevated CO₂ is variable (Curtis and Wang 1998), *D. antarctica* biomass increased by 46%, and *C. quitensis* by 33% under elevated CO₂, both slightly higher than the average for C₃ plants (approximately 20%) as compiled by Ainsworth and Long (2005).

4.4.2 Warming did not consistently enhance growth

In contrast, the effect of warming on growth is more complex than that of elevated CO₂, due to the integrated temperature responses of various processes involved in growth and biomass accumulation. Since photosynthesis did not thermally acclimate in either *D. antarctica* or *C. quitensis*, performance at the growth condition reflects a direct response to high measurement temperature. While *D. antarctica* responded positively, *C. quitensis* was not responsive to increases in measurement temperature. The capacity to assimilate CO₂ at the growth conditions should translate to a similar trend in biomass accumulation; however, this is not always the case.

In *D. antarctica*, the accumulation of both aboveground and belowground biomass was enhanced under moderate warming (+4 °C), as suggested by the greater A_{net} at the growth conditions. This result agrees with most moderate warming experiments across ecosystems, which observe a stimulation of plant productivity by 19-20% (Rustad et al. 2001, Lin et al. 2010). However, under a growth temperature of 20 °C, the stimulation of photosynthesis did not translate to higher biomass. Meanwhile, photosynthesis in *C. quitensis* did not acclimate to growth temperature or respond to measurement temperature. Under the growth conditions, 20 °C treatments had a lower A_{net} (approximately 35% the rate of a cooler-grown plant at the same CO₂ level); however, the poor photosynthetic performance of plants grown in warmer treatments was quite evident in biomass. Total biomass in the warmest treatments was 30 to 60% lower than that produced by a cooler-grown plants at the same growth CO₂, a response that could not be accounted for by the poor photosynthetic performance alone.

There could be a number of explanations for the mismatch in whole-plant biomass accumulation and leaf-level photosynthesis in warmer treatments in *D. antarctica* and *C. quitensis*. First of all, in *D. antarctica*, the aforementioned modifications in stomatal groove structure at high growth temperature could potentially account for the suppression of growth in the warmest treatments. As stomatal grooves became smaller to minimize water loss, CO₂ diffusion becomes more limiting. Gas exchange measurements of photosynthetic parameters were performed at a relatively constant vapor pressure deficit, which served to assess the capacity of the photosynthetic machinery itself. Under the

growth condition, however, this measured capacity was not realized due to the high VPD at warmer treatments. As evidenced by the decline in the C_i/C_a ratio in both species and changes in stomatal groove structure in *D. antarctica*, in warmer treatments, the pressure to conserve water was high enough that CO_2 diffusion was reduced, resulting in lower CO_2 assimilation and as a result, reduced growth. Likewise, the aforementioned decreasing C_i/C_a in *C. quitensis* at high temperature could also suggest CO_2 diffusion limitations, which could be amplified under extended exposure to the growth conditions, and resulted in lower biomass accumulation under warming.

Atkin et al. (2007) suggested that short-term changes in photosynthesis (A) and respiration (R) and more importantly, the balance between the two (the R:A ratio), play a key role in whole-plant CO_2 exchange. While some studies suggest the R:A ratio reaches homeostasis regardless of the intrinsic growth rate (Loveys et al. 2003), both acclimation and short-term response to temperature might disrupt this homeostasis (Campbell et al. 2007, Way and Yamori 2014). In species with little thermal plasticity in photosynthesis or respiration, such as *Plantago euryphylla* (Atkin et al. 2007), high growth temperatures suppress daily net carbon gain, as night time respiratory losses are a higher proportion of the carbon gained during the day. On the other hand, full thermal acclimation of respiration to a higher growth temperature and a lower night temperature could enhance biomass accumulation even though photosynthesis does not acclimate (Xiong et al. 2000). In the cases of *D. antarctica* and *C. quitensis*, while photosynthesis was stimulated under high leaf temperature, respiration rates did not show any thermal acclimation. Because growth temperatures were constant between day and night in this experiment, respiratory losses at night could be especially high in the warmest treatment.

4.4.3 *D. antarctica* and *C. quitensis* performance in future climates

Fowbert and Smith (1994) reported significant expansion in the populations of both *D. antarctica* and *C. quitensis* over the second half of the 20th century, which was attributed to the rapid warming in Antarctica over the same period. Enhanced growth has previously been observed in both species under warmer growth temperatures in the field (Day et al. 1999) and greenhouse (Xiong et al. 2000). My work has demonstrated that increasing growth temperatures by 4 °C in fact promoted growth in *D. antarctica*. Additionally,

elevated CO₂ promoted growth in both species, without any interaction between warming and elevated CO₂. Consequently, population growth in *D. antarctica* from 1960 to 2000 could have been a result of both warmer growth temperature and the increasing atmospheric CO₂, considering warmer temperatures over this period were coupled with rising CO₂. However, both moderate and severe warming suppressed growth in *C. quitensis*. One could postulate that the slower population growth in the second half of the 20th century in *C. quitensis* compared to *D. antarctica* could therefore have been due to the poor performance of the species at warm temperatures, without ruling out the differences in growth habits between the two species.

Although *D. antarctica* benefited from moderate warming, the trend of increasing plant productivity might not hold if warming intensifies. This experiment has also shown that growth was suppressed in both species at a growth temperature of 20 °C. This decrease in growth is not from a limitation in the photosynthetic machinery itself, but may be linked to either higher respiratory losses, CO₂ diffusion limitations, or other causes. Therefore, changes in other environmental conditions in Antarctica, such as the extent of night warming or the plant water status in future climates, could also alter the growth response of the two vascular plants. Based on my findings, under very high greenhouse gas emission scenarios, severe warming might decrease growth in both vascular plant species in Antarctica, which could potentially alter the carbon budget and nutrient dynamics of the terrestrial ecosystem of the continent.

Both *D. antarctica* and *C. quitensis* are key inputs of C and N to the intrinsically poor Antarctic soils (Beyer et al. 2000). Therefore, changes in the population sizes of these two species could affect the future carbon stocks in Antarctica, especially when the two species are differentially affected under future climates. The warming trend and altered species composition could impact the carbon pool in the soil and indirectly affect the growth of nonvascular vegetation (Day et al. 2008).

4.5 Future directions

To better evaluate the temperature and CO₂ response of *D. antarctica* and *C. quitensis*, future studies could use chlorophyll fluorescence to estimate mesophyll conductance (Harley et al. 1992). This method characterizes changes to the diffusion pathway of CO₂ from the intercellular air space to the site of carboxylation in the chloroplast, arriving at an estimate of mesophyll conductance. In this experiment, mesophyll conductance was assumed to be infinite, although studies have shown that it can vary with temperature and CO₂ (Bernacchi et al. 2002). Additionally, having an estimate of mesophyll conductance would allow calculations of the CO₂ concentration at the chloroplast (C_c), which is the CO₂ concentration used in carboxylation, and would offer a better estimate of V_{cmax} and J_{max} .

Thermal acclimation of photosynthesis in this study was evaluated by measuring gas exchange parameters under the growth temperature and again at a common temperature of 16 °C. This method, however, did not allow estimates of the optimal temperature of A_{net} , or any actual shifts in the temperature response curve. Future studies, therefore, should investigate the short-term temperature response of photosynthesis over a larger range of temperature and use the thermal optimum to evaluate thermal acclimation. Similarly, the acclimation response to elevated CO₂, or the lack thereof, is often linked to the pool of carbohydrates. Having an estimate of total non-structural carbohydrates, and soluble sugars, would allow a more established link between feedback inhibition and down-regulation of photosynthesis.

Future studies can design warming experiments that control vapor pressure deficit, which affects stomatal regulation. With a constant relative humidity, VPD increased with temperature and became a confounding factor in this experiment. As a result, CO₂ diffusion decreases when stomatal conductance is reduced by a high VPD. Although allowing VPD to fluctuate better reflects future climates, constant VPD experiments lend to better understanding of the underlying mechanism of temperature response of photosynthesis. Additionally, it would be interesting to emulate the daily temperature fluctuation in Antarctica, and potentially look at its effect on photosynthetic acclimation compared to a constant growth temperature. While the experimental period coincided

with the austral summer, exposure of *D. antarctica* and *C. quitensis* to a photoperiod much shorter than their summer could have unanticipated effects. Considering the very short growing season and long photoperiod in their native habitat, it would also be interesting to investigate the interplay of increasing temperature and constant photoperiod on the ability of plants to take advantage of the longer photosynthetic time and shorter period of respiratory losses.

While this study provided some insights into the response of *D. antarctica* and *C. quitensis* in future climates, extrapolating the result to the performance of the two species in Antarctica on a larger scale should be conducted with care. First of all, performance of plants grown in the lab could differ from that in the field, especially in terms of leaf anatomy (Romero et al. 1999) and photochemical efficiency (Casanova-Katny et al. 2010). Additionally, this experiment investigated vegetative growth only, leaving out the effects of temperature and CO₂ on the reproductive output of the two species. Even if only vegetative growth was considered, other factors such as the availability of ice-free surface, as well as suitable microhabitat including nutrients, light availability, or wind, could hinder the spread of both species despite the favorable temperature and CO₂ conditions. Future studies should investigate these topics to arrive at a better prediction of the performance of these two species under climate change.

4.6 Conclusions

This study investigated the photosynthetic and morphological responses of two Antarctic vascular plants, *Deschampsia antarctica* and *Colobanthus quitensis*, to warming and elevated CO₂. Overall, neither species showed thermal plasticity of the photosynthetic apparatus to increasing growth temperatures. *D. antarctica* showed some down-regulation of photosynthesis to elevated CO₂, but *C. quitensis* did not acclimate to elevated CO₂. In their growth environment, photosynthesis was stimulated by short-term increases in leaf temperature and atmospheric CO₂ in *D. antarctica*, and by elevated CO₂ in *C. quitensis*. However, these trends did not translate directly to growth. Biomass accumulation in both species was enhanced at elevated CO₂, but was suppressed under warming of +8 °C in *D. antarctica* and at all warmer temperatures in *C. quitensis*. Leaf

structures of *D. antarctica* were modified at high growth temperatures to prevent moisture stress, but this also presents a challenge for CO₂ diffusion that could potentially limit biomass accumulation at high growth temperature.

I have proposed physiological mechanisms that may help explain the documented enhanced growth in both Antarctic vascular species. My results also suggest that in future climates, both vascular species in Antarctica will benefit from elevated CO₂; however, severe warming can potentially suppress growth in both species, not due to damage to the photosynthetic apparatus, but likely from either enhanced respiratory losses or CO₂ diffusion limitations under warmer conditions. The study also offers useful insights for climate models predicting the carbon cycling of Antarctica under climate change. Scaling leaf-level gas exchange parameters to whole-plant performance to predict the performance of *D. antarctica* and *C. quitensis* needs to consider other abiotic factors, such as moisture availability.

References

- Ainsworth EA, Long SP (2005) What have we learned from 15 years of free-air CO₂ enrichment (FACE)? A meta-analytic review of the responses of photosynthesis, canopy properties and plant production to rising CO₂. *New Phytol* 165:351–372.
- Ainsworth EA, Rogers A (2007) The response of photosynthesis and stomatal conductance to rising [CO₂]: mechanisms and environmental interactions. *Plant Cell Environ* 30:258–270.
- Alberdi M, Bravo LA, Gutierrez A, Gidekel M., Corcuera LJ (2002) Ecophysiology of Antarctic vascular plants. *Physiol Plant* 115:479–486.
- Amthor JS (2000) Direct effect of elevated CO₂ on nocturnal in situ leaf respiration in nine temperate deciduous tree species is small. *Tree Physiol* 20:139–144.
- Anderson, JM (1986) Photoregulation of the composition, function, and structure of thylakoid membranes. *Ann Rev Plant Physiol* 37:93-136.
- Arp W. (1991) Effects of source-sink relations on photosynthetic acclimation to elevated CO₂. *Plant, Cell Environ* 14:869–875.
- Atkin OK, Evans JR, Siebke K (1998) Relationship between the inhibition of leaf respiration by light and enhancement of leaf dark respiration following light treatment. *Aust J Plant Physiol* 25:437-443.
- Atkin OK, Scheurwater I, Pons TL (2006) High thermal acclimation potential of both photosynthesis and respiration in two lowland *Plantago* species in contrast to an alpine congeneric. *Glob Chang Biol* 12:500–515.
- Atkin OK, Scheurwater I, Pons TL (2007) Respiration as a percentage of daily photosynthesis in whole plants is homeostatic at moderate, but not high, growth temperatures. *New Phytol* 174:367–380.
- Atkin OK, Tjoelker MG (2003) Thermal acclimation and the dynamic response of plant respiration to temperature. *Trends Plant Sci* 8:343–351.
- Bascuñán-Godoy L, García-Plazaola JI, Bravo LA, Corcuera LJ (2010) Leaf functional and micro-morphological photoprotective attributes in two ecotypes of *Colobanthus quitensis* from the Andes and Maritime Antarctic. *Polar Biol* 33:885–896.
- Bergstrom D, Chown SL (1999) Life at the front: history, ecology and change on southern ocean islands. *Trends Ecol Evol* 14:472–477.
- Bernacchi CJ, Pimentel C, Long SP (2003) *In vivo* temperature response functions of parameters required to model RuBP-limited photosynthesis. *Plant Cell Environ* 26:1419–1430.
- Bernacchi CJ, Portis AR, Nakano H, von Caemmerer S, Long SP (2002) Temperature response of mesophyll conductance. Implications for the determination of Rubisco enzyme kinetics and for limitations to photosynthesis *in vivo*. *Plant Physiol*

130:1992–1998.

- Berry JA, Björkman O (1980) Photosynthetic response and adaptation to temperature in higher plants. *Annu Rev Plant Physiol* 31:491–543.
- Beyer L, Bolter M, Seppelt RD (2000) Nutrient and thermal regime, microbial biomass, and vegetation of antarctic soils in the Windmill Islands region of East Antarctica (Wilkes Land). *Arct Antarct Alp Res* 32:30–39.
- Bravo LA, Griffith M (2005) Characterization of antifreeze activity in Antarctic plants. *J Exp Bot* 56:1189–1196.
- Bravo LA, Ulloa N, Zuniga GE, Casanova A, Corcuera LJ, Alberdi M (2001) Cold resistance in Antarctic angiosperms. *Physiol Plant* 111:55–65.
- Bromwich DH, Nicolas JP, Monaghan AJ, Lazza MA, Keller LM, Weidner GA, Wilson AB (2012) Central West Antarctica among the most rapidly warming regions on Earth. *Nat Geosci* 6:139–145.
- Campbell C, Atkinson L, Zaragoza-Castells J, et al. (2007) Acclimation of photosynthesis and respiration is asynchronous in response to changes in temperature regardless of plant functional group. *New Phytol* 176:375–389.
- Casanova-Katny MA, Zúñiga GE, Corcuera LJ, Bravo LA, Alberdi M (2010) *Deschampsia antarctica* Desv. primary photochemistry performs differently in plants grown in the field and laboratory. *Polar Biol* 33:477–483.
- Chapman W, Walsh JE (2007) A synthesis of Antarctic temperatures. *J Clim* 20:4096–4117.
- Chwedorzewska KJ, Gielwanowska I, Szczuka E, Bochenek A (2008) High anatomical and low genetic diversity in *Deschampsia antarctica* Desv. from King George Island, the Antarctic. *Polish Polar Res* 29:377–386.
- Convey P (2010) Terrestrial biodiversity in Antarctica - Recent advances and future challenges. *Polar Sci* 4:135–147.
- Convey P (1996a) Reproduction of Antarctic flowering plants. *Antarct Sci* 8:127–134.
- Convey P (1996b) The influence of environmental characteristics on life history attributes of antarctic terrestrial biota. *Biol Rev* 71:191–225.
- Convey P, Gibson JAE, Hillenbrand CD, Hodgson DA, Pugh PJA, Smellie JL, Stevens MI (2008) Antarctic terrestrial life - Challenging the history of the frozen continent? *Biol Rev* 83:103–117.
- Curtis PS (1996) A meta-analysis of leaf gas exchange and nitrogen in trees grown under elevated carbon dioxide. *Plant, Cell Environ* 19:127–137.
- Curtis PS, Wang X (1998) A meta-analysis of elevated CO₂ effects on woody plant mass, form, and physiology. *Oecologia* 113:299–313.
- Day TA, Ruhland CT, Grobe CW, Xiong F (1999) Growth and reproduction of Antarctic

- vascular plants in response in the field reductions and UV radiation to warming. *Oecologia* 119:24–35.
- Day TA, Ruhland CT, Xiong FS (2008) Warming increases aboveground plant biomass and C stocks in vascular-plant-dominated Antarctic tundra. *Glob Chang Biol* 14:1827–1843.
- Drake BG, Gonzalez-Meler MA, Long SP (1997) More efficient plants: A consequence of rising atmospheric CO₂? *Annu Rev Plant Physiol Plant Mol Biol* 48:609–639.
- Edwards JA (1972) Studies in *Colobanthus quitensis* (Kunth) Bartl, and *Deschampsia antarctica* Desv.: V. Distribution, ecology and vegetative performance on Signy Island. *Br Antarct Surv Bull* 28:11–28.
- Ellis RP (1976) A procedure for standardizing comparative leaf anatomy in the Poaceae. I. The leaf-blade as viewed in transverse section. *Bothalia* 12:65–109.
- Ellis-Evans J., Walton D (1990) The process of colonization in Antarctic terrestrial and freshwater ecosystems. *Proc NIPR Symp Polar Biol* 3:151–163.
- Farquhar GD, Sharkey TD (1982) Stomatal conductance and photosynthesis. *Annu Rev Plant Physiol* 33:317–345.
- Farquhar GD, von Caemmerer S, Berry JA (1980) A biochemical model of photosynthetic CO₂ assimilation in leaves of C₃ species. *Planta* 149:78–90.
- Field C, Berry JA, Mooney HA (1982) A portable system for measuring carbon dioxide and water vapour exchange of leaves. *Plant, Cell Environ* 5:179–186.
- Ferron FA, Simões JC, Aquino FE, Setzer AW (2004) Air temperature time series for King George Island, Antarctica. *Pesq Antárt Bras* 4:155–169.
- Fowbert JA, Smith RIL (1994) Rapid population increases in native vascular plants in the Argentine Islands, Antarctic Peninsula. *Arct Alp Res* 26:290–296.
- Fox AJ, Cooper APR (1998) Climate-change indicators from archival aerial photography of the Antarctic Peninsula. *Ann Glaciol* 27:636–642.
- Franzen LD, Gutsche AR, Heng-Moss TM, Higley LG, Sarath G, Burd JD (2007) Physiological and biochemical responses of resistant and susceptible wheat to injury by Russian wheat aphid. *J Econ Entomol* 100:1692–1703.
- Gianoli E, Inostroza P, Zúñiga-Feest A, Reyes-Diaz M, Cavieres LA, Bravo LA, Corcuera LJ (2004) Ecotypic differentiation in morphology and cold resistance in populations of *Colobanthus quitensis* (Caryophyllaceae) from the Andes of central Chile and the Maritime Antarctic. *Arctic, Antarct Alp Res* 36:484–489.
- Gielwanowska I, Szczuka E (2005) New ultrastructural features of organelles in leaf cells of *Deschampsia antarctica* Desv. *Polar Biol* 28:951–955.
- Gielwanowska I, Szczuka E, Bednara J, Gorecki R (2005) Anatomical features and ultrastructure of *Deschampsia antarctica* (Poaceae) leaves from different growing habitats. *Ann Bot* 96:1109–1119.

- Harley PC, Loreto F, Di Marco G, Sharkey TD (1992) Theoretical considerations when estimating the mesophyll conductance to CO₂ flux by analysis of the response of photosynthesis to CO₂. *Plant Physiol* 98:1429–36.
- Hikosaka K, Ishikawa K, Borjigidai A, Muller O, Onoda Y (2006) Temperature acclimation of photosynthesis: mechanisms involved in the changes in temperature dependence of photosynthetic rate. *J Exp Bot* 57:291–302.
- Holdgate MW (1977) Terrestrial ecosystems in the Antarctic. *Philos Trans R Soc London B, Biol Sci* 279:5–25.
- Holtom A, Greene W (1967) The growth and reproduction of Antarctic flowering plants. *Philos Trans R Soc* 252:323–337.
- Hopkins WG, Hüner NPA (2008) *An Introduction to Plant Physiology*. New York, NY, USA.
- IPCC (2014) *Climate Change 2014: Synthesis Report. Contribution of Working Groups I, II and III to the Fifth Assessment Report of the Intergovernmental Panel on Climate Change*. IPCC, Geneva, Switzerland, 151 pp.
- Jordan DB, Ogren WL (1984) The CO₂/O₂ specificity of ribulose 1,5-biphosphate carboxylase/oxygenase. *Planta* 161:308–313.
- Kattge J, Knorr W (2007) Temperature acclimation in a biochemical model of photosynthesis: A reanalysis of data from 36 species. *Plant, Cell Environ* 30:1176–1190.
- Kennedy AD (1995) Antarctic terrestrial ecosystem response to global environmental change. *Annu Rev Ecol Syst* 26:683–704.
- Kennedy AD (1993) Water as a limiting factor in the antarctic terrestrial environment - a biogeographical synthesis. *Arct Alp Res* 25:308–315.
- Komárková V (1985) Two native Antarctic vascular plants, *Deschampsia antarctica* and *Colobanthus quitensis*: a new southernmost locality and other localities in the Antarctic Peninsula area. *Arct Alp Res* 17:401–416.
- Lambers H, Chapin II FS, Pons TL (2008) *Plant physiological ecology*. Springer-Verlag New York, NY.
- Lamers PP, Janssen M, De Vos RCH, Bino RJ, Wijffels RH (2008) Exploring and exploiting carotenoid accumulation in *Dunaliella salina* for cell-factory applications. *Trends Biotechnol* 26:631–638.
- Larigauderie A, Korner C (1995) Acclimation of leaf dark respiration to temperature in alpine and lowland plant species. *Ann. Bot.* 76:245–252.
- Lewis JD, Wang XZ, Griffin KL, Tissue DT (2002) Effects of age and ontogeny on photosynthetic responses of a determinate annual plant to elevated CO₂ concentrations. *Plant Cell Environ* 25:359–368.
- Lin D, Xia J, Wan S (2010) Climate warming and biomass accumulation of terrestrial

- plants: A meta-analysis. *New Phytol* 188:187–198.
- Long SP (1991) Modification of the response of photosynthetic productivity to rising temperature by atmospheric CO₂ concentrations: Has its importance been underestimated? *Plant, Cell Environ* 14:729–739.
- Loveys BR, Atkinson LJ, Sherlock DJ, Roberts RL, Fitter AH, Atkin OK (2003) Thermal acclimation of leaf and root respiration: An investigation comparing inherently fast- and slow-growing plant species. *Glob Chang Biol* 9:895–910.
- Luo Y, Field CB, Mooney HA (1994) Predicting responses of photosynthesis and root fraction to elevated [CO₂] - Interactions among carbon, nitrogen, and growth. *Plant Cell Environ* 17:1195–1204.
- Mantovani A, Vieira RC (2000) Leaf micromorphology of Antarctic pearlwort *Colobanthus quitensis* (Kunth) Bartl. *Polar Biol* 23:531–538.
- Mawson BT, Cummins WR (1989) Thermal acclimation of photosynthetic electron transport activity by thylakoids of *Saxifraga cernua*. *Plant Physiol* 89:325–332.
- Maxwell K, Johnson GN (2000) Chlorophyll fluorescence - a practical guide. *J Exp Bot* 51:659–668.
- Medlyn BE, Barton CVM, Broadmeadow MSJ, Ceulemans R, de Angelis P, Forstreuter M, Jach ME, Kellomaki S, Laitat E, Marek M, Philippot S, Rey A, Strassemeier J, Laitinen K, Liozon R, Portier B, Roberntz P, Wang K, Jarvis PG (2001) Stomatal conductance of forest species after long-term exposure to elevated CO₂ concentration: A synthesis. *New Phytol* 149:247–264.
- Medlyn BE, Dreyer E, Ellsworth D, Forstreuter M, Harley PC, Kirschbaum MUF, le Roux X, Montpied P, Strassemeier J, Walcroft A, Wang K, Loustau D (2002) Temperature response of parameters of a biochemically based model of photosynthesis. II. A review of experimental data. *Plant, Cell Environ* 25:1167–1179.
- Montiel P, Smith A, Keiller D (1999) Photosynthetic responses of selected Antarctic plants to solar radiation in the southern maritime Antarctic. *Polar Res* 18:229–235.
- Moore DM (1970) Studies in *Colobanthus quitensis* and *Deschampsia antarctica*. *Br. Antarct. Surv. Bull* 23:63–80.
- Morison JIL, Lawlor DW (1999) Interactions between increasing CO₂ concentration and temperature on plant growth. *Plant, Cell Environ* 22:659–682.
- Oishi AC, Oren R, Novick KA, Palmroth S, Katul, GG (2010) Interannual invariability of forest evapotranspiration and its consequence to water flow downstream. *Ecosystems* 13:421–436.
- Parkhurst F (1982) Stereological methods for measuring internal leaf structure variables. *Am J Bot* 69:31–39.
- Parnikoza I, Convey P, Dykyy I, Trokhymets V, Milinevsky G, Tyschenko O,

- Inozemtseva D, ozeretska I (2009) Current status of the Antarctic herb tundra formation in the Central Argentine Islands. *Glob Chang Biol* 15:1685–1693.
- Parnikoza I, Kozeretska, I., Kunakh V (2011) Vascular plants of the maritime antarctic: origin and adaptation. *Am J Plant Sci* 02:381–395.
- Parnikoza IY, Maidanuk DN, Kozeretska IA (2007) Are *Deschampsia antarctica* Desv. and *Colobanthus quitensis* (Kunth) Bartl. migratory relicts? *Tsitol Genet* 41:36–40.
- Pearcy RW (1977) Acclimation of photosynthetic and respiratory carbon dioxide exchange to growth temperature in *Atriplex lentiformis* (Torr.) Wats. *Plant Physiol* 59:795–799.
- Poorter H, Niinemets Ü, Poorter L, Wright IJ, Villar R (2009) Causes and consequences of variation in leaf mass per area (LMA): A meta-analysis. *New Phytol* 182:565–588.
- Reynolds JF, Hilbert DW, Kemp PR (1993) Scaling ecophysiology from the plant to the ecosystem: A conceptual framework. In Ehleringer JR, Field CR (eds) *Scaling physiological processes: Leaf to globe*. Academic Press, San Diego, pp 127-140.
- Romero M, Casanova A, Iturra G, Reyes A, Montenegro G, Alberdi M (1999) Leaf anatomy of *Deschampsia antarctica* (Poaceae) from the Maritime Antarctic and its plastic response to changes in the growth conditions. *Rev Chil Hist Nat* 72:411–425.
- Rozema J, Boelen P, Blokker P (2005) Depletion of stratospheric ozone over the Antarctic and Arctic: Responses of plants of polar terrestrial ecosystems to enhanced UV-B, an overview. *Environ Pollut* 137:428–442.
- Ruhland CT, Day TA (2000) Effects of ultraviolet-B radiation on leaf elongation, production and phenylpropanoid concentrations of *Deschampsia antarctica* and *Colobanthus quitensis* in Antarctica. *Physiol Plant* 109:244–251.
- Rustad LE, Campbell JL, Marion GM, Norby RJ, Mitchell MJ, Hartley AE, Cornelissen JHC, Gurevitch J, GCTE-NEWS (2000) A meta-analysis of the response of soil respiration, net nitrogen mineralization, and aboveground plant growth to experimental ecosystem warming. *Oecologia* 126:543-562.
- Sage RF (1994) Acclimation of photosynthesis to increasing atmospheric CO₂: The gas exchange perspective. *Photosynth Res* 39:351–368.
- Sage RF, Kubien DS (2007) The temperature response of C₃ and C₄ photosynthesis. *Plant Cell Environ* 30:1086–1106.
- Salvucci ME, Ogren ML (1996) The mechanism of Rubisco activase: insights from studies of the properties and structure of the enzyme. *Photosynth Res* 47:1-11.
- Sharkey TD, Bernacchi CJ, Farquhar GD, Singsaas EL (2007) Fitting photosynthetic carbon dioxide response curves for C₃ leaves. *Plant Cell Environ* 30:1035-1040.
- Sierra-Almeida Á, Casanova-Katny MA, Bravo LA, Corcuera LJ, Cavieres LA (2007) Photosynthetic responses to temperature and light of Antarctic and Andean

- populations of *Colobanthus quitensis* (Caryophyllaceae). *Rev Chil Hist Nat* 80:335–343.
- Smith RIL (1994) Vascular plants as bioindicators of regional warming in Antarctica. *Oecologia* 99:322–328.
- Smith RIL (2003) The enigma of *Colobanthus quitensis* and *Deschampsia antarctica* in Antarctica. In: Huiskes AH., Gieskes WW., Rozema J, et al. (eds) *Antarctic Biology in a Global Context*. Backhuys Publisher, Leiden, The Netherlands, pp 234–239
- Stitt M (1991) Rising CO₂ levels and their potential significance for carbon flow in photosynthetic cells. *Plant, Cell Environ* 14:741–762.
- Thomson VP, Cunningham SA, Ball MC, Nicotra AB (2003) The effect of temporal scale on the outcome of trophic cascade experiments. *Oecologia* 134:578–586.
- Trumble JT, Kolodny-Hirsch DM, Ting IP (1993) Plant compensation for arthropod herbivory. *Annu Rev Entomol* 38:93–120.
- Turner NC, Schulze E-D, Gollan T (1984) The responses of stomata and leaf gas exchange to vapour pressure deficits and soil water content. *Oecologia* 63:338–342.
- Vaughan DG, Marshall GJ, Connolley WM, Parkinson C, Mulvaney R, Hodgson MA, King JC, Pudsey CJ, Turner J (2003) Recent rapid regional climate warming on the Antarctic Peninsula. *Clim Change* 60:243–274.
- von Caemmerer S, Evans JR, Hudson GS, Andrews TJ (1994) The kinetics of ribulose-1,5-bisphosphate carboxylase/oxygenase *in vivo* inferred from measurements of photosynthesis in leaves of transgenic tobacco. *Planta* 195:88–97.
- Wang D, Heckathorn SA, Wang X, Philpott SM (2012) A meta-analysis of plant physiological and growth responses to temperature and elevated CO₂. *Oecologia* 169:1–13.
- Way DA, Oren R (2010) Differential responses to changes in growth temperature between trees from different functional groups and biomes: a review and synthesis of data. *Tree Physiol* 30:669–688.
- Way DA, Yamori W (2013) Thermal acclimation of photosynthesis: On the importance of adjusting our definitions and accounting for thermal acclimation of respiration. *Photosynth Res* 119:89–100.
- Xiong FS, Day TA (2001) Effect of solar ultraviolet-B-radiation during springtime ozone depletion on photosynthesis and biomass production of Antarctic vascular plants. *Plant Physiol* 125:738–751.
- Xiong FS, Mueller EC, Day TA (2000) Photosynthetic and respiratory acclimation and growth response of antarctic vascular plants to contrasting temperature regimes. *Am J Bot* 87:700–710.
- Xiong FS, Ruhland CT, Day TA (1999) Photosynthetic temperature response of the Antarctic vascular plants *Colobanthus quitensis* and *Deschampsia antarctica*.

Physiol Plant 106:276–286.

Xu ZZ, Zhou GS (2006) Combined effects of water stress and high temperature on photosynthesis, nitrogen metabolism and lipid peroxidation of a perennial grass *Leymus chinensis*. *Planta* 224:1080–1090.

Yamasaki T, Yamakawa T, Yamane Y, Koike H, Satoh K, Kato S (2002) Temperature acclimation of photosynthesis and related changes in photosystem II electron transport in winter wheat. *Plant Physiol* 128:1087–1097.

Yamori W, Hikosaka K, Way DA (2014) Temperature response of photosynthesis in C₃, C₄, and CAM plants: temperature acclimation and temperature adaptation. *Photosynth Res* 119:101–117.

Appendix

Appendix A. Mean \pm SE of CO₂ gas exchange, chlorophyll fluorescence, leaf chemical and structural parameters, and biomass of *C. quitensis* grown in the 12/AC treatment. The treatment was under an aphid attack, which was likely to confound with the treatment effect. Data for this treatment were therefore removed from the thesis.

Parameters	Measured at 16 °C	Measured at growth temperature (12 °C)
V_{cmax} (μmol m⁻² s⁻¹)	57.57 ± 4.69	28.86 ± 5.82
J_{max} (μmol m⁻² s⁻¹)	148.85 ± 7.56	82.04 ± 12.24
A_{net} (μmol m⁻² s⁻¹)	10.81 ± 1.27	6.79 ± 1.59
F_v/F_m	0.80 ± 0.004	
ETR (μmol m⁻² s⁻¹)	144.01 ± 4.34	92.10 ± 12.30
C_i/C_a	0.76 ± 0.02	0.82 ± 0.05
R_{dark} (μmol m⁻² s⁻¹)	4.63 ± 0.28	2.27 ± 0.34
SLA (mm²/g)	0.022 ± 0.002	
Aboveground biomass (g/pot)	0.63 ± 0.14	
Belowground biomass (g/pot)	0.23 ± 0.03	
Total biomass (g/pot)	0.84 ± 0.14	
%C	36.83 ± 0.48	
%N	3.00 ± 0.10	

Appendix B. Permission to reuse images from the copyright holders. a) Permission from Elsevier to use a figure from Lamers et al. 2008, (Trends in Biotechnology, 26(11):631-638) as Figure 1.1 in this thesis; b) Permission from Oxford University Press to use a figure from Maxwell and Johnson 2000 (Journal of Experimental Botany, 51:659–668) as Figure 1.2 in this thesis.

a)

Apr 14, 2

This is an Agreement between VI NT Bui ("You") and Elsevier ("Elsevier"). It consists of your order details, the terms and conditions provided by Elsevier, and the payment terms and conditions.

All payments must be made in full to CCC. For payment instructions, please see information listed at the bottom of this form.

Supplier	Elsevier Limited
Registered Company Number	1982084
Customer name	VI NT Bui
License number	3846210631657
License date	Apr 11, 2016
Licensed content publisher	Elsevier
Licensed content publication	Trends in Biotechnology
Licensed content title	Exploring and exploiting carotenoid accumulation in <i>Dunaliella salina</i> for cell-factory applications
Licensed content author	Packo P. Lamers, Marcel Janssen, Ric C.H. De Vos, Raoul J. Bino, René H. Wijffels
Licensed content date	November 2008
Licensed content volume number	26
Licensed content issue number	11
Number of pages	8
Start Page	631
End Page	638
Type of Use	reuse in a thesis/dissertation
Portion	figures/tables/illustrations
Number of figures/tables/illustrations	1
Format	electronic
Are you the author of this Elsevier article?	No
Will you be translating?	No
Original figure numbers	Figure 3
Title of your thesis/dissertation	Photosynthetic acclimation to warming and elevated CO ₂ of two Antarctic vascular plant species
Expected completion date	Apr 2016
Estimated size (number of pages)	94
Elsevier VAT number	GB 494 6272 12
Price	0.00 CAD
VAT/Local Sales Tax	0.00 CAD / 0.00 GBP
Total	0.00 CAD

b)

Apr 14, 2016

This is a License Agreement between Vi NT Bui ("You") and Oxford University Press ("Oxford University Press") provided by Copyright Clearance Center ("CCC"). The license consists of your order details, the terms and conditions provided by Oxford University Press, and the payment terms and conditions.

All payments must be made in full to CCC. For payment instructions, please see information listed at the bottom of this form.

License Number	3847660412947
License date	Apr 14, 2016
Licensed content publisher	Oxford University Press
Licensed content publication	Journal of Experimental Botany
Licensed content title	Chlorophyll fluorescence—a practical guide:
Licensed content author	Kate Maxwell, Giles N. Johnson
Licensed content date	04/01/2000
Type of Use	Thesis/Dissertation
Institution name	None
Title of your work	Photosynthetic acclimation to warming and elevated CO ₂ of two Antarctic vascular plant species
Publisher of your work	n/a
Expected publication date	Apr 2016
Permissions cost	0.00 USD
Value added tax	0.00 USD
Total	0.00 USD
Total	0.00 USD

Curriculum Vitae

NAME **Vi Nguyen Tuong Bui**

POST-SECONDARY EDUCATION AND DEGREES

- 2014-2016** **MSc**, Biology (Environment and Sustainability Collaborative Program)
University of Western Ontario
London, ON
- 2006-2009** **BA**, summa cum laude, Environmental Studies
Mount Holyoke College
South Hadley, MA

HONOURS AND AWARDS

- 2015** **Honorable mention poster**
Fallona Interdisciplinary Research Showcase, University of Western Ontario
- 2015** **Physiology Section Best Student Presentation**
Botany Conference, Edmonton, AB
- 2015** **George H. Duff Travel Award**
Canadian Society of Plant Biologists
- 2015** **Environment and Sustainability Excellence Award**
University of Western Ontario
- 2015** **Environment and Sustainability Travel Award**
University of Western Ontario
- 2013** **Abby Howe Turner Award for Excellence in Physiology**
Mount Holyoke College
- 2012** **Summer Research Grant**
Howard Hughes Medical Institute for Undergraduate Research

TEACHING EXPERIENCE

- Winter 2015-16** Bio 2217 - Plants as a Human Resource
- Fall 2014-15** Bio 2601 - Organismal Physiology

PRESENTATIONS

- 2015** **Oral presentation**, Canadian Society of Plant Biologists Eastern Regional Meeting, Toronto, ON
Photosynthetic response of an Antarctic grass to warming and elevated CO₂
- 2015** **Poster presentation**, Fallona Family Interdisciplinary Showcase, University of Western Ontario, London, ON

- Wood anatomy of Scots pine and Norway spruce under warming and elevated CO₂
- 2015** **Oral presentation**, Botany Conference, Edmonton, AB
- Wood anatomy of Scots pine and Norway spruce under warming and elevated CO₂
- 2014** **Oral presentation**, Archbold Biological Station, Venus, FL
- Gases in grasses: Greenhouse gases in response to timing of fire and feral pig rooting in a subtropical semi-native grassland
- 2013** **Poster presentation**, Ecological Society of America, Minneapolis, MN
- Photosynthetic performance of *Chamaedaphne calyculata* after twelve years of fertilization at Mer Bleue Bog, Canada

ACADEMIC ASSOCIATIONS

- 2014-present** **Canadian Society of Plant Biologists**
- 2013-2014** **Ecological Association of America**
- 2013-2014** **American Statistical Association**

EXTRACURRICULAR ACTIVITIES

- 2014-present** **Board Member**, Thames Region Ecological Association, London, ON
- 2014-present** **Logistics Organizer**, Earth Day Colloquium, University of Western Ontario